MYCN-Dependent Expression of Sulfatase-2 Regulates Neuroblastoma Cells

Thesis submitted in accordance with the requirements of the
University of Liverpool for the degree of
Doctor in Philosophy

by

Valeria Solari

July 2014

TABLE OF CONTENTS

Abstract

Neuroblastoma (NBL) is the most common type of cancer diagnosed in the first year of life. It is a complex and heterogeneous disease that arises from the developing sympathetic nervous system. Despite numerous advances and the well-demonstrated role of MYCN in the pathogenesis of neuroblastoma, the mechanisms underlying its oncogenic function are not entirely understood and there is evidence that its function is, in part, dependent on the tumour microenvironment (TME). New and improved therapeutic targets are urgently required for this often lethal tumour. Heparan sulfate proteoglycans (HSPG) play a critical role in the interactions between tumour cells and the TME and their activities are dependent on the sulfation pattern, that is controlled by sulfotransferases, which add sulfate groups to the repeating disaccharide units, and sulfatases (SULFs), which selectively remove 6-O-sulfates. In this work an analysis of the expression of these enzymes in human neuroblastoma revealed higher levels of SULF2 specifically when the MYCN oncogene was amplified. Loss of expression of SULF2 in MYCN-amplified (A) cell lines was associated with a marked decrease in survival and an increase in apoptosis. Evidence is presented that SULF2 is a direct downstream target of MYCN since over-expression of MYCN in neuroblastoma cells increases SULF2 expression whereas a down regulation reduced SULF2 expression. Underlying the importance of SULF2 in neuroblastoma cell survival independently of MYCN, it is demonstrated that overexpression of SULF2 in MYCN-NA cells increases cell viability without increasing MYCN expression. Analysis of SULF2 protein expression in a large cohort of primary human neuroblastoma tumours also indicated a high level of expression in MYCN-A tumours and an almost complete absence of expression in MYCN-non A (NA) tumours. The data identify SULF2 as a new downstream target of MYCN and a key contributor to its oncogenic function in human neuroblastoma, which might have future implications for clinical therapies for high-risk NBL.

To my parents

To all children suffering from neuroblastoma

Acknowledgment

I gratefully acknowledge all the people who have supported me during my training and who have contributed to this thesis.

I want to thank my supervisors for their guidance. Professor Jerry Turnbull and Dr Edwin Yates: thank you for welcoming me in your laboratory. Their belief in my abilities made it possible for me to tackle this thesis and receive a Medical Research Council (MRC) Clinical Research Training Fellowship. I would like to thank Dr Yves DeClerck for hosting me in his lab at Children's Hospital Los Angeles and for his encouragement.

I am grateful to Professor Michael Höllwarth and Professor Prem Puri. I started my training in paediatric surgery under their guidance and they passed me on their enthusiasm for patients care and research and stimulated me to work rigorously. I was lucky to have worked with such outstanding surgeons and remarkable mentors.

My deepest gratitude goes to Professor David Warburton who made the collaboration with Dr DeClerck at Children's Hospital Los Angeles possible. He has continuously motivated me and built my confidence with his extraordinary mentorship and advice. He has always been inspirational and inspires huge loyalty. Beyond his scientific guidance I am grateful for his humanity and genuine interest in my wellbeing in and out of the lab. I am very greatful to Edwin Jesudason whose beguiling science writing and enquiring mind has been a help and inspiration for this fellowship and my training in paediatric surgery.

Thanks to the following people for providing their knowledge: Gianluca Turcatel for the lentiviral work, Esteban Fernandez for microscopy assistance, Professor Hiro Shimada for sharing his exceptional knowledge in neuroblastoma, Shahab Asgharzadeh for microarray data, Muller Fabbri and Kishore Challagundla for cell work and discussions; Michael Sheard for FACS analysis and Richard Sposto for assistance in statistics. My gratitude goes also to Sophie Thompson, Becky Miller, Scott Guimond and Toin van Kuppevelt.

Finally, I am very greatful to my friend Lucia Borriello for many stimulating discussions and for making tiring days in the lab fun!

Contributors and funding

This work was supported entirely by award of a Clinical Research Training Fellowship to V. Solari from the United Kingdom Medical Research Council (MRC).

This work was supervised by a dissertation committee consisting of Professor Jeremy E Turnbull and Dr Edwin A Yates (supervisors) and Prof Phil Rudland and Dr Roger Barraclough (as independent assessors) of the Department of Biochemistry at the University of Liverpool, UK, and Professor Yves A DeClerck of the Department of Biochemistry and Molecular Biology, University of Southern California (USC), Los Angeles, USA.

List of Figures

List of Tables

List of Abbreviations

7-AAD	7-aminoactinomycin
ADP	adenosine diphosphate
ATP	adenosine triphosphate
BMP	Bone morphogenetic protein
bp	base pair
BrdU	bromodeoxyuridine
cDNA	complementary DNA
CHLA	Children's Hospital Los Angeles
COG	Children's Oncology Group
DNA	De-oxy ribonucleic acid
FFPE	formalin fixed paraffin embedded
GAPDH	Glyceraldehyde 3-phosphate dehydrogenase
GDNF	Glial cell-derived neurotrophic factor
GFP	green fluorescent protein
GPOH	Gesellschaft für Pëdiatrische Onkologie und Hämatologie
HS	heparan sulphate
KD	knockdown
MYCN	v-myc avian myelocytomatosis viral oncogene neuroblastoma derived homolog
NDST	N-deacetylase/N-sulfotransferases
OST	O-sulfotransferase
PARP	Poly ADP ribose polymerase
PI-88	phosphomannopentaose sulfate-88
qRT-PCR	reverse transcription polymerase chain reaction
RNA	ribonucleic acid
SCR	scramble
siRNA	small interfering RNA
SULF	sulfotransferase

Chapter 1: Introduction and Research Objectives

1.1 Childhood cancer

Every year about 1,600 children in the UK and 8,500 in the United States are diagnosed with cancer under 15 years of age; accounting for just 0.5 % of the total cancer diagnoses in all ages. In Europe, approximately 1 in 500-600 children develop a malignant disease before the age of fifteen [Parkin et al., 1998] although rare paediatric cancers are, next to accidents, the second most common cause of childhood death in developed countries [Kaatsch, 2010; Basta et al., 2011]. Since the declaration of war on cancer by USA president Nixon in 1971, and despite some improvements, little has changed in standard cancer therapy, which still comprises surgery, chemotherapy and radiation. Paediatric tumours such as high-risk neuroblastoma still have very poor outcomes.

The seminal paper *The Hallmarks of Cancer* by Hanahan and Weinberg [Hanahan and Weinberg, 2011] suggested that all cancers can be described by a few principles. They describe tumour progression via eight “hallmarks” in a process analogous to Darwinian evolution, in which genetic changes provide a growth advantage to cells that have become cancerous.

Childhood cancer is very different from adult cancers in many ways. Adult cancers are mostly epithelial carcinomas, whereas paediatric cancers are principally haematological malignancies, tumours from the central nervous system (CNS), lymphomas and embryonal tumours (i.e., neuroblastomas, retinoblastomas, nephroblastomas, embryonal rhabdomyosarcomas and germ cell tumours. The aetiology of childhood cancers remains unclear. Adult

tumours result from a multistep process that develops over several years or even decades. Childhood tumours have a much shorter carcinogenic process and environmental factors such as lifestyle, that are so significant in adults, have a very small aetiology, given the short time available between oncogenic exposure and disease [Grimmer et al., 2006]. Only 10 % of childhood cancers have a clear genetic predisposition that can be inherited from a parent, or occur *de novo* in the gametocytes before fertilisation. Germ line mutations are very rare in children. Over the last few decades many efforts have been focused on finding somatic mutations in human cancer, with the aim of identifying precise treatments for specific mutations. However, DNA mutations amongst paediatric tumours, and especially in NBL, are sparse, emphasizing the challenge of identifying new therapeutic targets for these tumours. Interestingly, even when excluding patients with known genetic conditions, many childhood cancers are associated with congenital anomalies [Miller RW, 1969]. One only has to think of what can happen when twinning goes awry; the spectrum of anomalies and embryology is extensive and ranges from monozygotic twins to conjoined twins, malformed external parasitic twins, fetus-in-fetu, to “fetaform” teratomas and finally teratomas. The idea of cancer as a “devolutionary” state has been noted in the early last century by scientists like Theodore Boveri [Boveri T, 2008], who recognised that cancer cells are similar to those seen during early embryonic development. So, one may ask; is the problem of cancer looked at in the wrong way?

In contrast to conventional explanations for cancer, the unifying theory of cancer by Davies and Lineweaver [Davies and Lineweaver, 2011] explains

cancer as an evolutionary throwback and atavistic state, in which cancer cells are under the control of ancient programs. The same genes that have been passed on from very early ancestry and are present during normal embryonic life as cells, differentiating into specific organs, are switched on in cancer. The earlier the embryonic stage, the more basic will be the genes guiding development. This theory seems to be appropriate for paediatric tumours, in which many genetic pathways controlling early development such as MYCN and Wnt are re-activated or, as in NBL, the tumour can undergo spontaneous regression and/or mature from a malignant to a benign state [Brodeur 2003; Beckwith and Perrin 1963; Ikeda et al. 1981; Haase et al. 1988].

In 1889 the English surgeon Stephen Paget proposed in his theory of the “seed and soil” of cancer, that metastasis relies on the cross-talk between the cancer cells (“the seed”) and the specific organ microenvironment (“the soil”) [Paget, 1889]. Numerous pieces of evidence illustrate the importance of the tumour microenvironment for tumour progression and therapeutic responses [Hanahan and Coussen, 2012; Whiteside 2008; Joyce and Pollard, 2009]. The microenvironment of the tumour can not only support the development of cancer, but also adversely impact the efficacy of clinical therapy [Quail and Joyce 2013; Hanahan and Coussen, 2012]. Anti-microenvironment therapy against blood vessels with the aim of starving the tumour was pioneered by the paediatric surgeon Judah Folkman [Folkman, 1971] and a drug was later approved by the US-FDA in 2004 for colorectal cancer and lung carcinoma, HER2 negative breast cancer and glioblastoma [Carmeliet and Jain, 2011; Jain et al., 2006; Ferrara 2009]. Clinical trials were encouraging but high efficacy

requires additional cytotoxic chemotherapy. A comprehensive understanding of the biological mechanism of the tumour microenvironment is required for successful therapeutic targeting [Valastyan and Weinberg, 2011]. Most studies are focused on the protein component, while other essential key regulators of the ECM, such as heparan sulfate proteoglycans (HSPGs), are largely neglected. Similar to other atavistic structures, heparan sulfate (HS) appeared in early metazoan life and is known to regulate the activity of many extracellular proteins and extracellular matrix components [Esko and Selleck, 2002; Häcker et al., 2005; Turnbull, 2007]. Recent evidence shows the role of HS in the tumour microenvironment [Sasiskeran et al., 2002; Iozzo 2005; Sanderson et al., 2005; Phillips et al., 2012]. Early evidence in the 1980's showed that neuroblastoma has altered sulfation with an increase in 6O-sulfation [Hampson et al., 1983; Hampson et al., 1984]. Extensive reports in the literature showed that cellular transformation and behaviour in malignancy correlates with changes in HS expression and structure including 6O-sulfation [Jayson et al., 1998; Delcommenne et al., 2012]. Similarly our preliminary data revealed that neuroblastoma cells and tissue have increased levels of HS and of 6O-sulfation by disaccharide analysis (*see* Appendix 1). Little is known about the host microenvironment of NBL. Studying the glycobiological aspect of this developmental tumour, in which the microenvironment and embryological genes, such as MYCN, play a critical role, could represent a novel molecular direction and a missing link.

1.2 Neuroblastoma

1.2.1 Historical and general background

"Mit einer gewissen Zaghaftigkeit erwähne ich hier noch einer geschwulstartigen Bildung, nähmlich partieller Hyperplasien der Marksubstanz der Nebennieren. Bekanntlichist von vielen neueren Beobachtern diese Substanz für eine wesentlich nervöse angesehen worden, [Virchow, 1865]; *{"It is with a certain diffidence that I bring up here another tumour-like condition, namely partial hyperplasia of the marrow substance of the adrenal glands."}*. It is with these words that in 1864 just 5 years after Darwin's "*The Origin of Species*", the concept of neuroblastoma was introduced by the great pathologist Rudolf Virchow in his seminal work "*Die Krankhaften Geschwülste*" (*"The morbid growths"*). However, the first description of this enigmatic tumour was a misconception as the sympathetic ganglion cells were thought to be less important and the tumour was classified as a type of glioma. Only at the beginning of the 20th century James Homer Wright recognised the tumour originates from primitive neuronal cells and coined the term "Neuroblastoma", as the cells were associated with fibrils similar to neuroblasts [Lee et al., 2002]. Felix Marchand recognized that NBL is a tumour that arises from the sympathetic nervous system and the adrenal gland [Cheung, 2005]. In 1953 the paediatric surgeon Robert E Gross opined that "extensive and radical surgery has a definite place under certain circumstances and can lead to permanent cure" [Gross et al., 1959].

From the beginning of the 20th century there have been many attempts to make a prognostic evaluation from the histological features of this tumour [Beckwith

and Martin, 1968; Mäkinen 1972; Wahl 1914; Landau 1911]. A grading system proposed by Hughes was not successful [Hughes et al., 1974]. In 1983, Shimada proposed a classification system that was based on the unique principle of age-linked evaluation of morphological indicators [Shimada et al., 1984]. In 1992 Joshi *et al* proposed histological grading using the mitotic rate (MR: low ≤10/10 high power field, high >10/10 high-power fields) and calcification [Joshi et al., 1992]. In 1994 the International Neuroblastoma Pathology Committee was created to establish a prognostically significant and biologically relevant classification. Five years later in 1999 the Committee developed the International Classification based on the original Shimada Classification with some modifications [Shimada et al., 1999], (*see* Chapter 1.2.5).

1.2.2 Aetiology of neuroblastoma

Numerous studies evaluated the potential risk factors for neuroblastoma, but no causal factors were identified. The role of birth characteristics and reproduction history has been extensively studied [Yang et al. 2000]. Inconsistent results were reported concerning maternal history of prior miscarriage, caesarian section and vaginal infection during pregnancy, as well as sexually transmitted diseases [Michalek et al., 1996]. A recent review found no increased overall risk for neuroblastoma in children born after assisted conception [Williams et al., 2013]. Reports also conflict regarding the relationship between pre-term birth (<37 weeks gestation) and low birth weight (<2500 gr), [Johnson and Spitz, 1985; Hamrick et al., 2001]. No correlation was found between parental occupation and the cancer [Bunin et al., 1990]. Studies from Toronto suggest

that the rate of neuroblastoma was reduced by 60 % with the mandatory folic acid fortification of flour and by multivitamin supplementation [French et al., 2003; Goh et al., 2007].

1.2.3 Clinical and surgical features

Neuroblastoma is described as enigmatic as it can present in several ways depending on the site of the primary tumour, presence of metastasis and production of metabolic by-products [Cheung, 2005]. It commonly presents with an abdominal mass, pain and distension. Hypertension is present in 25 % of children due to the production of catecholamine and encasement of renal vessels. Bone pain and limp are the result of metastatic disease in the bones. General cancer symptoms such as weight loss, fever and anaemia are often present. Tumours in the paraspinal region can present as tetraplegia due to the extension in the intervertebral foramen and compression of the spinal cord. When the growth is in the neck and involves the stellate ganglion it can cause Horner syndrome with miosis, ptosis and enophtalmos and heterochromia of the iris. Bone metastasis of the orbit causes bilateral ecchymosis called “raccoon eyes” or “panda eyes” [Cheung, 2005]. Patients with stage I or II disease and mediastinal tumours often present with cerebellar ataxia with opsomyoclonus and nystagmus (involuntary muscle contractions and random movements of the eye). This is believed to be caused by an autoimmune response with the production of antigen-antibody complexes that cross-react with Purkinje cells of the cerebellum. These are some of the more common clinical manifestations of this tumour. Rarely neuroblastoma can present as a

“mirror-syndrome” when foetal catecholamine induces symptoms in the mother via the placenta. In addition there are distinct associations of neuroblastoma with other disorders such as neurofibromatosis type 1 [Origone et al., 2003], Beckwith-Wiedermann syndrome [Shuman et al., 1993], Hirschsprung’s disease (Maris et al., 2002; Raabe et al., 2008], Ondine’s syndrome [Stovroff et al., 1995] and cardiovascular malformations [Lin et al., 2005; George et al., 2004]. Some of these relationships have been explained on the basis of the abnormalities of neuronal crest development (*see* 1.2.8).

The paediatric surgeon plays an essential role in the management of children with neuroblastoma. Not only is the paediatric surgeon often the first physician to examine a symptomatic child and raise the suspicion of this cancer, but is required to provide an adequate tissue sample for histological and molecular diagnosis and, importantly, conduct good tumour resection. Surgical removal of neuroblastoma is frequently a very challenging task and the mainstay of treatment. It requires a safe resection with full preservation of adjacent organs and vital structures, such as vessels and nerves. The tumour encases the major vessels, making en-block resections often impossible, however, invasion is very rare; it has not been reported to go beyond the adventitia and media. Surgical resection can be the only treatment required for low-risk neuroblastomas but it is also widely accepted that aggressive resection of loco-regional disease should be attempted to reduce the mass of the disease. Haase reported that surgical resection for stage III tumour can downstage the patient, thereby improving the outcome [Haase et al., 1989].

1.2.4 Histopathology

Neuroblastoma belongs to the tumours of peripheral neuroblastoma group and comprises a distinct entity from the other “small blue round cell” tumours, central primitive neuroendocrine tumours (cPTEN) and Ewing’s sarcoma/peripheral primitive neuroendocrine tumour (pPTEN), despite some immunological overlaps.

In 1999, the International Neuroblastoma Pathology Committee (INPC) made a recommendation for terminology and morphological criteria of peripheral neuroblastic tumours by adopting the modified Shimada Classification [Shimada et al., 1999]. The INPC is a morphological classification designed to be prognostically significant and biologically relevant, that was established in 1999 [Shimada et al., 1999] and revised in 2003 [Peuchmaur et al., 2003]. It classifies two prognostic groups; i.e. favorable histology (FH) and unfavorable histology (UH) groups. The histological features are evaluated from tissue removed by surgery or biopsy before starting chemotherapy/irradiation therapy. Metastatic sites are also eligible for MKI (Mitosis Karyorrhexis Index) calculation, except for bone marrow.

The peripheral neuroblastic tumours are divided into 4 categories, and two distinct prognostic groups (‘favourable histology’ and ‘unfavourable histology’), based on grade of neuroblastic differentiation, Schwannian stromal development and mitotic karyorrhexis index, (Table 1.1). The four categories are:

- Neuroblastoma (Schwannian stroma poor)
- ganglioneuroblastoma intermixed (Schwannian stroma rich)

- ganglioneuroblastoma nodular (composite, Schwannian stroma rich/stroma dominant/stroma poor)
- ganglioneuroma (Schwannian stroma dominant, mature or maturing).

International Neuroblastoma Pathology classification			**Original Shimada classification**	**Prognostic group**
Neuroblastoma		**(Schwannianstroma-poor)**	**Stroma-poor**	
	Favourable		Favourable	Favourable
	<1.5 yrs	Poorly differentiated or differentiating & low or intermediate MKI tumour		
	1.5–5 yrs	Differentiating & low MKI tumour		
	Unfavorable		Unfavourable	Unfavourable
	<1.5 yrs	a) undifferentiated tumour		
		b) high MKI tumour		
	1.5–5 yrs	a) undifferentiated or poorly differentiated tumour		
		b) intermediate or high MKI tumour		
	≥5 yrs	All tumours		
Ganglioneuroblastoma, intermixed		**(Schwannianstroma-rich)**	**Stroma-rich Intermixed (favourable)**	**Favourable**
Ganglioneuroma		**(Schwannianstroma-dominant)**		
	Maturing		Well differentiated (favourable)	Favourable
	Mature		Ganglioneuroma	
Ganglioneuroblastoma, nodular		**(composite Schwannianstroma-rich/dominant/poor)**	**Stroma-rich nodular (unfavourable)**	**Unfavourable**

Table 1.1 Prognostic evaluation of peripheral neuroblastic tumours according to the International Neuroblastoma Pathology Classification (Shimada System) [Shimada H et al., 1999[b]].

MKI: mitosis-karyorrhexis index

1.2.5 Staging and Classification

Over the years there have been several staging systems proposed for neuroblastoma. The International Neuroblastoma Staging System (INSS) developed by Brodeur et al. (Brodeur et al., 1988, Brodeur et al., 1993) classifies patients into stages 1-4s and takes into account the local and distant extent of the disease as well as the surgical resectability of the tumour (Table 1.2). This is a post-operative staging system that takes into account tumour size and location relative to the midline and the presence of metastatic disease. However, it depends on the extent of surgical resection of the primary tumour in patients with non-metastatic disease. Recently, a new staging system was developed that takes into account pre-treatment imaging of the tumour and bone marrow pathology, instead of surgical resection, which is surgeon dependent and thus varies from institution to institution (Table 1.3), [Monclair et al., 2009].

Stage	Description
1	Localised tumour confined to area of origin; complete excision, with or without microscopic residual disease; ipsilateral and contralateral lymph nodes negative (nodes attached to primary tumour and removed en-bloc with it might be positive)
2A	Unilateral tumour with incomplete gross excision; ipsilateral and contralateral lymph nodes negative
2B	Unilateral tumour with complete or incomplete excision; positive ipsilateral, non-adherent regional lymph nodes; contralateral lymph nodes negative
3	Tumour infiltrating across the midline with or without lymph node involvement; or unilateral tumour with contralateral lymph node involvement; or midline tumour with bilateral lymph node involvement or bilateral infiltration (unresectable). The midline is defined as the vertebral column.
4	Dissemination of tumour to distant lymph nodes, bone, bone marrow, liver, or other organs, except as defined for stage 4S
4S	Localised primary tumour as defined for stage 1, 2A or 2B with dissemination limited to liver, skin, and/or bone marrow (limited to infants younger than 1 year). Marrow involvement should be minimal (i.e., <10% of total nucleated cells identified as malignant by bone biopsy or by bone marrow aspirate). More extensive bone marrow involvement would be considered stage 4 disease. The results of the MIBG scan, if performed, should be negative for disease in the bone marrow.

Table 1.2 The International Neuroblastoma Staging System (INSS) of neuroblastoma.

Stage	Description
L1	Localised tumour not involving vital structures as defined by the list of image-defined risk factors and confined to one body compartment
L2	Locoregional tumour with presence of one or more image defined risk factor
M	Distant metastatic disease (except stage MS)
M5	Distant metastatic disease in children younger than 18 months with metastases confined to skin, liver, and/or bone marrow

Table 1.3 The new International Neuroblastoma Risk Group Staging System (INRGSS).

1.2.6 Prognostic factors

Current prognostic factors used by the COG Neuroblastoma study group for patients stratification and assignment to protocol are: Age (<18 months *vs* >18 months), Stage (1, 2 and 4s *vs* 3, 4), ploidy (diploid *vs.* hyperploid), International Neuroblastoma Pathology Classification (Shimada System: Favourable *vs.* Unfavourable Histology; *see* Table 3), MYCN status (A *vs*. NA), 1pLOH (present *vs.* absent) and 11qLOH (present *vs.* absent), [Cohn et al., 2009, Shimada et al., 1999[a], Shimada et al., 1999[b]].

1.2.7 Current treatment strategies and outcomes

NBL is difficult to treat despite aggressive treatment modalities. Children with NBL and lack of MYCN amplification have a 93 % survival rate compared to the 10 % event-free survival (EFS) rate in children with MYCN amplification [Brodeur, 2003]. The majority of patients with NBL belong to the high-risk group and their treatment involves chemotherapy, aggressive surgical resection, myeloablative chemotherapy and autologous bone marrow transplantation

(ABMT), radiotherapy, immunotherapy and ^{131}I-MIBG infusion. As the survival rates remain poor, new approaches are needed.

1.3 Glycosaminoglycans (GAGs) and Heparan Sulfate (HS)

The complex interplay between cancer cells ("the seed") and growth factors are mediated in a dynamic three-dimensional extracellular matrix (ECM), ("the soil"), [Paget, 1889]. The ECM plays a crucial role in the tumour microenvironment (TME) that goes beyond the formation of a scaffold. The interaction between the tumour cells and their surroundings is a dynamic process that changes upon modification of the ECM. Several hallmarks of cancer, induction of angiogenesis, avoiding immune destruction and tumour promoting inflammation involve close interaction between malignant cells and the ECM [Hanahan and Weinberg, 2011]. Therefore, cancer biology can only be understood through a non-simplified approach that includes the study of the TME. Glycosaminoglycans (GAGs) are major components of the ECM and evidence supports their role in the progression, invasion and metastasis of tumours, especially in the case of heparan sulfates (HS) [Sasisekharan et al., 2002]. GAGs are long, unbranched polysaccharides units on the cell surface and extracellular matrix (ECM) attached to a core protein in the form of proteoglycans. They bind to many growth factors, ligands and cytokines. There are four major classes of GAGs, hyaluronic acid (HA), keratan sulfate (KA), chondroitin sulfate (CS) and heparan sulfate (HS).

HS is a linear anionic sulfated polysaccharide chain (measuring from ~5 to ~70 kDa) and composed of alternating monosaccharide units, N-acetylated

or N-sulfated glucosamine units (N-acetyl D-glucosamine, GlcNAc, or N-sulfo-D-glucosamine, GlcNS) and hexuronic acid (either D-glucuronic acid, GlcA, or L-iduronic acid, IdoA). There are 23 disaccharide units but not all are equally prevalent. HS has a domain structure, where long stretches of Glc-A-GlcNAc repeating units (NA domains) are intermixed with regions of higher sulfation (S domains) flanked by areas of intermediate levels of sulfation (NS domains) [Whitelock and Iozzo, 2005; Esko and Selleck, 2002]. The HS chain is then further modified, mainly in the N-sulfated regions, through C-5 epimerization of GlcA to IdoA, O- sulfation at C-3 and C-6 of GlcN and O-sulfation at C-2 of GlcA and IdoA [Casu et al., 2001]. There is also the recent suggestion by Rudd [Rudd et al., 2012] that the commonly occurring disaccharides can be explained by a branched biosynthetic structure in which the branch point corresponds to the modification of GlcA-GlcNAc to IdoA-GlcNAc, a relatively rare event or more commonly, GlcA-GlcNS to IdoA-GlcNS. These two events give rise to the two branches. All this gives HS a high structural diversity that is based on HS chain length, arrangement of structural features (N-, O- sulfation, N-acetylation, etc) and sulfation status. The blockbuster drug and anticoagulant heparin, another GAG family member, which contains the same disaccharide units and linkage type as HS, is considered to be more homogeneous and highly sulfated than HS [Gallagher and Walker, 1985]. On average, around 2.7 sulfate groups are present within the disaccharide units of heparin and 0.6-1 within HS [Hileman et al., 1998; Conrad 1998].

HS primarily controls cancer progression by regulating the interaction between cells and signalling molecules such as growth factors and cytokines.

FGF2-HS interactions are probably the best studies example. Binding of FG2 to its receptor causes phosphorylation of the receptor's tyrosine kinase domain and causes increased growth and migration in several cancers [Su et al., 2006; Plotnikov et al., 1999]. In order for FG2 to bind, the HS chain requires N-sulfated glucosamine units and 2-O-sulfated iduronic acid units [Guimond et al., 1993; Jia et al., 2009]. Alongside, for HS to bind to FGFR they require 6-O-sulfates glucosamine residues in addition to 2-O-sulfated iduronic acid and N-sulfated glucosamine residues [Guimond et al., 1993; Sugaya et al., 2008]. HS is also essential to other signalling pathways such as Wnt [Ai et al., 2003], VEGF [Narita et al., 2006; Makinen et al., 1999] and TGFbeta [Lyon et al., 1997] and FGF [Pantoliano et al., 1994; Kan et al., 1993; Yayon et al., 1991; Rapraeger et al., 1991]. Cancer cells have also inherently altered proteoglycan structures due to errors in the biosynthetic enzymes that regulate HS organisation. Despite the recently increased attention to the ECM, some of its components such as HS are still neglected. The expression profiles of the core proteins along with the side-chain modification enzymes (NDSTs, SULFs, etc) have not been fully determined in many cancers.

The 6-O-sulfation of HS has been shown to be important for binding and activation of many signalling molecule involved in cell proliferation, adhesion and migration [Ori et al., 2008]. These include FGFs such as FGF1, FGF4, FGF7 and FGF10 [Kreuger et al., 2001; Pye et al., 2000; Ashikari-Hada et al., 2004; Kreuger et al., 2005], HGF [Ashikari-Hada et al., 2004; Lyon et al., 1994], VEGF [Ono et al., 1999], PDGF [Feyzi et al., 1997], fibronectin [Mahalingam et

al., 2007] and chemokines. Furthermore, in the case of FGF2, although 6-O-sulfates are not necessary for binding, they are required for promoting the growth factor activity [Guimond et al., 1993; Ishihara et al., 1995]. The structural basis for this is that the 6-O-sulfates are required for interaction of HS with the FGF receptor [Pellegrini et al., 2000; Schlessinger et al., 2000], and the functional interaction involves a protein “canyon” involving both ligand and receptor molecules to create specific interactions with HS motifs [Mohammadi et al., 2005]. It is worth noting that effects of altered sulfation on HS interactions and functions may be due not only to lack of essential sulfate groups for direct interactions, but also on altered saccharide conformation, which can be induced by differences in sulfation patterns and therefore indirectly altering the binding characteristics for proteins [Rudd et al., 2007].

1.3.1 HS chain synthesis and its biosynthetic enzymes

The synthesis of HS is a non-template enzymatic driven multi-step process. The synthesis of HS chains is initiated in the endoplasmatic reticulum (ER) with the synthesis of the core protein and continued in the Golgi apparatus using sugars imported from the cytoplasma. The synthesis involves a series of biosynthetic enzymes that form a linear polymer of repeating disaccharide of hexuronic acid and glucosamine with different sulfations at various points. The HS biosynthetic pathway has 3 stages, 1) biosynthesis of a tetrasaccharide linkage region, 2) chain initiation/elongation, and 3) chain modification (Figure 1.1).

Stage 1: biosynthesis of the tetrasaccharide linker region of HS

This occurs in the lumen of the Golgi apparatus and involves the attachment of the tetrasaccharide linker region (four monosaccharides) to a serine within the conserved attachment site of the core protein.

Stage 2: chain initiation/elongation

After the tetrasaccharide linkage region is formed, other enzymes form the HS chain backbone (chain initiation and polymerization). A GlcNAc residue by N-acetyl-glucosaminyltransferase I (GlcNAcT-I) is added and the chain elongation proceeds by N-acetyl-glucosaminyltransferase II (GlcNAcT-II) and glucuronyltransferase II (GlcAT-II) activities that add (1,4) α D-GlcNAc and (1,4) βD-GlcA residues in alternating sequences to the polysaccharide chain [Lidholt et al., 1992]. The glycosyltransferases are encoded by the exostin (EXT) gene family [Takei et al., 2004]. The chain will now act as a substrate for modification by sulfotransferases in the HS biosynthesis.

Stage 3: Chain modification

After Stage 2 the HS backbone is composed of repeating disaccharide units of D-glucuronic acid and N-acetyl D-glucosamine $(GlcA\text{-}GlcNAc)_n$ that are unsulfated and not yet epimerized. The HS chain is then subject to further modifications by a series of enzymes: N-deactylase/N-sulfotransferase (NDST), C5 epimerase (C5-Epi), 2-O-sulfotransferase (2-OST), 6-O-sulfotransferase (6-OST) and 3-O-sulfotransferase (3-OST). These sulfotransferases are membrane bound and located in the Golgi. Three different 6-O-sulfotransferase (6-OSTs) have been cloned, seven 3-OSTs as well as four isoforms of the NDSTs [Aikawa and Esko, 1999; Esko and Lindahl 2001; Habuchi et al., 2000].

Only one C-5 epimerase and one 2-OST have been identified. The exact functionality of all the different enzymes and isoforms has not yet been identified.

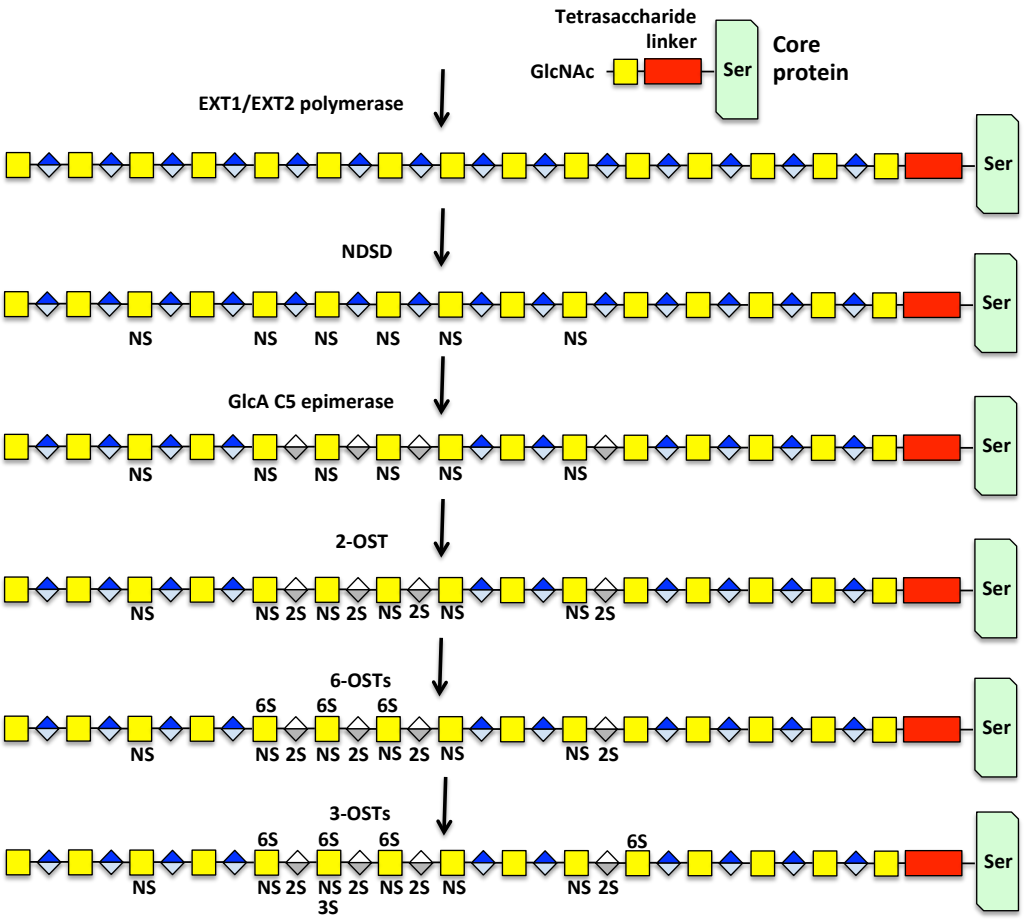

Figure 1.1 HS chain is biosynthesised on a core protein. Not all biosynthesis or modification steps occur in a linear sequence. Some modification steps depend on previous steps to occur first, whereas others are independent.

Full details and regulation of the biosynthetic pathways of the HS chain are not entirely known. Rudd et al. [Rudd et al., 2012] proposed a novel forked biosynthetic pathway for HS where all common HS disaccharides are synthesised through a common route, the major branch, giving rise to the

commonly occurring disaccharides GlcA-GlcNS and subsequent modifications by epimerase, 2-OST and 6-OST; and a minor branch starting from IdoA-GlcNAc, which contains the minor disaccharides.

N-deactylase/N-sulfotransferase

NDST is the first modification enzyme in the HS biosynthetic pathway. The actions of NDST are believed to determine the subsequent modifications, especially epimerization, 2-O- and 3-O-sulfation. NDST is a dual function enzyme. N-deacetylase activity removes the acetyl group from the GlcNAc residue to a $GlcNH_2$ residue; N-sulfotransferase activity transfers a sulfo group to the primary amine group to form a GlcNS residue. Four isoforms of NDST have been identified in the human genome [Aikawa and Esko, 1999]. It is believed that the different isoforms have different substrate specificities, and knockout experiments in mice have begun to distinguish their *in vivo* functions. NDST1 is the most expressed isoform. Conditional knockout of NDST1 showed several physiological roles, including the development of mammary gland [Crawford et al., 2010], neutrophil trafficking [Wang et al., 2005] and inhibition of tumour angiogenesis [Fuster et al., 2007]. The absence of NDST1 caused respiratory distress and neonatal death [Fan et al., 2000]. These were attributed to the changes in O-sulfations and epimerisation of HS. NDST2 knockout mice were viable but had abnormal connective tissue mast cells [Forsberg et al., 1999]. NDST1 and NDST2 were found to be up-regulated in hepatocellular cancer [Tátrai et al. 2010]. NDST3 knock out mice are also fertile with subtle haematological and behavioural changes [Pallerla et al., 2008]. The NDST4

gene has been reported to be a tumour suppressor gene in human colorectal cancer [Tzeng et al., 2013]. The difficulty in analysing these enzymes is that the expression of the NDST isoforms may be both translationally and post-translationally regulated [Grobe and Esko, 2002].

6-O-sulfotransferases

There are three members of the HS 6-OST family. Isoform 1 is strongly expressed in liver, 6-OST2 mainly in spleen and brain, and 6-OST3 is expressed throughout the body in most mouse tissues [Habuchi et al., 2000]. HS 6OSTs catalyze the transfer of a sulfo group to the C6 position of glucosamine residue (GlcN) to form 6-O-sulfo glucosamine. 6-O-sulfation occurs predominantly at the GlcNS residue, generating a GlcNS6S moiety. However, in some cases, it can also occur at the GlcNAc residue, generating a GlcNAc6S moiety; 6-O-sulfation is the only type of sulfation that occurs at the GlcNAc residue. Three isoforms of 6OST have been identified with many similarities. The 6-O-sulfation by 6OST1 predominantly occurs at the GlcNS residues, while other 6OST isoforms can modify GlcNAc to yield GlcNAc6S. Furthermore, 6OST1 prefers the IdoA-GlcNS over GlcAGlcNS while 6OST2 favours GlcA-GlcNS more than IdoA-GlcNS. 6OST3 acts equally on both disaccharide structures. 6OST2 has two transcript variants encoding different isoforms [Habuchi et al., 2003]. 6OST1 null mice had growth retardation, abnormal lung and eye development, and impaired placental function and did not survive long after birth [Irie et al., 2002]. 6OST1 and 6OST2 were described as being overexpressed in ovarian cancer and human colorectal cancer

[Backen et al., 2007; Raman et al., 2010]. 6OST1 was reported to be up-regulated in hepatocellular cancer [Tátrai et al., 2010]. The enzyme 6OST1-3 was down-regulated, in glioblastoma [Wade et al., 2013].

2-O-sulfotransferase

2OST transfers a sulfo group to the 2-OH position of IdoA or GlcA (with a preference for IdoA) within HS and is the only sulfation that occurs on the uronic acid units. [Kobayashi et al., 1997]. 2OST is also the only HS sulfotransferase that exists as a single isoform. Bullock *et al* described renal agenesis, eye and skeletal defects in 2OST-null mice, which die soon after birth [Bullock et al., 1998]. This enzyme may have a preference for IdoA-GlcNS over IdoA-GlcNAc substrates, notably just after the proposed "branch" in the pathway [Rudd et al., 2012]. A report in the literature shows that this enzymes is over-expressed in prostate cancer cell lines and tissue, where its expression correlates with increasing metastatic potential [Ferguson and Datta, 2011].

3-O-sulfotransferase

The last family of enzymes that are involved in the HS modification are the 3-O-sulfotransferase with seven different isoforms [Shworak et al., 1997; Shworak et al., 1999; Mochizuki et al., 2003]. The 3-OSTs catalyze sulfuryl transfer to the 3-hydroxyl position of various glucosamine residues. 3-O sulfation of glucosamine residues of HS occurs with low frequency. Alterations of these enzymes have been reported in various tumours. Methylation-associated silencing of the isoform 3-OST2 was found in primary human breast, colon, lung

and pancreatic cancer [Miyamoto et al., 2003] and in malignant melanoma [Furuta et al., 2004]. Furthermore, down regulation of isoforms 3-OST4, 3-OST5 and 3-OST6 have been reported in invasive breast ductal carcinoma [Fernandez-Vega et al., 2013].

1.3.2 Remodelling of HS chain and Sulfotransferases (SULFs)

The synthesized HS chain is released from the cell in proteoglycan form and located on the cell surface or in the ECM [Iozzo, 2005]. HSPGs on the cell surface can either be shed by cleavage of the core protein or by cleavage of the HS chain by extracellular heparanase. Bound ligands can so be released to diffuse away from the cell. Until recently it has been thought that no further modification of HS occurs but, the discovery of a novel class of enzymes that edit the 6-O sulfation status, has altered that view [Dhoot et al., 2001; Morimoto-Tomita et al., 2002]. In fact, additional control of the HS structure takes place at the cell surface, where degrading enzymes modify post-synthetically the HS chain.

The sulfatase enzymes SULF1 and SULF2 change the sulfation status of HSPGs outside the cell. SULF1 was identified for the first time in quail embryos in [Dhoot et al., 2001], SULF2 was cloned later from mouse and human [Morimoto-Tomita et al., 2002]. The substrate specificity of the SULFs is unclear. However, they remove the 6-O sulfate groups from HS (GlcNS) with preference for the 6-O sulfate present on trisulfated disaccharides (IdoA2S-GlcNS6S) within S-domains of HS and to a lesser extent on disulfated disaccharides (UA-GlcNS6S) [Ai et al., 2003; Lamanna et al., 2008]. No effect

on other 6-O sulfate disaccharides was observed, implying a requirement for N-sulfate groups. However, it is still unclear if SULF2 has substrate specificity for other disaccharide motifs in HS. No effects on other 6-O sulfated disaccharide were observed. Studying knock-out mice gave some information; single SULF1 or SULF2 knock out mice had normal viability and no phenotypical and histological changes, suggesting an overlapping function of the two enzymes. However, double SULF1/2 knock-out mice had several congenital abnormalities and a higher neonatal mortality rate [Lamanna et al., 2006; Lamanna et al., 2008; Ai et al., 2007; Holst et al., 2007].

Both SULFs are very similar in structural organisation but divergent in sequence identity and their biochemical activities are still controversial. SULFs differ from other sulfatase enzymes, as they are extracellular endosulfatase (intra-chain) enzymes that act at neutral pH. This differs from lysosomal sulfatases, which are active in an acid environment and remove sulfate esters from the termini of chains [Morimoto-Tomita et al., 2002; Rosen and Lemjabbar-Alaoui, 2010].

SULFs are large proteins of approximately 870 amino acids (aa) with a unique structural organisation consisting of four domains: a cleavable signal peptide, a catalytic domain (CAT), a central hydrophilic domain (HD) and a C-terminal region (C-ter) [Morimoto-Tomita et al., 2002; Tang and Rosen, 2009]. The signal peptide and two sulfatase-related domains (approx. 374 aa and 118 aa) are separated by a hydrophilic domain (HD) of approx. 350 aa. SULFs are formed as pre-proteins (125 kDa). The pro-protein is cleaved within the hydrophilic domain by a furin-type proteinase resulting in 75 kDa and 50 kDa

fragments [Uchimura et al., 2006], which are then joined by disulfide bonds (Figure 1.2). It has been shown that this cleavage is essential for activation of SULF2 [Nagamine et al., 2010]. Blocking the furin cleavage had little or no effects on the secretion of the SULFs and enzymatic activity. However the localisation of the SULFs into the lipid rafts was reduced when furin-type cleavage was prevented [Tang and Rosen, 2009]. An altered localisation of the SULFs in the lipid rafts could be responsible for optimal signalling and possible non-enzymatic functions of the SULFs. The exact functions of the furin-type cleavage of the SULFs are unknown. CAT domain is highly homologous to the conserved catalytic domains of all eukaryotic sulfatases. The CAT domain is located in the amino-terminal 75 kDa unit and contains a post-translational modification, an α-formylglycerin (FGy) residue resulting from oxidation of a conserved cysteine, which is essential for enzyme activity (critical cysteine residue “C”), [Dierks et al., 1997]. The HD domain is the unique feature of the SULFs, has no homology with any other protein sequences and is essential for recognition and endosulfatase activity on HS and for cell surface localisation of the SULFs. Mutated SULF enzymes with deleted HD domains have arylsulfatase activities, but lack endosulfatase activity against HSPGs [Tang and Rosen, 2009]. The C-ter domain has unknown function but, it has homology with the C-ter region of the lysosomalsulfatase. The C-ter 50 kDa subunit is required for both the arylsulfatase and the endosulafatse of the enzymes. SULF1 and SULF2 are highly homologous in all domains, consistent with their unclear functional differences. The SULFs and particularly SULF2 have been shown to regulate the interaction of many ligands with HS such as

VEGF, FGFs, TGF, SDF-1 (CXCL12), [Ori et al., 2008]. Through their ability to regulate the 6-O sulfation in the functional S-domains of HS, the SULFs can regulate ligand binding/activation, which can result in enhancement or repression of signalling. This depends on the isoform (SULF1 or SULF2) the protein ligands and the biological context. For example, quail SULF1 was initially identified for its ability to promote Wnt signalling because its action reduced its affinity for Wnt enabling the formation of a HS/Wnt/Frizzled functional complex [Ai et al., 2003]. Similar SULFs enhance BMP signalling by regulating its inhibitor Noggin [Otsuki et al., 2010; Viviano et al., 2004]; and GDNF during neuronal development [Ai et al., 2007]. In contrast SULFs down regulate FGF1, VEGF, TGFβ [Ashikari-Hada et al., 2004; Ori et al., 2008]. Additionally, SULF1 has been shown to either enhance or repress sonic hedgehog (Shh) during neuronal development [Danesin et al., 2006]. SULFs are well expressed in embryonic tissues [Danesin et al., 2006; Dhoot et al., 2001]. In zebrafish both SULFs were broadly expressed in various tissues, whereas SULF2 expression was entirely restricted to the CNS [Gorsi et al., 2010]. During embryogenesis, SULFs also promote oesophageal innervation, bone skeletal system [Ai et al, 2007; Holst et al., 2007; Lamanna et al., 2006]. In the mouse embryo at E14.5 and E16.5, SULF1 and SULF2 were expressed in many embryonic tissues, including the floor plate of the neuronal tube, bone, cartilage, skeletal muscle and lung [Ai et al., 2007]. Interestingly, SULF1 and SULF2 were reported to be essential for neuronal crest migration *in vivo* in *Xenopus tropicalis* [Guiral et al., 2010].

However, the distinct roles of the two isoforms SULF1 and SULF2 are not well

understood. First, one of the enzyme could be more labile than the other resulting in low steady stale levels in some organs/tissues. Second, the activity of one of the SULFs could be inhibited by unknown factor(s). Third, one of the enzymes could be more diffusible and thus able to desulfate more HS in some particular environments; fourth, SULF1 and SULF2 could undergo different protein cleavage *in vivo* [Tang and Rosen, 2009]. Fifth, native HS may have distinct structures that are more susceptible to desulfation by either SULF1 or SULF2.

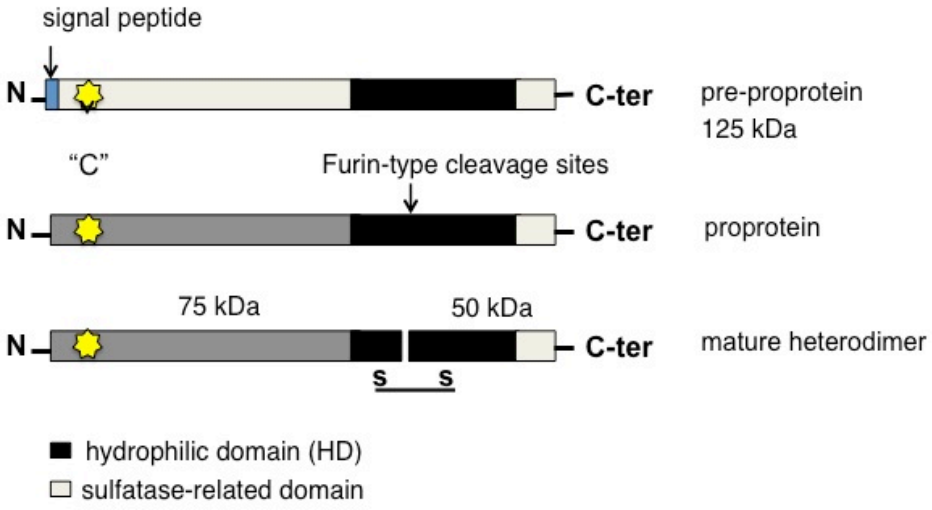

Figure 1.2 SULF synthesis as a pre-protein. The yellow star indicates the conserved sulfatase-specific cysteine residue necessary for enzyme activity.

1.3.3 SULFs in cancer

Increasing evidence indicates an important role for the SULFs in cancer [Bret et al., 2011; Rosen and Lemjabbar-Alaoui, 2010]. Elevated SULF2 levels have been correlated to aggressive hepatocellular cancer (HCC) [Yang et al., 2011], pancreatic cancer [Rosen and Lemjabbar-Alaoui, 2010], head and neck squamous cell carcinoma [Bret et al., 2011], gastric cancer [Hur et al., 2012],

non-small-cell lung carcinoma (NSCLC) [Lemjabbar-Alaoui et al., 2010], oesophageal cancer [Lui et al., 2012], glioblastoma multiforme [Phillips et al., 2012]. Overall, it was shown that an overexpression of SULF1 reduces the growth of cancer cell lines [Lai et al., 2003]. Low SULF1 expression levels were found in hepatocellular carcinoma (HCC), specific types of breast cancer, kidney, gastric and bladder cancers [Lai et al., 2003; Lai et al., 2004; Rosen and Lemjabbar-Alaoui, 2010]. Some reports showed an overexpression of SULF1 in gastric, pancreatic, brain, oesophageal and lung carcinoma [Bret et al., 2011; Nawroth et al., 2007; Lui et al., 2012; Rosen and Lemjabbar-Alaoui, 2010]. SULF2 has been shown to reverse ligand interactions with heparin causing their release. It is this mechanism that allows cells that secrete SULF to communicate with their tumour microenvironment by releasing sequestrated growth factors that can then act back to the cell. By this action they can activate multiple key signalling pathways (e.g., Wnt, Shh and PDGF). SULFs seem to have overlapping function in development where, despite their role in regulating many signalling pathways, they do not seem to be obligatory. In cancer the SULFs seem to be a driver of carcinogenesis. Such examples are given by FGF-2 dependent proliferation of tumours [Turner et al., 2010]. HS reduces the binding of GDNF to HS allowing the interaction with its receptor to produce GDNF signalling [Davies et al., 2003]. Recently, SULF2 was identified as a transcriptional target of the tumour suppressor p54 [Chau et al., 2009].

Of the two isoforms, SULF2 has been shown to be a more attractive therapeutic target for cancer due to its overexpression in several tumours [Rosen and Lemjabbar-Alaoui, 2010; 2010; Bret et al., 2011; Lui et al., 2012]. SULF2

antagonists may be particularly valuable in ligand-dependent tumours. SULF2 is an extracellular enzyme where it can be easily targeted by low molecular weight compounds, making it a druggable target. SULF2 as targets for anticancer therapies are discussed in Chapter 6.

1.4 The MYCN oncogene

MYCN is member of the MYC family and is a DNA binding helix-loop-helix/leucin zipper protein that forms an obligate heterodimer with the partner protein MAX [Wenzel et al., 1991]. MYCN and MAX contain DNA binding motifs and the active protein initiates transcription when bound to its DNA binding sires of which the E-box motif is the most frequent [Thomas et al., 2004]. The exact mechanism that MCYN uses to mediate its oncogenic effects is not exactly known. It is known that MYCN amplification increases cell proliferation by shortening the time used to progress through the cell cycle [Dang, 2012]. MYCN is also known to increase the susceptibility of cells entering apoptosis after cell stress such as DNA damage and hypoxia and to increase genomic instability [Leder et al., 1986]. MYCN establishes a delicate balance between pro- and anti-apoptotic molecules that might be easily perturbed by various insults [Leder et al., 1986]. The guardian of the genome p53 has been reported to be a direct transcriptional target of MYCN [Carr-Wilkinson et al., 2011]. MYCN is also a transcriptional activator of MDM2, which is a negative regulator of p53 [Slack and Shohet, 2005]. Deregulated expression of MYCN can also be present without MYCN amplification, as MYCN is downstream of other oncogenic signal transduction pathways [Valentijn et al., 2012]. The apoptosis-

sensitive phenotype induced by MYCN via the MDM2-p53 pathway is relatively rare in NBL as p53 is rarely mutated [Keshelava et al., 2001; Moll et al., 1995]. The mechanisms by which MYC family members induce apoptosis are not fully understood. It is known that MYCN overexpression induces apoptosis in cells from the nervous system but not so frequently in NBL cells [Lutz et al., 1998]. Knocking MYCN out in MYCN-addicted tumours represents a very effective therapeutic strategy [Puissant et al., 2013]. MYCN induced SULF2 transcription may be another important mechanism by which MYCN sensitises cells to proliferation or apoptosis.

1.4.1 MYCN in development and neuroblastoma

MYCN is a strong oncogene that is naturally expressed only in embryonic life particularly neural tissue [Schwab, 2004]. During development MYCN is expressed at gastrulation and other early stages of embryogenesis before neurulation and somitogenesis [Moodley et al., 2013]. During later stages of development MYCN expression becomes limited to the peripheral and central nervous system and structures derived from the neuronal crest. Mice with a deletion of MYCN have a reduced number of mature neurons in the sympathetic ganglia during embryonic development [Soucek et al., 2008; Arvanitis and Felsher, 2006]. MYCN is responsible for tumour progression and expansion and induces genomic instability in cell culture [Whitfield and Soucek, 2012].

MYCN was one of the first genetic defects identified in NBL and high levels and/or amplification are associated with aggressive tumour phenotype and poor

survival [Slamon et al., 1986]. MYCN is the strongest indicator for aggressive tumour progression and is observed in 15 to 20 % of all NBL tumours with amplification, meaning an increase of the gene copy number. MYCN has recently also been identified in adult tumours such as, retinoblastoma, prostate cancer and triple-negative breast cancer [Dang, 2012; Gurel et al., 2008; Palaskas et al., 2011]. MYCN amplification refers to the increased number of copies of the gene within a cell. MYCN amplified (A) NBL cells usually have between 50 to 100 extra copies of the gene, DNA amplicons are identified by fluorescence in-situ hybridisation (FISH) analysis.

1.4.2 MYCN therapeutic targets

MYCN has long been regarded as an undruggable target. Normal proliferating cells also use MYCN for renewal. Several strategies aimed to interrupt the MYCN-MAX dimerization [Clausen et al., 2010; Follis et al., 2008; Brockmann et al., 2013; Park et al., 2004], to inhibit MYCN-MAX DNA binding and to interfere with key MYCN target genes such as repression of miR-26a have been proposed [Kota et al., 2009]. Interestingly, recent reports showed that an inhibitor of the BET bromodomain inhibited MYCN and impaired growth and inducted apoptosis in NBL [Puissant et al., 2013].

1.5 Research Objectives

The main hypothesis of this study is that HSPGs and their sulfation status are involved in the regulation of NBL cell survival. Identifying alterations in HSPG

structure “signatures” and their effects on tumour behaviour represents a therapeutically relevant goal, with potential impact in the clinic.

The objectives of this study are to:

1. Examine the expression of HS and its biosynthetic enzymes in different NBL cell lines. Work under this aim will help to establish the relevance of different populations of NBL tumour cells and their HS profile, and may lead to a novel marker/s.
2. To validate the findings in primary human NBL tissue and identify any correlation to clinical outcome and behaviour. Work with this aim is concerned with extending the observation from the *in-vitro* to the human *in-vivo* situation.
3. Investigate the effects of the alteration of HS sulfation on the activity of NBL cell lines *in vitro* by knock-down and over-expression techniques. Work with this aim will highlight the importance such HS changes in NBL cell survival and introduce the possibility of new therapeutic targets.
4. To identify any possible association between HSPGs profile and a clinically relevant marker of poor outcome, such MYCN amplification. Work with this aim may lead to the development of a clinical relevant link between sulfation status and outcome.

1.6 Thesis overview

This thesis will explore the role of HS and its sulfation status in NBL. It provides the first report of the implications of Sulfotransferase 2 (SULF2) levels in NBL cell survival and a link to the proto-oncogene MYCN, a marker of poor outcome.

The subsequent Chapters of this thesis will deal with each of the Specific objectives as follows:

Chapter 1 provides an introduction to the research work presented in this thesis. It describes the research background and objectives.

Chapter 2 will describe the materials and methodologies used.

Chapter 3 will focus on the expression of HS biosynthetic enzymes in a series of NBL and other cancer cell lines. A candidate enzyme amongst several biosynthetic and modification enzymes that modify the HS chain (SULF2) is identified in NBL cell lines with amplification of the MYCN oncogene (MYCN-A).

Chapter 4 analyses the effects of SULF2 alteration on modulating the biological behaviours of NBL cells such as cell proliferation and survival. Reduction of SULF2 expression in NBL cells was demonstrated to significantly reduce the proliferation of MYCN-A NBL cells and increase apoptosis. SULF2 was shown to be a down-stream target of MYCN by demonstrating that over-expression of MYCN in NBL cell lines increases SULF2 expression and *vice versa* (Knockdown of MYCN reduced the expression of SULF2). The importance of SULF2 in neuroblastoma survival was then demonstrated independently of MYCN by over-expressing SULF2 in MYCN-NA NBL cells resulting in an increase in cell viability without increasing MYCN expression.

Chapter 5 describes the expression of SULF2 in in a large panel of primary human NBL tumour tissue with and without MYCN-A. Additional data from a large cohort of human tumours confirms the gene expression of SULF2 in high-risk patients with MYCN amplified NBL. Here we also show the effects of SULF2 knockdown in a mouse model on NBL.

Chapter 6 will include a general discussion of the thesis results, present suggestions for future directions and work, with particular reference to translational applications.

Chapter 2: Material and Methods

2.1 Cell lines and cell cultures

Eight human NBL cell lines with and without MYCN amplification and other human cell lines were grown under established conditions at 37 °C in a humidified incubator containing 95 % air and 5 % CO_2 atmosphere. Human NBL cell lines CHLA-255, CHLA-255-MYCN, CHLA-90, CHLA-16, SMS-SAN and SK-N-RA were cultured in complete medium consisting of Iscove's modified Dulbecco's medium (IMDM) supplemented with 20 % FCS, 2 mM L-glutamine and penicillin (100 U/ml) and streptomycin (100 μg/ml), (pen/strep). Cell lines NB-19, SK-N-BE2, A549, HT-1080, SHEP, SHEP-2, SHEP-21N, HT-1080 and HBMEC were grown in RPMI-1640 (Mediatech) supplemented with 10 % (vol/vol) FCS with penicillin-streptomycin (pen-strep; Invitrogen). Cell line SK-NSH, HeLa, C8161 and fibroblasts, were grown in DMEM with 10 % FCS and penicillin-streptomycin. The cell lines used are shown in Table 2.1.

To facilitate mycoplasma detection (MycoAlertMycopplasma Detection Kit; Lonza, #LT 07-418) cells were grown without antibiotics for at least 2 passages, for which all of the cells tested negative. Cell lines' identity was confirmed by genotype analysis using AmpFISTR Identifier kit PCR Reagents and Gene Mapper ID v3.2 (Applied Biosystems).

Cell line	Type	MYCN	Stage	Age	Therapy	Tissue source	References
CHLA-255	Neuroblastoma	NA	4	–	PD + 13-cis	Brain	Keshelava et al., 1998
CHLA-255-MYCN	Neuroblastoma transfected	A*	–	–	–	–	Song et al., 2007
CHLA-90	Neuroblastoma	NA	4	102 m	PD-BMT	Bone marrow	Keshelava et al., 2001
SK-N-SH	Neuroblastoma	NA	4	48 m	PD	–	ATCC HTB-11
SHEP	Neuroblastoma subclone	NA	4		PD	Bone marrow	Biedler et al., 1978
SHEP-2N	Neuroblastoma transfected	NA	–	–	–	–	Lutz et al., 1996
SHEP-tet 21N	Neuroblastoma transfected	A*	–	–	–	–	Lutz et al., 1996
NB-19	Neuroblastoma	NA	4	12 m	PD	Bone marrow	Riken
CHLA-136	Neuroblastoma	A	4	36 m	PD-BMT	Bone marrow	Keshelava et al., 2001
SK-N-BE2	Neuroblastoma	A	4	24 m	PD	Bone marrow	ATCC CRL-227
SMS-SAN	Neuroblastoma	A	4	36 m	Dx	Bone marrow	Reynolds et al., 1986
SK-N-RA	Neuroblastoma	A	4	-	PD	Bone marrow	Keshelava et al., 1998

Cell line	Type	MYCN	Morphology	Age	Tissue source	References
HeLa	Adenocarcinoma	NA	epithelial	31 y	Cervix	ATCC CCL-2
A549	Lung squamous carcinoma	NA	epithelial	58 y	Lung	ATCC CCL-185
MG-63	Osteosarcoma	NA	fibroblast	14 y	Bone	ATCC CRL-1427
MDA-MB-231	Human Breast adenocarcinoma	NA	epithelial	51 y	Pleural effusion	ATCC HTB-26
HT-1080	Human Fibrosarcoma	NA	epithelial	35 y	Connective tissue	ATCC CCL-121
C8161	Human Melanoma	NA	epithelial	Middle age	Abdominal wall metastasis	Bregman and Meyskens, 1983
Fibroblast	Human foreskin	NA	fibroblast	Newborn	foreskin	ATCC CRL-2522
HBMEC	Brain endothelial	NA	endothelial	Unknown	Brian cortex	ScienCell Research Laboratories #1000
HEK 293T	Human embryonic kidney	NA	Epithelial	Fetus	Embryonic kidney	ATCC CRL-1573

Table 2.1 Cell lines and culture conditions used.

Dx (Diagnosis) = cell lines derived from samples of patients prior treatments
PD (Progressive disease) = cell lines derived from samples of patients who relapsed after chemotherapy
PD-BMT = cell lines derived from samples of patients who relapsed after chemotherapy and bone marrow transplant
13-cis = 13-cis-retinoic acid
m = months; y = years
NA = non-amplified; A = amplified

2.2 Real-Time Reverse transcription (RT)-PCR

RNA was isolated from lysed cells using aRNeasy® Mini kit (Qiagen, #74104) according to the manufacturer's protocol 'Purification of total cellular RNA'. The NanoDrop^{TM} ND-100 Spectrophotometer (Nano Drop Technologies, Inc., USA) was used to determine the concentration and to assess the quality of the RNA (absorbance ratio 260 nm : 280 nm between 1.9 and 2.1).

Total RNA (1μg) was reversed transcribed using Superscript III Reverse Transcriptase (Invitrogen, # 18020-051) according to the instructions provided by the manufacturer.

Gene expression of enzymes involved in the HS chain regulation was performed using LightCycler® 480 (Roche); [Table 2.2]. The expressions of RNA were measured against the housekeeping genes GAPDH and β-actin.

Abbreviation	Gene	Oligonucleotides	RefSeq No
2OST1 F	2-O-Sulfotransferase-1	TCTTGGAAAACCAGATCCAGA	NM_012262.3
2OST1 R		CTCGGACTTCGTGTCTTGC	
3OST1 F	3-O-Sulfotransferase-1	CCAGCCCAGGAGCCTATT	NM_005114
3OST1 R		CAGCAGGGAAGCCTCCTA	
3OST2 F	3-O-Sulfotransferase-2	GGATTCCCTTGCTTGAAAAA	NM_006043
3OST2 R		TTTTGATTTGCCCAAGCATC	
6OST1 F	6-O-Sulfotransferase-1	CTCTTCTCCCGCTTCTCCA	NM_004807
6OST1 R		CTCGTAGCAGGGTGATGTAGTAGA	
6OST2L F	6-O-Sulfotransferase-2 l	CAAAGACCCGGAACACATCT	NM_001077188
6OST2L R		CTCAAGTACCGGGACACTGG	
6OST2S F	6-O-Sulfotransferase-2 s	TGCGATCTTCTCCAAGATTTTC	NM_147175
6OST2S R		ACGATCACGGCAAATAGGAA	
6OST3 F	6-O-Sulfotransferase-3	TCTTCTCCCGCTTCTCCA	NM_153456
6OST3 R		CCCGTAACATTGTGATGTAATAGAA	
SULF1 v1 F	Sulfatase-1 variant 1	CGCTGCCACCTTATCTCTG	NM_001128205.1
SULFf1 v1 R		TGTTCAAGAGAAGTGAAGAATCCA	
SULF1 v2 F	Sulfatase-1 variant 1	CAGACAGCCTGTGAACAACC	NM_015170.2
SULF1 v2 R		ATTCGAAGCTTGCCAGATGT	
SULF2 v1 F	Sulfatase-2 variant 1	GTGACAGCGGGGACTACAAG	NM_018837
SULF2 v1 R		CGACTGCGGACATAGCTG	
SULF2 v2 F	Sulfatase-2 variant 1	CGAATCCCACATCTGTTTCA	NM_198596
SULF2 v2 R		CCCTCTTCACTCGCAGATTC	
NDST1 F	NDST1	CACAAAGGCATCGACTGGTA	NM_001543.4
NDST1 R		AGAAGTCGGAGGTGGTGTTG	
NDST2 F	NDST2	CAGGCCTGACGTCGAATC	NM_003635.2
NDST2 R		GTCAGCAAAGTTCAATCTCTTCC	
NDST3 F	NDST3	CACAGGGGGATTGATTGGTA	NM_004784.2
NDST3 R		CAAACAAAAAGTCGGTAGTGACA	
NDST4 F	NDST4	CTTGTCCCCAAAGCCAAG	NM_022569.1
NDST4 R		GGATCTTCATGTGATCGTTGG	
GAPDH F	GAPDH	AACGGGAAGCTTGTCATCAA	NM_002046
GAPDH R		TGGACTCCACGACGTACTCA	
Beta-actin F	Beta-actin	CCAACCGCGAGAAGATGA	X00351
Beta-actin R		CCAGAGGCGTACAGGGATAG	

Table 2.2 HS biosynthetic enzymes and their primers used for qRT-PCR. v = variant, L = long, S = short, F = forward, R + reverse.

2.3 Western Blotting

Adherent cells were harvested in Pierce IP Lysis Buffer with the addition of Halt Protease Inhibitor Cocktail (Thermo Scientific, #78430). Cell lysates were left on ice for 20 min then cleared by centrifugation at 12,000 g for 15 min at 4 °C. Protein concentration was measured by the bicinchonic acid (BCA) protein assay kit (Pierce BCA™ Protein Assay Kit; Pierce Biotechnology, #23225). After denaturation at 100 °C for 5 mins with a 2.5 % p-mercaptoethanol loading buffer, equal amounts of protein (40 μg/lane) were resolved by electrophoresis in a 10-20 % gradient acrylamide gel containing 0.1 % SDS (Bio-Rad Laboratories, #456-1084). Gels were transferred to protein nitrocellulose membranes (Bio-RadLaboratories, #162-0115) by semi-dry blotting. Membranes were blocked by Odyssey® Blocking buffer (LI-COR Biosciences, #927-40000) for 1 h at room temperature and then incubated overnight at 4°C with the primary antibody diluted in Odyssey Blocking Buffer with 0.1 % (v/v) Tween-20. Membranes were washed and then probed for 1 h at room temperature with an anti-mouse IgGIRdye 680 (LI-COR, #926-32220) and/or an anti-rabbit IgGIRdye 800 (Li-Cor #926-32211) as secondary antibodies at a dilution of 1:5000.

2.4 Immunocytochemistry and confocal microscopy

Cells were seeded (5 x 10^4 /mL) into 24-well plates on round glass coverslips and grown for 12-24 h then rinsed with PBS and fixed with 4 % (w/v) paraformaldehyde for 10 min at room temperature. After washing, non-specific binding was blocked with 10 % (v/v) normal goat serum for 1 h at room temperature. Cells were incubated overnight at 4 °C with the primary antibody

diluted in PBS with 1% (v/v) normal goat serum. Phage-display antibodies against HS (HS3B7V, HS4E4V, HS3A8V and RB4CD12) were supplied by Professor T. van Kuppevelt (Nijmegen, The Netherlands). Cells were rinsed with PBS and a rabbit polyclonal VSV-G tag antibody (Abcam, #ab1874) was applied (1:200 dilution v/v) for 1 h at room temperature. AlexaFluor®-488 goat anti-rabbit IgG (H+L) and AlexaFluor®-594 goat anti-mouse IgG (H+L) conjugated secondary antibodies (Life Technologies, #A-11012 and A-11001; respectively) were used at a concentration of 2 μg/ml in PBS with 1 % (v/v) normal goat serum for 1 h. Hoechst 33342 was used as a nuclear counterstain (1 μg/ml; Life Technologies, #H3570). Cells were mounted with ProLong (Life Technologies, #P36930). When double staining for SULF2 and HS with the phage display antibodies was performed, both primary antibodies were incubated together followed by VSV-G tag antibody incubation and finally by the secondary fluorescent conjugated Alexafluor antibodies. Controls included the omission of either the primary antibody or the VSV-tag (phage display antibodies) or pretreatment with 2.5 mU of heparinase I (from *Flavobacterium heparinum*, EC 4.2.2.2.7), heparinase II (from *Flavobacterium heparinum*, no EC number) and heparitinase (from *Flavobacterium heparinum,EC* 4.2.2.2.8), (IBEX Technologies, Montreal, Canada). Fluorescence and differential interference contrast (DIC) images were captured using LSM 710 confocal microscope with a 63 x 1.4 Plan-APOCHROMAT oil-immersion objective lens (Carl Zeiss Microscopy, Thornwood NY, USA).

2.5 Immunohistochemistry of primary NBL tumours

Archival formalin fixed paraffin-embedded (FFPE) tissue sections of human primary NBL were obtained from the Children's Oncology Group (COG) Neuroblastoma Biology Study with the approval of the CHLA Institutional Review Board. Samples were obtained without patient identification.

Tissue section (5 µm) were deparaffinised, rehydrated and subjected to heat-induced epitope retrieval with citrate buffer pH 6.0 using a microwave. Endogenous peroxidase was blocked with Bloxall (Vector Laboratories, #SP6000). Sections were stained using the Universal Staining Kit (Vector Laboratories, #PK-6100). The primary antibody against SULF2 (Novus Biologicals; same as used in Western Blot) was used at dilution 1:250 and incubated overnight at 4 °C. Antibody binding was visualised by 3,3'-Diamonobenzidine (DAB), (Vector Laboratories, #SK-4100) and cell nuclei counterstained with Mayer's haematoxylin. Negative control included the omission of the primary antibody.

Samples were also classified for the following parameters, age at diagnosis, clinical stage, MYCN status, mitosis-karhyorrhexis index (MKI), DNA index, degree of neuroblastic differentiation and favourable vs. unfavourable histology group according to the international Neuroblastoma Pathology Classification [Shimada et al., 1984; Shimada et al., 1999] and overall and event-free survival (EFS). Unfavourable histology (UH) tumours were either MYCN amplified (A) or MYCN non-amplified (NA) whereas all tumours with favourable histology (FH) were MYCN NA amplified.

2.5.1 Microscopic evaluation of Sulf2 in primary NBL tissue

Light microscope (Zeiss Axioplan) was used to take images (objective lenses magnification of 4 x, 10 x and 20 x and 63 x). Brown DAB reaction was considered positive for SULF2. A minimum of ten representative fields from each tissue section (central and peripheral tumour area) were photographed digitally using a Zeiss AxioObserver.Z1 microscope equipped with 20 x0.8 and 63 x1.4 Plan-APOCHROMAT objective lenses and an AxioCam MR colour CCD camera (Carl Zeiss Microscopy). Files were saved in TIFF format (1600 x 1200 pixels).

2.5.2 Digital Image Analysis

DAB staining in the 20x digital images was quantified using Fiji ImageJ software [Schindelin et al., 2012] in the following manner. Brown DAB and blue hematoxylin staining were separated into different images with the Color Deconvolution function using the H DAB matrix. The DAB image was then thresholded at 0-100 to include only the darkest pixels; staining lighter than 100 intensity units was considered non-specific background and disregarded in the quantitation. The integrated density (ID) and area (A) of thresholded pixels were quantified and optical density (OD) was calculated with the formula OD = log [IDmax÷ (ID + IDmax – 255 × A)], where IDmax = 255 × 1388 ×1040, the maximum possible ID for an 8-bit image of 1388 × 1040 pixels. The samples were also classified for MYCN amplification and risk (high vs. low), according to the International Neuroblastoma Pathology Classification [Shimada et al., 1999].

2.5.3 Statistical Calculation of Required Tissue Samples and Analysis

Preliminary data indicated that the estimated within group standard deviation of $\log_{10}$OD values for SULF2 expression by IHC is 0.138. (The $\log_{10}$ scale is used to stabilize the variance) The average difference observed between these three groups in preliminary analyses was 0.24 on the $\log_{10}$ scale. This corresponds to just under a halving or doubling of geometric mean OD between any two groups, and is a reasonable benchmark for sample size computation. Based on a one-way, three group (A-UH, NA-UH, NA-FH) ANOVA with 10 samples per group, and with Type I error of 5 %, there will be at least 90 % power to detect a maximum difference of 0.24 between and two groups. Other analyses in the one-way or two-way ANOVA setting of SULF2 expression by disease stage, age, metastatic disease, and other features of the tumour or patient will have similar power provided that there is reasonable balance among subgroups. For example, a comparison two groups (e.g., metastatic *vs.* non-metastatic disease) with a sample allocation of 1:3 will have at least 90% power to detect a 0.20 $\log_{10}$change in OD. Hence it was accepted that there would be sufficient power to detect plausible and potentially relevant differences in SULF2 expression. Slides were then requested from the COG Committee from 30 patients with NBL (10 for each group: A-UH, NA-UH and NA-FH).

2.6 Transfection of Neuroblastoma cells

Either small interfering RNA (siRNA) or short hairpin RNA (shRNA) was used to knockdown the expression of SULF2. For SULF2 over-expression the vector pcDNA3.1(-) was used.

2.6.1 Small interfering RNA (siRNA) of SULF2 in neuroblastoma cells

Cells were seeded in cell culture plate and grown overnight to obtain 60-70% confluence at the time of transfection. Transfections of siRNA were performed in OptiMEM medium in the presence of 7.5 µl Lipofectamine RNAiMAX (Invitrogen, #13778-075) and a final siRNA concentration of 10nM siRNA oligonucleotides (siRNA#1 *fwd* GGUGCUACAUCCUAGAGAA, siRNA#1 *rev* UUCUCUAGGAUGUAGCACC, siRNA#2 *fwd* GGACAACACGUACAUCGUA and siRNA#2 *rev* UACGAUGUACGUGUUGUCC) were obtained from Life Technologies (Silencer Select for SULF2, #4392420, s31805 and s31806 and negative control #AM4611).

2.6.2 SULF2 overexpression in neuroblastoma cells

Two human SULF2 overexpressing constructs, a full length SULF2 [Addgene, plasmid #13004: pcDNA3.1/Myc-His(-)-HSULF2] and a catalytically inactive SULF2 (S2ΔCC)form with a mutation that changed cysteine 88 to alanine [Addgene, plasmid #13006 pcDNA3.1/Myc-His(-)-HSULF2 deltaCC] were used. Plasmid DNA was extracted (Qiagen, Plasmid Maxi kit, #12162) and DNA subcloning was performed by restriction enzyme digest technique. Cutting was done at cloning sites with XhoI and HindIII. Digested DNA was run on a 0.8 % agarose gel and the insert and vector band was cut out of the gel and purified (Qiagen, QIAquick Gel Extraction Kit, #28704). Insert was ligated into the pcDNA3.1(-) vector (Invitrogen #V795-20) using T4 DNA ligase enzyme (New England Biolabs #) in a 1:3 vector : insert molar ratio. Subcloned DNA was transformed into chemically competent *E. coli* (Invitrogen, One Shot TOP10

Chemically Competent E. coli, #C4040-10). Reaction was plated on LB agarose plates with 100µg ampicillin followed by selection of single colonies. DNA was extracted (Qiagen, Plasmid Mini Kit, #12123) and analysed by sequencing using T7 primer (Genewiz, San Diego, USA). Cells were grown in antibiotic free IMDM medium for 24 hours prior to plasmid DNA transfection. Transfection was performed when cells were ~80 % confluent. For 6-well dishes plasmid DNA (2.5 µg) and Opti-MEM (250 µl) were mixed together and Lipofectamine 2000 (Invitrogen, #11668-019) (10 µl) and Opti-MEM (250 µl) were mixed together for 5 min at RT. The diluted plasmid DNA and the diluted Lipofectamine 2000 were mixed together for a further 10 min at RT to allow the formation of DNA-Lipofectamine complexes. Complexes were added to cultured cells, which were used in experiments following 48 h incubation. For control cells the equivalent amount of empty pcDNA3.1/(-) was added in place of plasmid DNA. Neomycin was used for selection.

2.6.3 SULF2 short-hairpin RNA (shRNA) construct and subcloning by restriction enzyme digest

When using shRNA to knockdown SULF2, we observed that within 7-10 days SULF2 positive cells outgrew the SULF2-knockdown cells (shown by a decreased ratio of EGFP-positive to total cells). This limited the time available for in-vivo experiments. To avoid this, we aimed to use a *tet* regulated vector to allow control of the gene expression of SULF2. For shRNA we used two previously publishes target regions of SULF2 GGAGTGGTGGTGTCAATAA (1143) and GCTGAAGCTGCATAAGTGC (1413) and AACAGTCGCGTTTGCGACTGG as a control (scramble) [Nawroth et al., 2007].

First, we used the pLVTHM empty backbone (Addgene plasmid#12247) (Figure 2.1) to insert the SULF2 oligonucleotides with the appropriate enzyme restriction site (iRNAi program for Mac, The Netherlands Cancer Institute, Amsterdam, The Netherlands), (Table 2.3). Second, the inserted sequences were then subcloned into a *tet*-inducible shRNA lentiviral vectors pLVCT-tTR-KRAB (Addgene plasmid #11643) containing a GFP reporter gene and *tet*-inducible H1 promoter (Figure 2.2).

Oligonucleotides were resuspended at a concentration of 2µg in a total volume of 50µl annealing buffer (10mN Tris, pH7.5, 50mM NaCl, 1m EDTA) and annealed in a PCR thermocycler (starting at 95°C for 2 minutes then gradually cooled to 25°C over 45 minutes). The empty vector was cut at the ClaI site and the annealed oligonucleotides were inserted by ligation (T4 ligase, #T0202; New England BioLabs Inc., USA) at an oligonucleotide to vector ratio of 3:1 (Figure 2.3). Reactions were then transformed in One Shot® TOP 10 chemically competent E. Coli cells (Invitrogen, #C4040-10), following the manufacture's instructions. The bacteria were then grown on LB agar plates containing 100 µg/mL ampicillin at 37°C overnight. Single colonies were isolated from stab cultures and grown in LB broth with 100 µg/mL ampicillin for ~16 hours in a 37°C shaking incubator. Stocks were made for long-term storage in 50 % (v/v) glycerol and kept at -80°C. Plasmid DNA was prepared using commercially available kits (Qiagen, Mini Prep Kit #27104 and/or EndoFree Plasmid Maxi Kit #12362). Plasmid deposition was verified by sequencing (GENEWIZ) using the human H1 promoter forward primer TCGCTATGTGTTCTGGGAAA and/or SP6 forward primers

ATTTAGGTGACACTATAG. PCR with H1 and SP6 was also employed to check the insert into the vector (Annealing Temp 50°C) and run on a 1 % (w/v) agarose gel. Additionally, DNA samples were sent for sequencing analysis using the H1 primer (GeneWiz, San Diego, CA; USA). Confirmed sequences were then used to subclone into the pLVCT-tTR-KRAB vector (Figure 2.3).

The empty pLVCT-tTR-KRAB vector and the pLVTHM vector with the inserted SULF2 sequences were digested with restrictions enzymes FspI (#R0135, New England BioLabs) and MscI (#R0534 New England BioLabs) following the manufacture's instructions and run on a 1 % (w/v) agarose gel (Figure 2.3). Desired bands of recipient plasmid and donor vector were cut and DNA recovered (QIAquick Gel Extraction Kit #28704; Qiagen). DNA ligation, transformation and colonies isolation were performed as above. Antarctic phosphatase (#M0289, New England BioLabs) was used after each ligation. The empty donor LVT-tTR-KRAB vector (after digestion with FspI and MscI and separated on agarose gel) that was without the AmpR-promoter region was used as a control on the LB plates (no growth). Sequencing (GeneWiz) was used to confirm accurate subcloning using the H1 primer.

SULF2 1143 S	5' – CGCATCGATCCCC**GCTGAAGCTGCATAAGTGC**TTCAAGAGA**GCACTTATGCAGCTTCAGC**TTTTTAATCGATCGC
SULF2-1143 AS	5'- GCGATCGATTAAAAA**GCTGAAGCTGCATAAGTGC**TCTCTTGAA**GCACTTATGCAGCTTCAGC**GGGGATCGATGCG
SULF2 1413 S	5'- CGCATCGATCCCC**GGAGTGGTGGTGTCAATAA**TTCAAGAGA**TTATTGACACCACCACTCC**TTTTTAATCGATCGC
SULF2 1413 AS	5' – GCGATCGATTAAAAAGGAGTGGTGGTGTCAATAATCTCTTGAATTATTGACACCACCACTCCGGGGATCGATGCG
SULF2 Scr S	5'-CGCATCGATCCCC**AACAGTCGCGTTTGCGACTGG**TTCAAGAGA**CCAGTCGCAAACGCGACTGTT**TTTTAATCGATCGC
SULF2 Scr AS	5'-GCGATCGATTAAAAAACAGTCGCGTTTGCGACTGGTCTCTTGAACCAGTCGCAAACGCGACTGTTGGGGATCGATGCG

Table 2.3 SULF2 shRNA oligonucleotides with restriction sites. ClaI restriction site are highlighted in red, vector loop is shown in blue. SULF2 sequences are in bold.

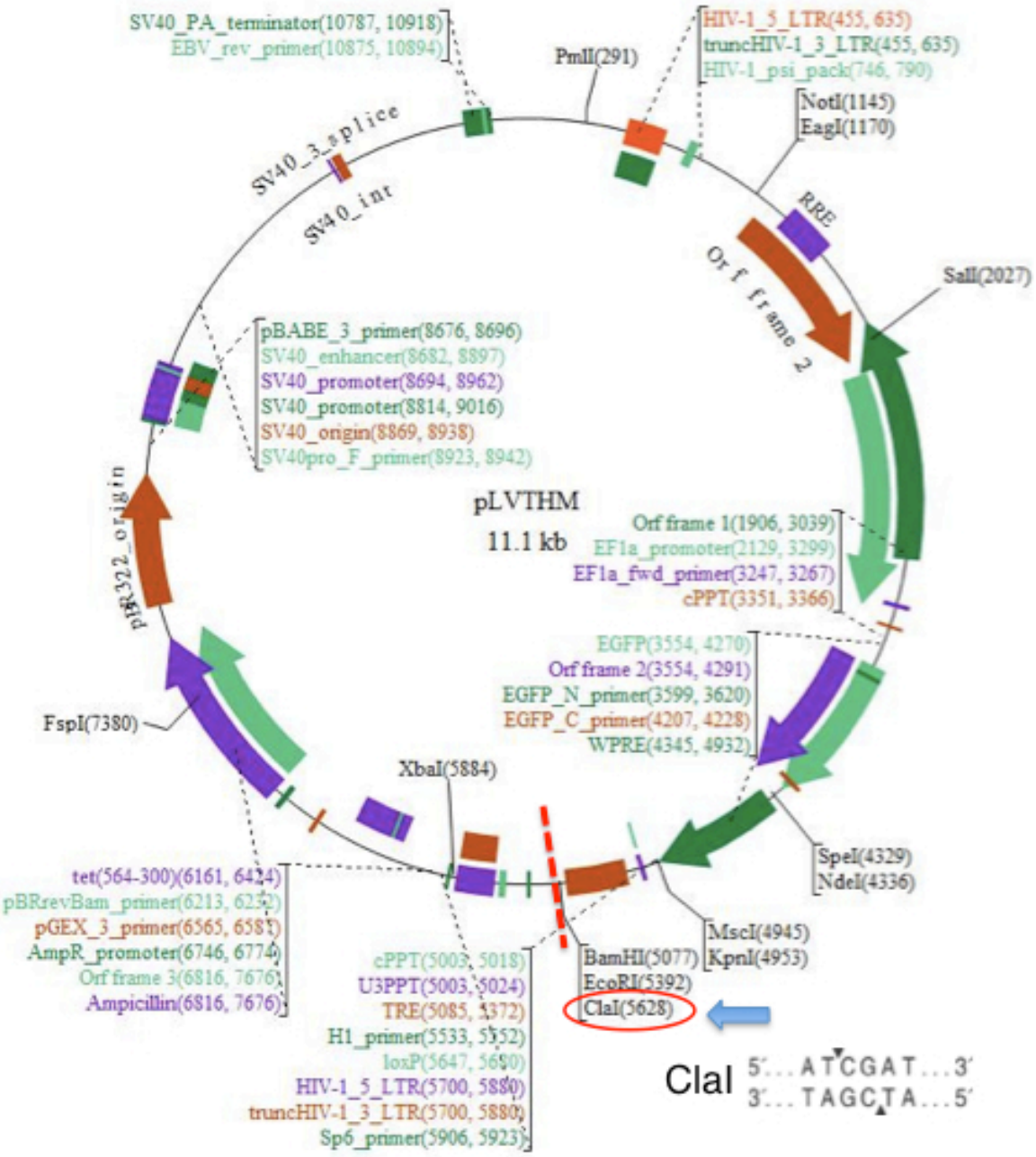

Figure 2.1 pLVTHM vector. The ClaI site (red dashed line) was used to insert the SULF2 oligonucleotides.

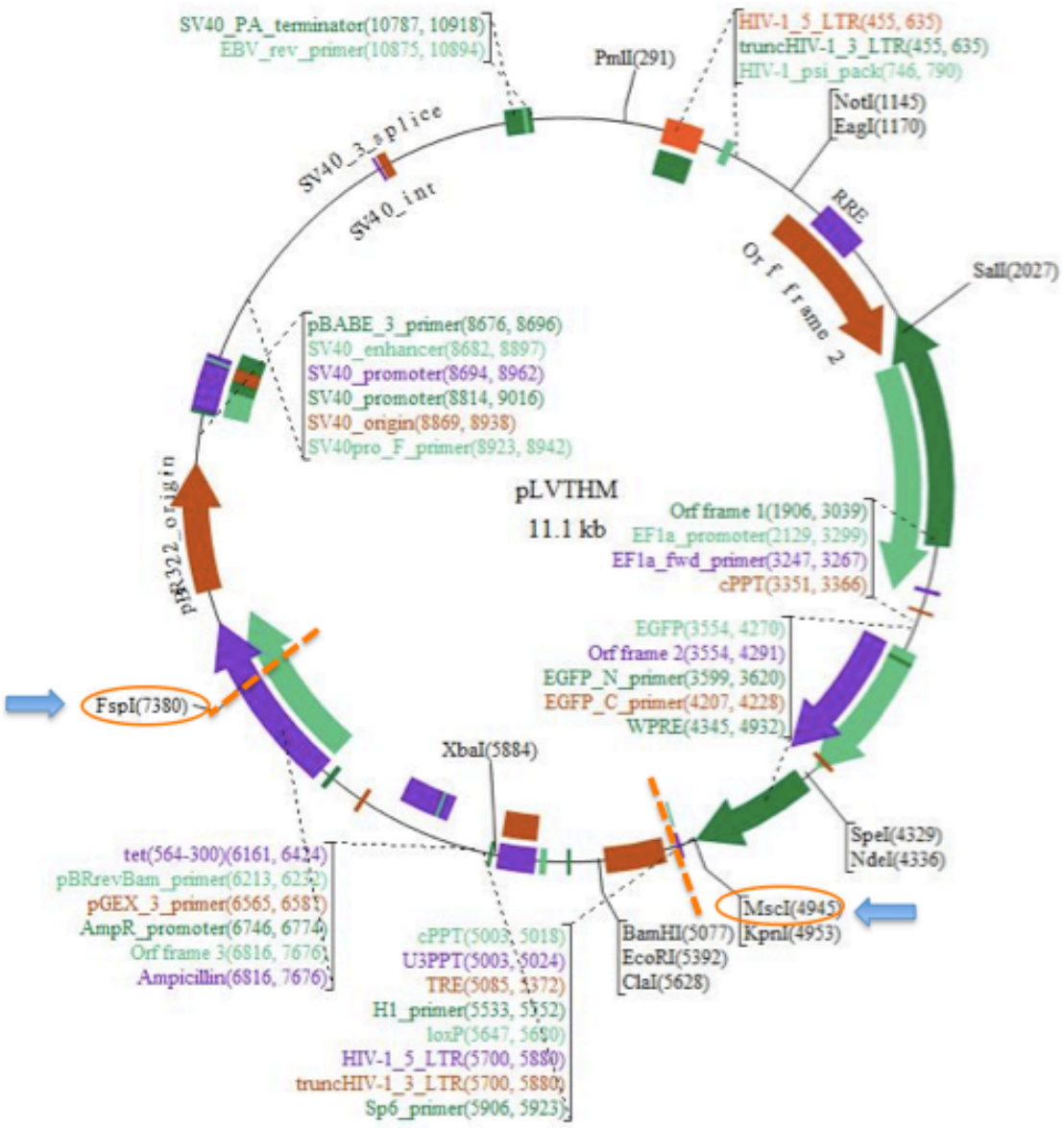

Figure 2.2 Subcloning from the pLVTHM vector by restriction enzyme digestion. The pLVTHM vector containing the SULF2 sequence inserted at ClaI site is cut out at FspI and MscI sites (orange dashed line) to allow ligation into the new vector (Figure 2.2).

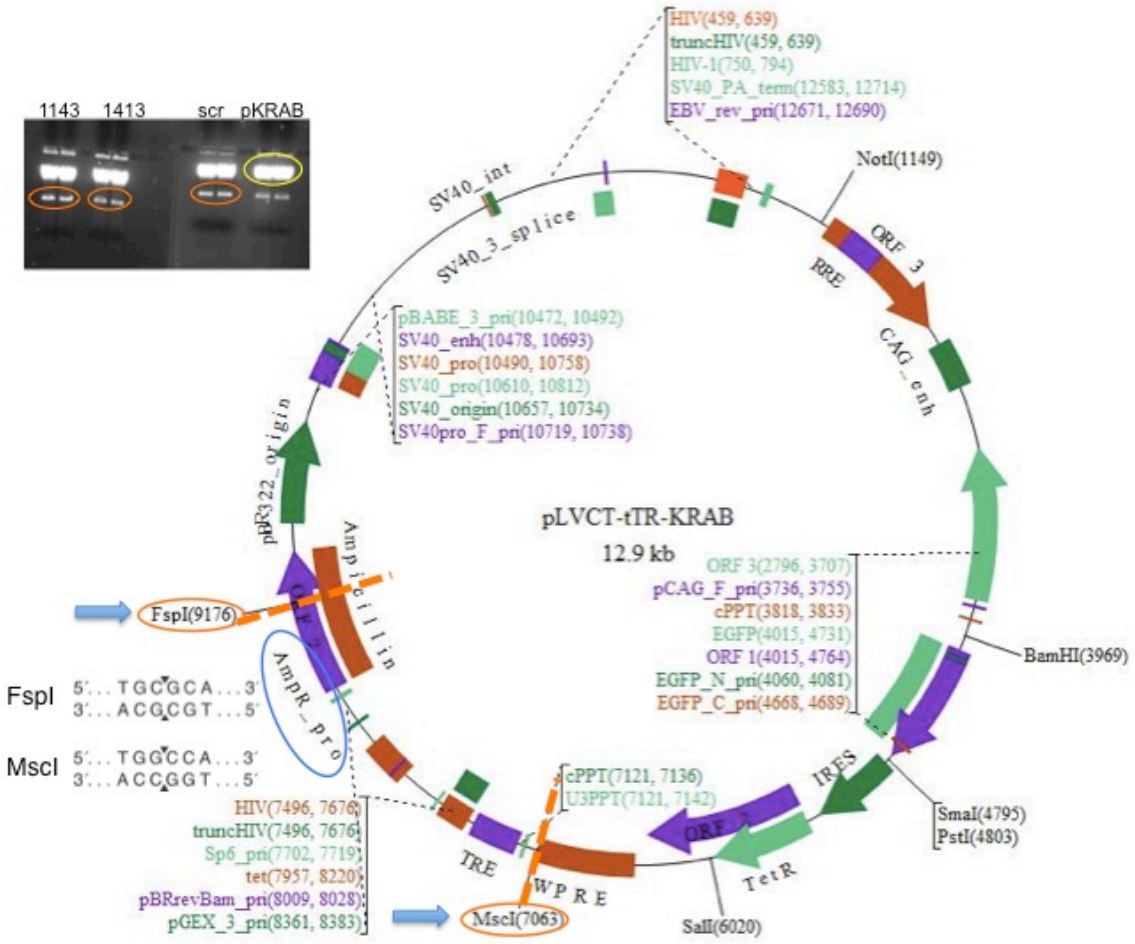

Figure 2.3 Subcloning into pLVCT-tTR-KRAB vector. The recipient pLVCT-tTR-KRAB vector is digested with the enzymes MscI and FspI (empty vector marked in yellow on agarose gel – top left image) to allow insertion of the SULF2 sequence cut out from the pLVTHM vector (orange circle on agarose gel – top left image).

2.6.4 Lentivirus production

For transfection 2.5 x 10^6 293T cells (ATCC #11268) were seeded into each 10-cm cell culture dish and grown overnight to reach ~60-70 % confluence. Ten µg of the transfer vector plasmid pLVTHM, 2 µg of the envelope plasmid pMD2.G (Addgene, Plasmid #12259) and 2 µg of packaging plasmid pCMVR8.74 (Addgene, Plasmid #22036) were mixed with 2.5 M $CaCl_2$ and HBS (pH 7.12) and added to each 10-cm dish. The following day cells were washed with Dulbecco's PBS (DPBS) and incubated with DMEM medium

supplemented with 10mM sodium butyrate and 20mM HEPES for 18 h. Cells were then washed with DPBS and incubated with DMEM containing 20mM HEPES for further 48 h. The viral supernatant was removed and filtered through a 0.45 µm vacuum filter and ultracentrifuged at 26.000 rpm for 90 min at 4 °C. The pellet was resuspended in DPBS and stored at -80°C. NBL cells were grown in a 12-well plate to ~50 % confluency and transfected with the produced shRNA SULF2 regions 1144, 1413 and the scramble. Successfully transfected cells (5 x 10^6 cells) were sorted by FACS 3 days after transfection.

2.7 Cell viability assays

Crystal violet was used for cell viability. Cells were grown and transfected with siRNA as described above in 96-well flat-bottomed micro titer plate. After 48 h cells were then fixed with 4 % (w/v) paraformaldehyde and subsequently, stained with 1 % (w/v) crystal violet for 30 min and then rinsed with PBS. Cells were also grown in 96-well plates (2x10^4 cells /well) and transfected with siRNAas described above. CellTiter-Glo Luminescent cell viability assay (Promega #G7570) was used following the manufacturer's instructions.

2.8 Apoptosis

For apoptosis assays, cells were grown in a 96-well plate in a final 50 µl volume under the same conditions and analysed for caspase 3/7 activity (ApoLive-Glo Multiplex Assay; Promega #G6410). For Annexin V assessment, cells were grown in 6-well plates (4x10^5 cells/well) and Annexin V and propidium iodide staining (PI) was done in accordance to manufacturer's instructions (FITC

Annexin V Apoptosis Detection kit, BD Biosciences #556547). FACS scan flow cytometer was used with the CellQuestPro software. Western blotting was used to assess caspase-3 and PARP cleavage (see **2.3** Western Blotting).

2.9 Cell cycle analysis

Cell cycle analysis was performed using BrdUincorporation (FITC BrdU Flow kit, BD Pharmingen #552598). Annexin V and BrdU were analysed on a Beckman FACScan flow cytometer using CellQuestPro software.

2.10 Statistical analysis and graphs

All numerical data were calculated as means ± standard deviations (SD) or standard errors of the mean (SEM). Differences between groups were compared using Student's t- test (ANOVA). Statistical analysis for the gene expression microarray data was performed with R Project Software (version 3.0.1) with one-way ANOVA followed by Wald's test for comparing differences between multiple groups and correcting for multiple testing when appropriate. Differences were considered significant at $p < 0.05$. Graphs were created using GraphPad Prism 6 Software.

Chapter 3: SULF2 expression in MYCN amplified neuroblastoma

3.1 Introduction

HSPGs have an essential role in the interaction between cancer cells and the tumour microenvironment (TME) and are involved in many processes including cell proliferation, adhesion, migration and invasion [Esko and Lindahl, 2002; Esko and Selleck, 2002; Iozzo, 2005; Sasisekharan et al., 2002]. Their function has largely been attributed to sulfation motifs in HS chains that are controlled by regulatory enzymes such as biosynthetic sulfotransferases that add sulfate groups, and by extracellular sulfatases that selectively remove 6-O-sulfates [Vives et al., 2014]. Sulfate groups modulate the binding and interaction of HS with several growth and signaling factors.

The increasingly reported importance of sulfatase enzymes such as the SULFs to cancer cells and their microenvironment has led us to question their role in NBL. Early work in the 1980's analysed the biochemical composition of HSPGs of NBL cells *in vitro* identifying distinct HS populations from cells and from the medium [Maresh et al., 1984; Hampson et al., 1983; Hampson et al., 1984]. Recent evidence showed that children with solid tumours and with NBL have high levels of heparanase, the endoglycosidase enzyme that cleaves HS chains into large oligosaccharide fragments, and that this correlates with responses to treatment [Zheng et al., 2009; Shafat et al., 2007]. HS remains an under-researched, but vital "missing link" in enabling proteins to be regulated to support or suppress cancer growth and development. A comprehensive analysis on the expression of HSPGs in NBL has not been carried out to date. Here, in *Chapter 3,* the expression of HS and some of its biosynthetic and modification enzymes in NBL cell lines are investigated.

3.2 Hypothesis and Aims

The hypothesis of this chapter was that human NBL have a distinct HS molecular phenotype that may be associated with tumour behaviour.

To test the above hypothesis the specific aims of this chapter were:

- To examine the expression of key enzymes that control the sulfation patters of HS in human NBL and other cell lines
- To characterize the expression of HS in NBL cell lines
- To identify gene expression changes in HS enzymes that may be linked to specific NBL characteristics

3.3 Results

3.3.1 Expression of heparan sulfate biosynthetic and modification enzymes in cell lines

To test the hypothesis, the gene expression of several enzymes that regulate the sulfation of HS was analysed by RT-PCR technology. Overall, 8 NBL cancer cell lines were studied (CHLA-255, CHLA-90, SK-N-SH and SK-N-RA, CHLA-136, SK-N-BE2, SMS-SAN and NB-19); (Table 1.2). In order to evaluate whether any changes in gene expression were relevant to neuroblastoma, changes in HS biosynthetic enzyme expression was also checked in other 6 cancerous non-NBL cell lines (A-549 lung carcinoma, MG-63 osteosarcoma, HT-1080 fibrosarcoma, HeLa cervical cancer, MDA-MB-231 breast cancer and C-8161 melanoma) and non-cancerous human cell lines (human brain microvascular endothelial cells - HBMEC and human fibroblasts). The rationale behind this experiment was that a significant difference in expression (up- or down-regulation) between neuroblastoma cell lines (or a subgroup of cell lines) and the other cell lines, would identify enzyme(s) with a role in neuroblastoma

pathogenesis. Genes were selected (Table 3.1) with a focus on 2 major families of biosynthetic enzymes, the HS O-sulfotransferases (OSTs) and the N-deacetylase/N-sulforansferases (NDSTs) that increase sulfation of HS chains during their biosynthesis, and on the SULFs that remove 6-O-sulfate from glucosamine residues of HS extracellularly. The gene expression analysis was very informative as it revealed the most highly expression of SULF2 mRNA in the neuroblastoma cell lines (Figure 3.1). Particularly, mRNA for this enzyme was more abundantly expressed (-ΔCT >15) in 4 neuroblastoma cell lines (CHLA-136, SK-N-BE(2), SMS-SAN and NB-19) when compared to the other cell lines (Figure 3.1 and Figure 3.2). All the neuroblastoma cell lines that had the high levels of SULF2 were MYCN-A. The significantly lower levels of SULF2 mRNA in the MYCN-NA neuroblastoma cell lines expressed were comparable to the levels of the other non-neuroblastoma cell lines ($p<0.01$). Interestingly, the melanoma cell line C8161 (also a neuronal crest derived tumour like neuroblastoma) showed significantly elevated expression of SULF2. Overall, the relative expression of SULF1 mRNA was not significantly different amongst the MYCN-A and MYCN-NA neuroblastoma cell lines ($p=0.15$). When comparing the MYCN-A and MYCN-NA neuroblastoma cells, no significant changes in expression were observed uniquely in all lines for 2OST1, 3OST1, 6OST1 and 6OST2. 6OST3 had low levels of expression on 2 out of 4 MYCN-A neuroblastoma cell lines (SK-N-BE(2) and SMS-SAN) when compared to the MYCN-NA (SK-N-SH and SK-N-RA). The highest 6OST3 mRNA expression was present in the melanoma cell line C8161 (Figure 3.2). The expression of all NDSTs was also unaltered among the neuroblastoma cell lines; with the lowest

levels for the isoform NDST4 (Figure 3.1). NDST3 had the lowest levels in the non-neuroblastoma cell lines (Figure 3.2).

These findings showed that SULF2 mRNA was significantly increased in neuroblastoma cell lines when MYCN was amplified. Interest was then focused on SULF2 in neuroblastoma.

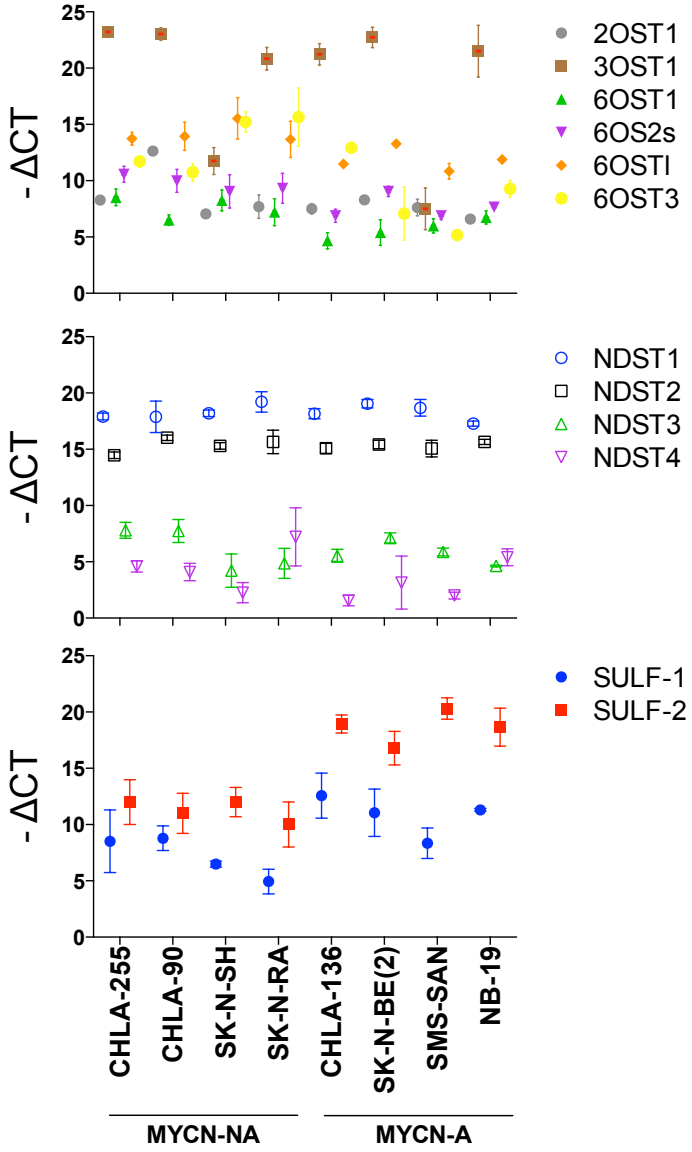

Figure 3.1 mRNA expression of sulfation modifying enzymes in neuroblastoma cell lines measured by qRT-PCR. cDNA from neuroblastoma cells was obtained by reverse transcription. The amount of RNA for each enzyme was determined by qRT-PCR as described in Materials and Methods. The data represent the negative mean ΔCT ± S.E.M. [-(value of gene – control value of GAPHD)] from 3 aliquots of samples obtained each from 3 separate experiments. Higher -ΔCT expression values represent higher level of expression. Statistical significance was determined using Student's t-test (* indicates $p < 0.05$). MYCN-NA = non amplified; MYCN-A = amplified. See Table 2.2 for oligonucleotides/gene information.

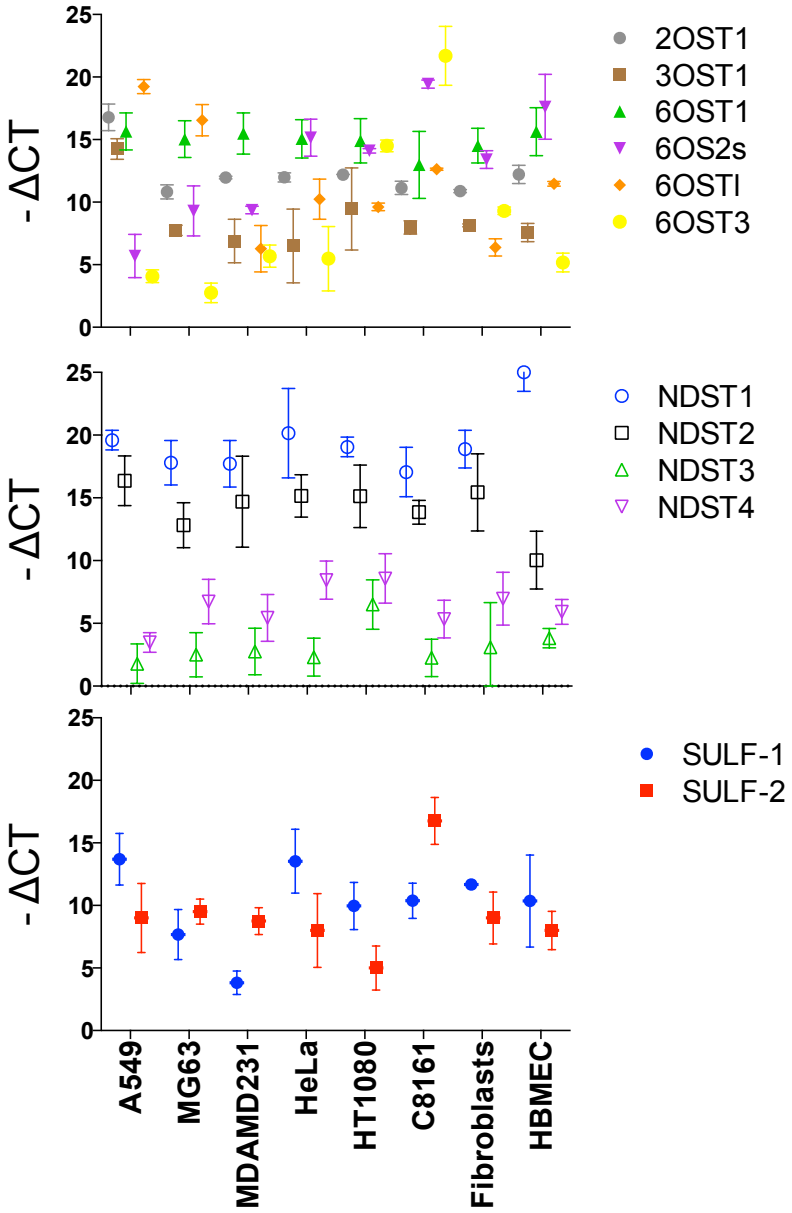

Figure 3.2 mRNA expression of sulfation modifying enzymes in non-neuroblastoma cell lines measured by qRT-PCR. See Table 2.2 for oligonucleotides/gene information.

To further assess the expression of the HS biosynthetic enzymes in NBL, the qRT-PCR findings were validated at the protein level by Western blot analysis. This study confirmed that SULF2 protein was abundantly present in the cell lysate of the four neuroblastoma cell lines with MYCN amplification when compared to the four MYCN-NA cell lines in which the MYCN protein was

absent or expressed at very low levels (Figure 3.3). The 125-kDa component in the detergent lysate corresponds to the unprocessed pre-protein of SULF2 [Morimoto-Tomita et al., 2002]. Additionally, the processed form is expressed (data not shown), in keeping with the reports in the literature [Lemjabbar-Alaoui et al., 2010]. However it is not well known what functional differences the processed and unprocessed forms may exhibit, but dominant negative effects of the unprocessed forms cannot be excluded.

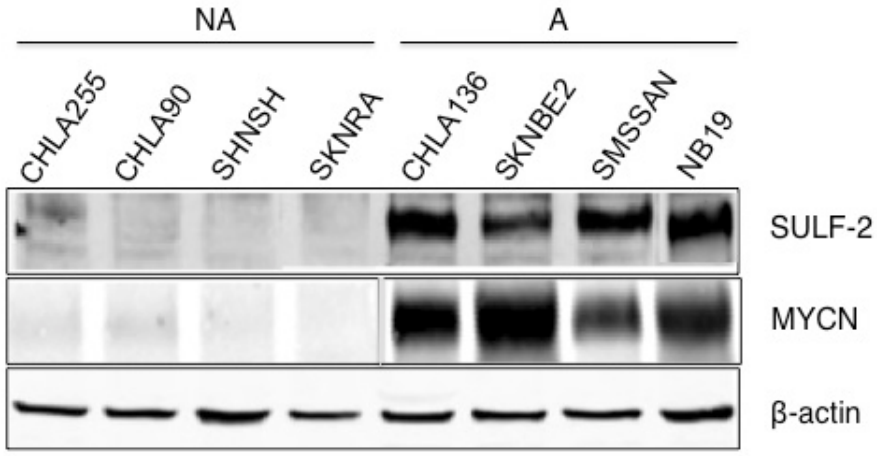

Figure 3.3 SULF2 is specifically overexpressed in MYCN-A neuroblastoma cell lines. Western blot analysis of SULF2 in 8 neuroblastoma cell lines was performed as indicated in *Materials and Methods*. From left, lanes 1-4 are MYCN-NA cell lines and lanes 5-8 are MYCN-A cell lines.

3.3.2 Neuroblastoma cells have distinct sulfated heparan sulfate epitopes

To examine the expression of HS on the surface on NBL cell lines, the 10E4 antibody was used; this is a mouse anti-human HS antibody that targets common HS epitopes containing extended N-sulfated domains, possibly also

mixed with NAc sequences [David et al., 1992; van den Born et al., 2005]. 10E4 was localized homogenously on cell surface of all NBL cells with slightly higher expression in the MYCN A cell lines SKNBE(2) and SMS-SAN (MYCN A), (panel iii and iv, Figure 3.4) when compared to the MYCN NA cell lines CHLA-255 and CHLA-90, (panel i and ii, Figure 3.4). The 10E4 antibody reacts with an epitope that is present in native HS chains and consist of mixed N-sulfated and N-acetylated heparan sulfate [van den Born et al., 2005]. There are no reported colocalisation studies with 10E4 and SULF2 and we did not double stain the NBL cells as both have the same source (raised in mouse). It is unclear why an elevated SULF2 levels might correlate with an increased levels of HS by the 10E4 antibody.

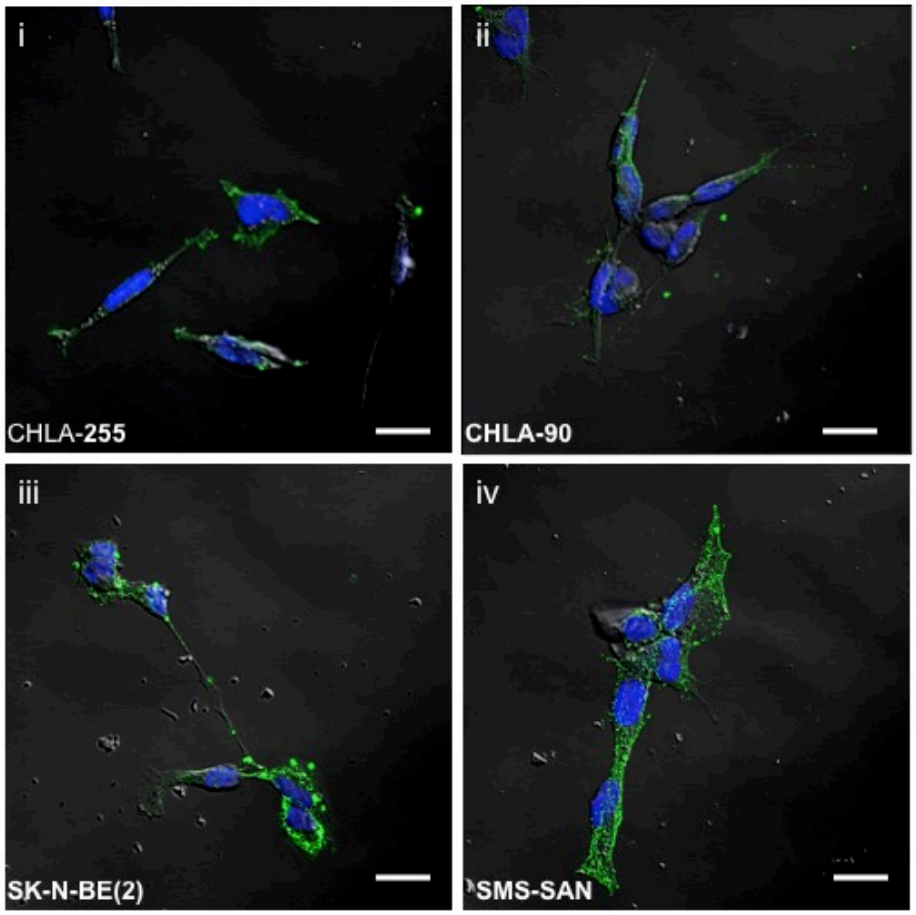

Figure 3.4 Immunocytochemistry to detect heparan sulfate in NBL cell lines. Panels i to vi were stained with an anti-HS antibody (10E4). Panels i-ii represent MYCN non-amplified NBL cell lines, panels iii-vi are MYCN amplified cell lines. DAPI was used to stain cell nuclei (blue). Scale bars are 20 µm.

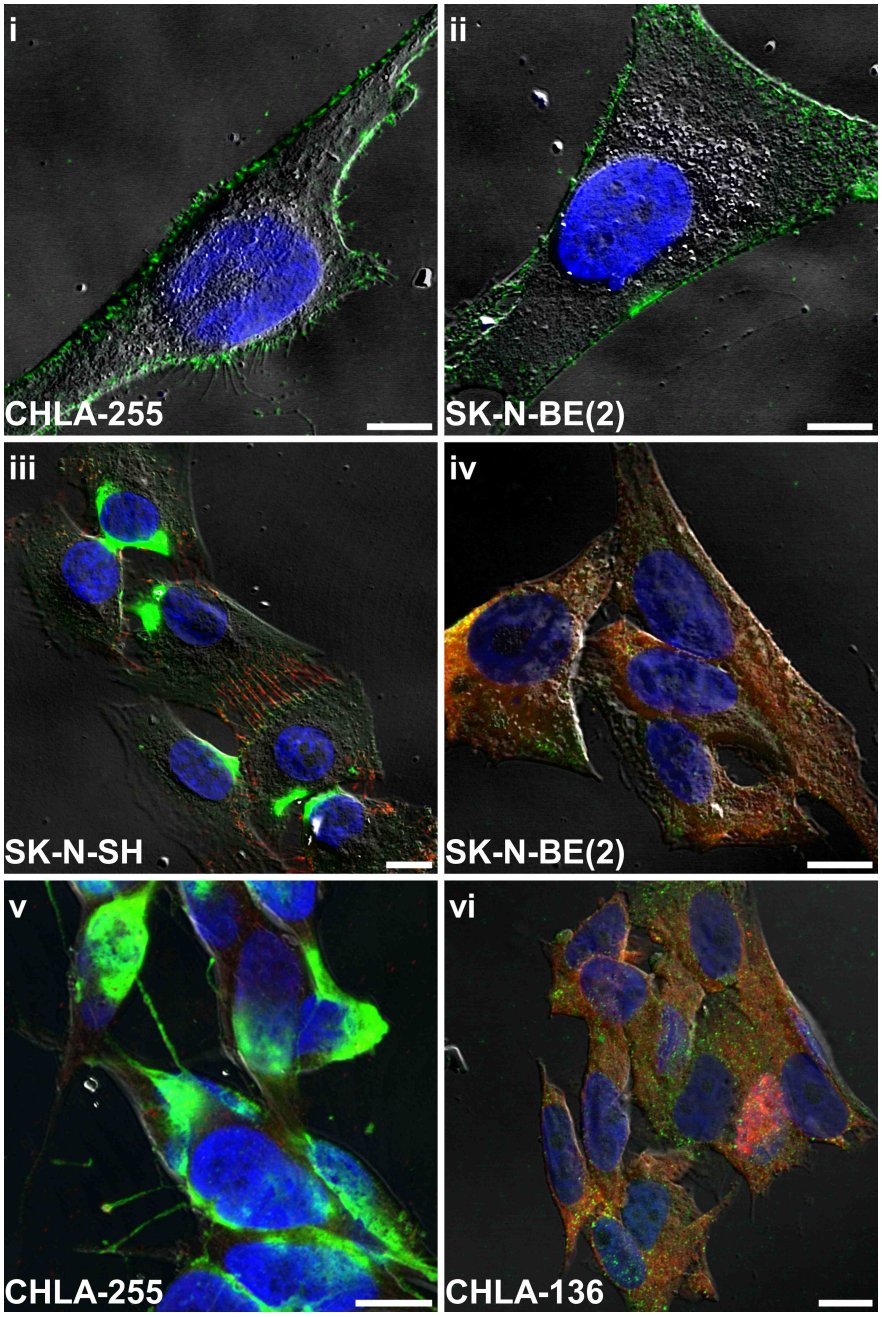

Figure 3.5 SULF2 (red) and HSPG (green) in neuroblastoma cells in culture by immunofluorescence. Panels on the left represent MYCN-NA cells, whereas panels on the right are MYCN-A cells. Panels i and ii were stained with an anti-HSPG antibody (HS3B7V). Panels iii to vi were double stained with an anti-HSPG phage display antibody (HS3B7V) that specifically recognizes highly 6-O-sulfated epitopes (green) and with an anti-SULF2 antibody (red). DAPI was used to stain cell nuclei (blue). Scale bars are 20 µm.

To determine whether over-expression of SULF2 in neuroblastoma cells was affecting the sulfation pattern of HSPG, immunocytofluorescence studies were conducted using an antibody against SULF2 and phage display antibodies against HSPG (Figure 3.5). We then used a panel of phage display antibodies. The phage display antibody HS3B7V recognised the presence of similar levels of IdoUA-GlcNS6S containing domains at the cell surface of both MYCN-A and MYCN-NA cell lines (Figure 3.5, panel i and ii). The phage display antibody HS3A8V that recognizes highly sulfated domains within HS that depend on 6-O-, N-sulfated glucosamine (GlcNS6S) and sulfated iduronic acid (IdoUA2S) over non-sulfated iduronic acid (IdoUA), [Dennissen et al., 2002] with the preferred sequence GlcNS6S-IdoUA2S-GlcNS6S, was then employed. These epitopes are potential substrates for SULF2 [Ai et al., 2003] and are typical components of HS but, are not present at high levels. Using immunocytochemistry staining on fixed NBL cells, the level of HS3A8V was significantly lower in MYCN-A cell lines, which expressed high levels of SULF2 (Figure 3.5, panels iii to vi). No staining was seen in the absence of primary antibody (Figure 3.6). The data indicated that among the enzymes controlling the pattern of sulfation of HSPG, SULF2 was the only one that was clearly differentially expressed in MYCN-A cell lines when compared to all other cell lines. SULF2 and HS stained by the phage display antibodies did not show any co-localisation. They also consistently demonstrated that the presence of higher levels of SULF2 was associated with a significant decrease in the level of sulfation of HSPG in these cells. These correlative data suggested a potentially important role of SULF2 in the pathogenesis of MYCN-A driven neuroblastoma.

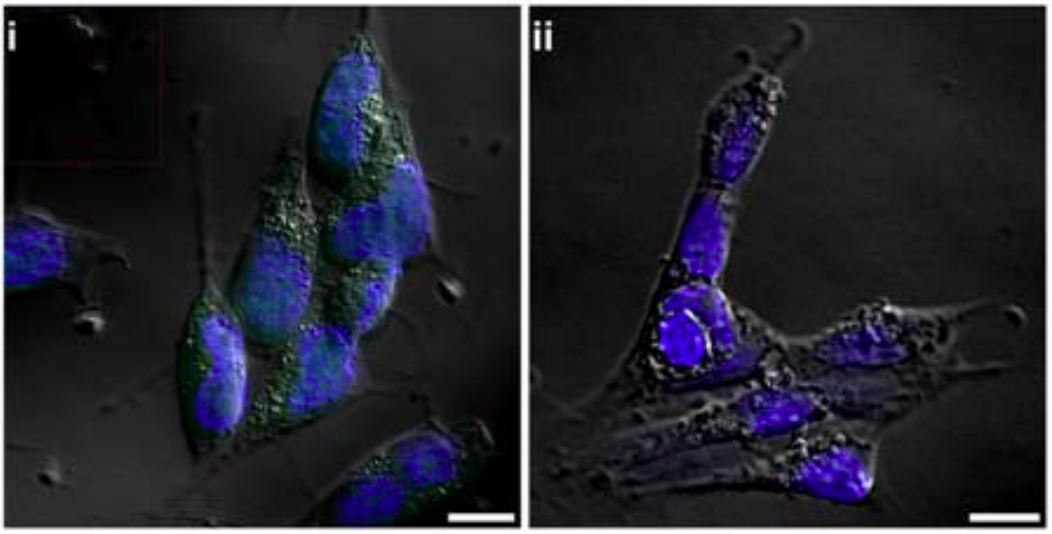

Figure 3.6 Confocal microscopy of negative controls for immunofluorescence staining. Endogenous heparan sulfate was digested with heparitinase and then stained with phage-display antibody HS3A8V using Alexa-fluor-488 (i). As a second control, omission of the primary antibody anti-SULF2 (2B4) was used and stained with Alexafluor-594 (ii). DAPI staining (blue) reveals the nuclei. Scale bars are 20 μm.

3.4 Discussion

The main findings of this Chapter were 1) SULF2 is high in NBL cell lines when compared to other cell lines and particularly when MYCN is amplified (A); 2) NBL cell lines that are MYCN-A have decreased expression of 6-O sulfation epitopes on their surface.

This is the first comprehensive analysis of the expression patterns of HSPGs and their modifying enzymes in human NBL.

Here we observed, first, that SULF2 is highly expressed in a series of NBL cell lines when MYCN is amplified. Our experiments started by screening 16 cell lines (8 NBL and 8 cancer and normal cell lines) for several HS biosynthetic enzymes that regulate HS sulfation and found that SULF2 was

highly expressed in NBL cell lines in which MYCN is amplified when compared to other cell lines. The same cell lines also had abundant protein levels of SULF2 by WB analysis. SULF1 was present in all NBL cell lines examined but was always lower than the levels of SULF2 and showed no significant differences amongst the cell lines. It has frequently been reported in the literature that SULF1 and SULF2 are not always expressed in cancer cell lines. For example in non-small cell lung carcinoma (NSCLC) [Lemmjabbar-Alaoui et al., 2010] showed that of a total of 18 cell lines, all of which are tumorigenic in immunocompromised mice, SULF2 was present in seven and SULF1 in three, while the remaining eight did not express either. Nawroth et al. reported that SULF1 is expressed in 15/24 and SULF2 in 23/24 human pancreatic adenocarcinoma cell lines [Nawroth et al., 2007]. We found that both SULFs mRNAs are expressed amongst all 16 cell lines tested. The differences in the results may be due to the more efficient gene expression analysis we used in our experiments with a much more sensitive detection by real-time qPCR, compared to standard RT-PCR and gel electrophoresis. Our gene expression data showed that the melanoma cell line C8161 had very high levels of SULF2 similarly to the NBL with MYCN A. This is of interest as melanoma is also a neural crest derived tumour like NBL and high expression levels of SULF2 were identified in tissue from patients with high-grade uveal melanoma when compared to low grade [Bret et al., 2011]. In the study by Iwao K et al [Iwao et al., 2009] it was demonstrated that HS regulates optical and cranial neural crest development through TGF-β_2 signaling; the disruption of HS caused several developmental facial and eye abnormalities. Similarly, in *Xenopus tropicalis,*

neural crest migration required SULFs (SULF1 and SULF2); when the SULFs were ectopically expressed in the environment, there was a disruption of neural crest cell migration [Guiral et al., 2010]. This showed that SULFs and especially SULF2 play a role in neural crest migration and therefore possibly in NBL development. In our study, the SULF2 overexpression was also shown at the protein level in the same NBL cell lines and correlated with the gene expression profiles. To the best of our knowledge no study in the literature analysed a colocalisation of SULF2 and MYCN during development. This might be of interest in neural crest development where both factors are reported to be essential [Guiral et al., 2010; Schwab, 2004; Soucek et al., 2008; Arvanitis and Felsher, 2006]. SULF2 is present on the cell surface and is secreted into the ECM by cancer cells, where it regulates elements of oncogenesis [Phillips et al., 2012] and it can probably be produced also by other cell types such as the cancerous stroma [Phillips et al., 2012; Bret et al., 2011]. The secreted SULF2 might have deleterious non-autonomous effects that alter the tissue microenvironment influencing cellular phenotype. To date, a comprehensive analysis of the secreted sulfatases in cancer is lacking.

Second, it is thought that levels of 6-O sulfation are inversely related to SULF2 expression. Immunocytochemistry and FACS analysis with phage display antibodies showed that overall 6-O sulfation is not elevated in NBL cells where SULF2 is highly expressed on cell surface. This finding is in agreement with reported data in the literature where cells with high levels of SULF2 have low levels of 6-O sulfation [Phillips et al., 2012; Lemmjabbar-Alaoui et al., 2010], showing that the enzymes function depends on its activity as a

endosulfatase of HSPGs. Similarly in our preliminary experiments (See Appendix 1) 6-O sulfation was increased in the two MYCN NA NBL cell lines (SHEP and SHSY5Y) that express very low levels of SULF2. In the same way, the NBL cells studied by Hampson et al., with high levels of 6-O sufation might have been MYCN NA [Hampson et al., 1983; Hampson et al., 1984].

The HS3A8V antibody reacts with trisulfated disaccharide motifs of HS [Dennissen et al., 2002] and because it is less abundant on the cell surface of NBL cells that have high SULF2 levels, it can be assumed that SULF2 remodels the sulfation profile of HS locally.

Chapter 4: The effects of SULF2 alteration on neuroblastoma cell lines

4.1 Introduction

NBL is an aggressive childhood cancer that accounts for 10 % of all childhood cancers and for approximately 15 % of all cancer deaths in children [Maris and Matthay, 1999]. High-risk NBL tumours with MYCN amplification (A) still have a high mortality rate despite multimodal therapies and new therapies that are effective against multidrug resistant NBL are needed.

In Chapter 3 increased SULF2 levels were observed in high-risk NBL cell lines when MYCN was amplified and associated with a decrease in 6-O-sulfation on cell surface HS. Recently it has been shown that SULF2 was overexpressed in a series of human cancers [Lui et al, 2012; Bret et al., 2011] and it has been directly implicated in driving tumourgenesis in human glioma and non-small lung carcinoma. Here it was associated with low levels of 6O-sulfation [Phillips et al., 2012; Lemjabbar-Alaoui et al., 2010]. Furthermore the reduction of SULF2 expression decreased the growth of gliomas and decreased the activity of PFGFRalpha and downstream signalling pathways [Phillips et al., 2012]. Similarly, in non-small cell lung carcinoma the down regulation of SULF2 induced cell death and apoptosis [Lemjabbar-Alaoui et al., 2010]. Overexpression of SULF2 promoted carcinogenesis in the lung [Lemjabbar-Alaoui et al., 2010]. Several methods were used to test the effects of SULF2 alterations by siRNA on apoptosis and viability. We measured the proliferation after SULF2 KD in two NBL cell lines with MYCN A using two assays. First, we used the CellTiterGLow (CTG) luminescence assay, which indirectly measures the number of viable cell by quantifying the amount of ATP present in a

metabolically active cell while concurrently inhibiting ATPases. This assay has been shown to be sensitive and give a stable luminescent output. Second, we used a classic fluorescent BrdU incorporation with cell cycle analysis by FACS with 7-AAD allowing the enumeration and characterisation of cells that are actively synthesising DNA (BrDU incorporation) in term of other cell cycle positions defined by 7-AAD staining.

In this chapter we focus on measuring the effects of loss of SULF2 on apoptosis. Apoptosis is the most common form of programmed cell death and since many features overlap among different forms of cell death we used various techniques. Caspases are cysteine-dependent aspartate-specific proteases involved in the execution of both intrinsic and extrinsic apoptosis [Lakhani et al., 2006.] Caspase-3 is one of the most effective caspases [Lakhani et al., 2006] and the proenzyme is activated by cleavage, which allows the formation of two dimerised and active subunits. Cleaved caspase-3 also cleaves and activates caspase-7; both have some overlapping roles that are common to the intrinsic and extrinsic apoptotic pathways [Lakhani et al., 2006]. Casapse-3 controls DNA fragmentation, whereas caspase-7 is more important for loss of cell viability [Lakhani et al., 2006]. PARP is cleaved by caspase-3 and 7 and is involved in DNA repair, differentiation and chromatin structure formation [Germain et al., 1999]. Caspase-3 and 7 activation is an indication that apoptosis will initiate whereas PARP activation is an indication that the cell is actually undergoing apoptosis. Additionally we analysed caspase-3 and PARP cleavage (89 kDa fragment containing the catalytic domain) by western blotting.

We use siRNA technology to knockdown SULF2 expression, using a previously reported SULF2 overexpression transfection [Lemjabbar-Alaoui et al., 2010] and SHEP cells with the tet21N system, which express MYCN in the presence of tetracycline [Lutz et al., 1996].

Here in *Chapter 4* we focus on the effects of SULF2 on growth and apoptosis in NBL cell lines. We also study the correlation of SULF2 to MYCN and provide evidence for a downstream target.

4.2 Hypothesis and Aims

In *Chapter 3* it has been shown that SULF2 is predominantly overexpressed in NBL cell lines are MYCN amplified. This raises the question whether:

- SULF2 has a role in the survival of NBL cell lines that are MYCN amplified
- MYCN amplification regulates SULF2 expression

Therefore, the aims of this chapter were:

- To examine the effects of SULF2 knockdown and overexpression on the survival of NBL cell lines *in-vitro*
- To study the effects of MYCN alterations on SULF2 expression

4.3 Results

4.3.1 Knockdown of SULF2 expression in MYCN amplified neuroblastoma cells results in loss of cell viability

To evaluate whether increased SULF2 levels in neuroblastoma were of biological importance, the effects of down-regulation of SULF2 expression in MYCN-A neuroblastoma cell lines were analysed. Two MYCN-A cell lines with strong expression of SULF2 [SK-N-BE(2) and NB-19] were transfected with either specific SULF2 siRNA (SULF2 siRNA 1 or 2 and a combination of both), or with a control siRNA. Both siRNA transfected cell lines showed a marked reduction in the expression of SULF2 compared to the control cells (>85-90%) (Figure 4.1, A). The knockdown (KD) of SULF2 did not cause a reduction of the expression of MYCN in either cell line. The KD of SULF2 in these cells resulted in a significant reduction in cell density in culture when compared to scramble-transfected controls as shown by crystal violet staining (Figure 4.1, B).

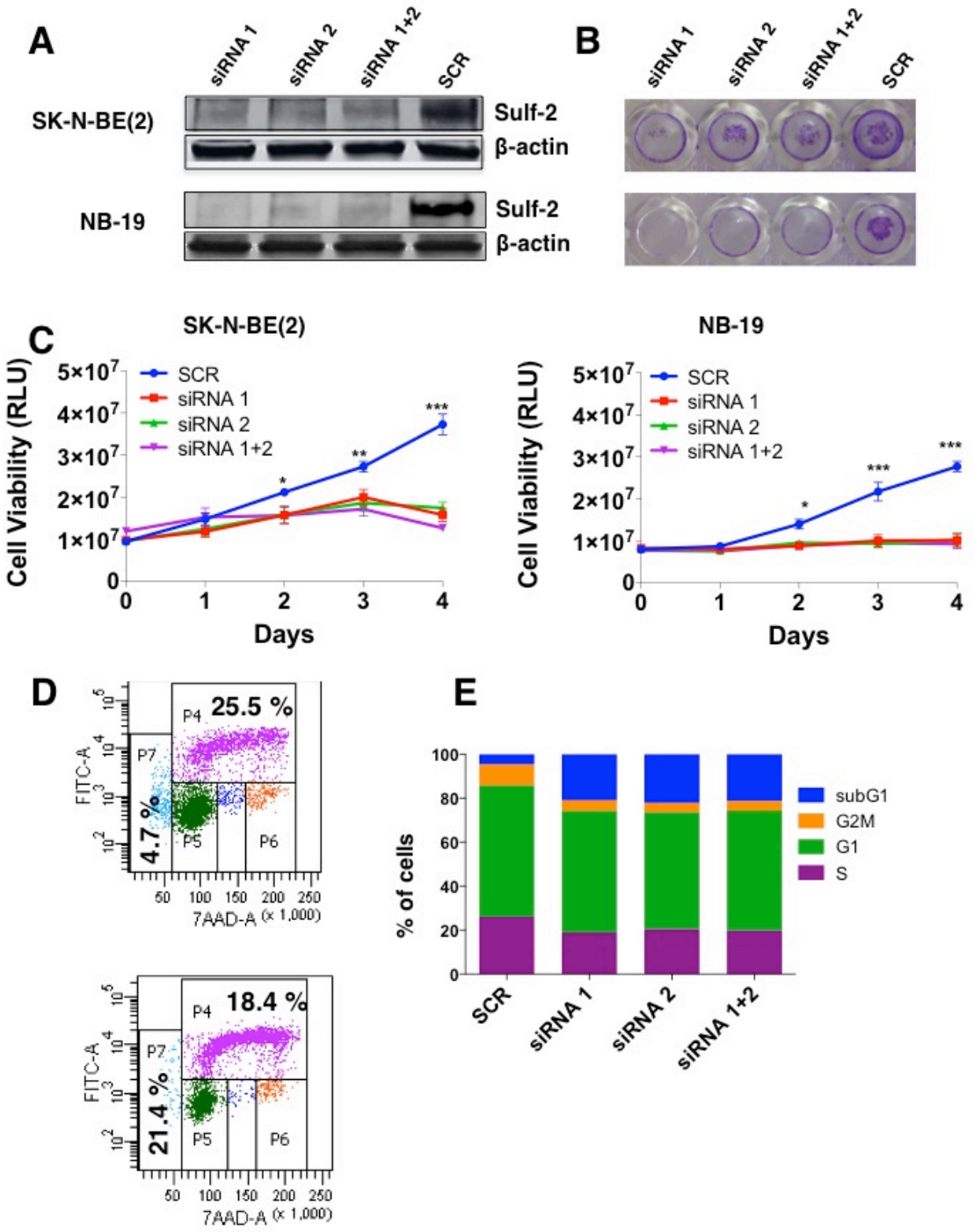

Figure 4.1 Knock down of SULF2 expression in neuroblastoma cells.

Knock down of SULF2 results in loss of viability. MYCN-A SK-N-BE(2) and NB-19 neuroblastoma cells were transfected with siRNA for SULF2 and examined for survival and proliferation as described in Materials and Methods. A, Western blot analysis of SULF2 expression on cell lysates obtained 48 hours after transfection with SULF2

siRNA and scrambled siRNA (scR). B, Representative crystal violet stains of cells in culture 48 hours after transfection. C, Cell viability was measured at the indicated time by the CellTiter-Glo luminescent cell viability assay as indicated in Materials and Methods. The data represent the mean (+/- SD) fluorescence units (RLU) of quadruplicate samples in 3 separate experiments (n=12); (* $p < 0.05$; ** $p < 0.01$; *** $p < 0.0001$). D, NB-19 cells were incubated with BrdU for 2 hours, harvested, permeabilised and stained with PI. The presence of BrdU and PI was then examined by flow cytometry. The data are representative of 2 experiments showing similar results. Top panel: Cells transfected with SCR; bottom panel: cells transfected with siRNA 1 + 2. E, Bar diagram of the distribution of cells in phases of cell cycle according to PI content from the experiments shown in D.

It was then demonstrated that loss of SULF2 expression in these MYCN-A cells [SKNBE(2) and NB-19] resulted in a significant decrease in cell viability when compared to the control transfection (Figure 4.1, C and D). The data thus indicated that SULF2 is required for cell viability in MYCN-A neuroblastoma cells. To determine whether the presence of SULF2 stimulated cell proliferation, the effect of SULF2 KD on cell cycle and BrdU incorporation was examined in MYCN-A NB-19 cells. This analysis revealed a significant decrease in the percentage of BrdU positive cells in S phase from 25.5% to 18.4% (Figure 4.1, D). An analysis of the cell cycle distribution of the cells revealed a decrease in the percentage of cells in S phase and in G2 (from 9.5% to 4.4%) and an increase in the sub- G0 cell population (from 4% to 22%) suggesting that SULF2 is a requisite for cell cycle entry and may protect cells from apoptosis (Figure 4.1, E). We did not investigate the effects on cell proliferation and survival of MYCN overexpression as these are well reported in the literature [Lutz et al.,1996]. We also did not study the effects of SULF2 KO in MYCN NA NBL cell lines as these cells already had very low expression levels of SULF2.

4.3.2 SULF2 protects MYCN amplified neuroblastoma cells from apoptosis

To test the hypothesis that SULF2 protects neuroblastoma cells from apoptosis, the level of caspase 3/7 was measured in cells in which SULF2 was knocked down by siRNA. Consistent with a protective effect of SULF2 on apoptosis, the data indicated an increase in caspase 3/7 activity upon SULF2 KD in SK-N-BE(2) and NB-19 cells in 72 hours (Figure 4.2, A). The increase in apoptosis upon SULF2 KD was confirmed by Western blot analysis, which demonstrated an increase in cleaved poly ADP ribose polymerase (PARP) and cleaved caspase-3 in SULF2 siRNA transfected SKNBE(2) and NB-19 cell lines (Figure 4.2, B). This corresponded to an increase in Annexin-V positive cells at 48 hours in NB-19 cells (Figure 4.2, C). The data thus indicated that SULF2 plays an important role in the viability of MYCN-A neuroblastoma cells, not only by promoting cell proliferation but also by protecting cells from spontaneous apoptosis.

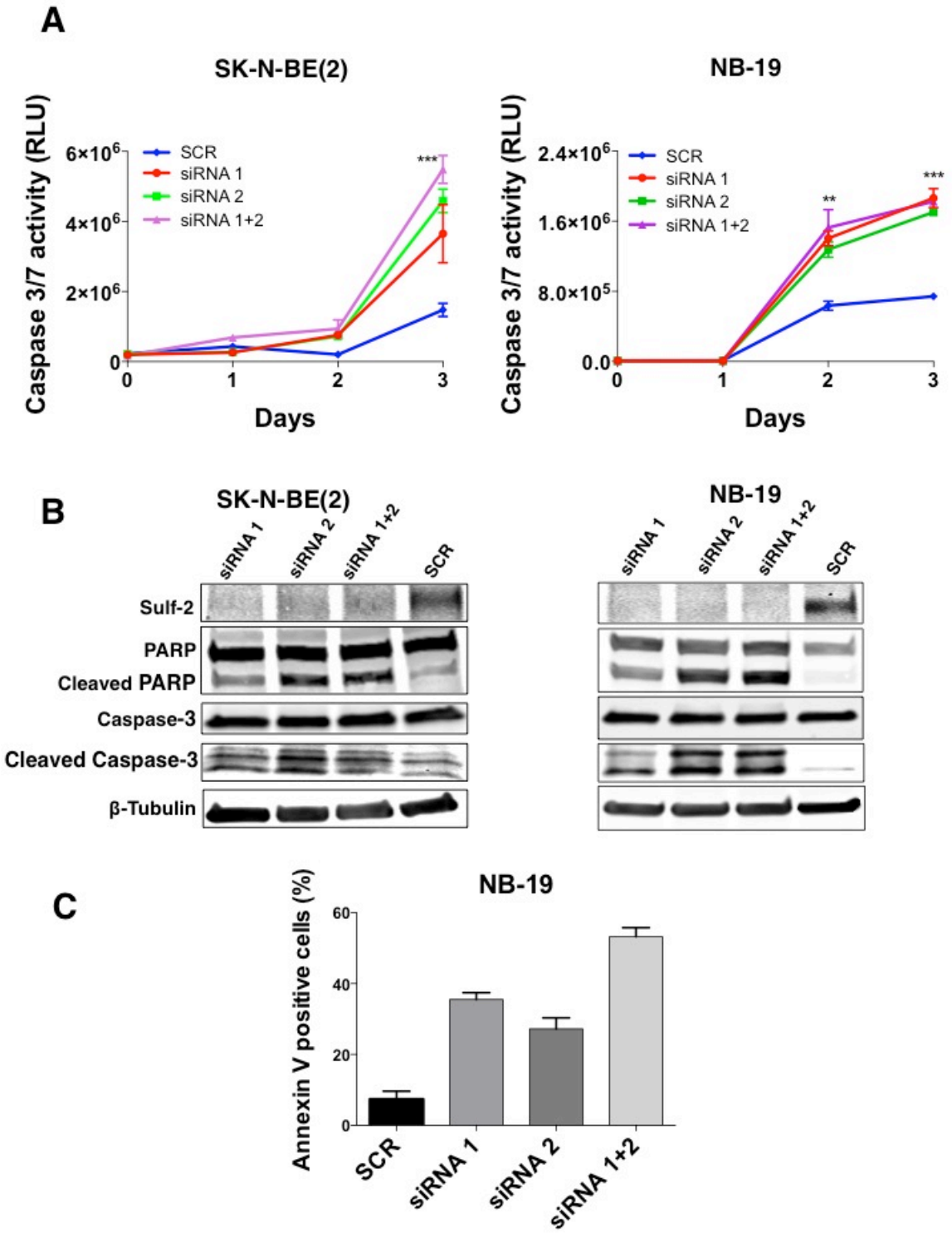

Figure 4.2 Loss of SULF2 expression induces apoptosis.

(A) Caspase 3/7 activity in SULF2 siRNA transfected SK-N-BE(2) and NB-19 cells was measured using the ApoLive-Glo system as indicated in Materials and Methods. The data represent the mean (±SD) luminescence units (RUL) of triplicate sample from one experiment and are representative of 3 independent experiments showing similar results. (B) Western blot analysis of SK-N-BE(2) and NB-19 cells transfected with

SULF2 siRNA and a scramble control, and harvested 48 hours after transfection. (C) Apoptosis in cells transfected as indicated in A, was determined by flow cytometric analysis of Annexin V/PI staining in NB-19 cells transfected with SULF2 siRNA and scramble control. Values are mean ± S.E.M. of three independent experiments. *$p < 0.05$.

4.3.3 SULF2 is a possible down stream target of NMYC and promotes cell viability

The correlation between MYCN and SULF2 expression in cell lines combined with the observation that loss of SULF2 expression decreases the viability of MYCN-A cells, suggested that SULF2 could be a downstream target of MYCN. To test this hypothesis, we wanted to examine the effects of SULF2 overexpression in a NBL cell line that does not express (or have very low levels) of MYCN. For this purpose we used the cell line CHLA-255 as it has almost undetectable levels of SULF2 and was easy to transfect with the plasmid vector. For this experiment we used two constructs overexpressing SULF2, one containing the wild-type (WT) human SULF2 and another with an inactive mutant of SULF2 (pcDNA3.1ΔCC).

Transfection of the cell line CHLA-255 with the overexpressing vectors resulted in an increase of SULF2 expression (Figure 4.3, A) in both the WT and an inactive SULF2 mutant. Induced SULF2 overexpression did not affect MYCN expression. This demonstrated that SULF2 might be downstream and not upstream of MYCN. Consistent with a protective role of SULF2 against apoptosis, we also demonstrated an increase in viability of SULF2-overexpressing CHLA-255 cells over 4 days in culture but not of cells overexpressing the inactive mutant or of untransfected parent cells (Figure 4.3, B).

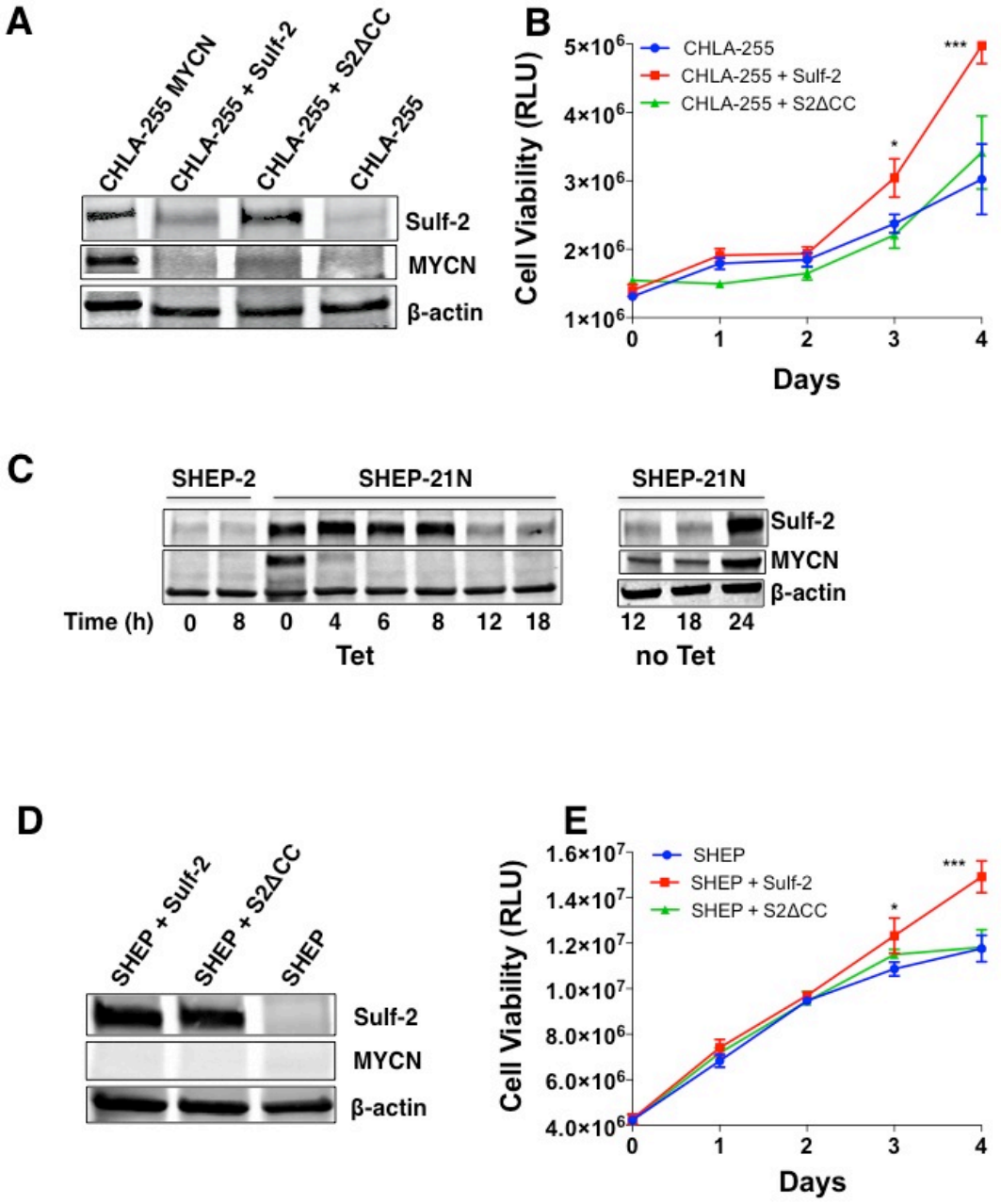

Figure 4.3. SULF2 is a target of MYCN and promotes cell viability.

(A) CHLA-255 cells were stably transduced with MYCN cDNA, a SULF2 WT cDNA, a mutant inactive SULF2 (S2ΔCC) or an empty vector control and examined for SULF2 and MYCN expression by Western blot analysis after 48 hours. β-actin was used as a loading control. (B) CHLA-255 cells transfected as indicated in (A) were cultured for 4 days and examined for viability at the indicated time points as described in Figure 4.3 C. The data represent the mean (±SD) luminescence units (RLU) of triplicate samples

(4 samples in 3 different experiments; n=12). (C) SHEP-21N cells were treated with tetracycline (Tet) at indicated time points (0-18 hours), and after 18 hours Tet was removed from the medium, and cells were kept in culture for another 24 hours. MYCN and SULF2 expression in cell lysates was examined by Western blot analysis at indicated times. (D) SHEP-2 cells were transduced with either SULF2 WT or an inactive mutant SULF2 (S2ΔCC) cDNA and examined for SULF2 and MYCN expression by Western blot analysis. (E) Cell viability was analysed by CellTiter-Glo over time. The data represent the mean (± S.E.M.) luminescence (RLU) of triplicate samples (4 samples in 3 different experiments; n=12). *$p<0.05$; ***$p<0.001$. All experiments were conducted at least three times.

4.3.4 MYCN regulates SULF2 expression in NBL cells

We next investigated the effects of a stable transfection with MYCN in the NBL cell line CHLA-255 that normally does not express (or have minimally detectable levels of) MYCN [Song et al., 2007]. This analysis revealed that overexpression of MYCN in CHLA-255 cells was associated with a corresponding increase in SULF2 expression (Figure 4.3, A) indicating a direct link between MYCN and SULF2. This observation was confirmed using the neuroblastoma cell line SHEP-21N, a subclone of the cell line SHEP (which has barely detectable levels of MYCN and SULF2) transfected with a tetracycline regulated (tet-off) MYCN expression vector [Rossler et al., 2001]. In the absence of tetracycline, these cells stably express MYCN and also SULF2 (Figure 4.3, C), which is consistent with our previous data.

In contrast, treatment of SHEP-21N cells with tetracycline resulted in loss of MYCN protein expression after just 4 hours as anticipated and a progressive decrease in SULF2 protein at 12 and 18 hours. Removal of tetracycline resulted consistently in rapid re-expression of MYCN that was followed later (24 hours) by re-expression of SULF2. These data further demonstrated that SULF2 is a

downstream target of MYCN. To confirm that SULF2 had no effect on MYCN expression, we overexpressed WT SULF2 or a loss of function mutant SULF2 as control in MYCN-NA parent SHEP-2 cells. Neither of these experiments had an effect on MYCN expression (Figure 4.3, D), which is consistent with the results obtained from MYCN-NA CHLA-225 overexpressing SULF2. Importantly, overexpression of SULF2 in MYCN-NA SHEP cells increased cell survival demonstrating again that, although a target of MYCN, SULF2 stimulates neuroblastoma cell survival by an MYCN independent mechanism (Figure 4.3, E). Possible non-autonomous or paracrine effects of SULF overexpression are not explored in this thesis. To provide evidence that SULF2 is a downstream target of MYCN we also performed a CHIP assay to assess the promoter region of SULF2 to MYCN (*see* Appendix 2).

4.4 Discussion

In this chapter two novel observations that shed light on the important role that the pattern of sulfation of HSPG plays in MYCN-driven neuroblastoma pathogenesis are reported.

First SULF2 was identified as playing a unique pro-tumorigenic role among the numerous enzymes controlling the sulfation of HSPG in NBL. Both SULF1 and SULF2 have been shown to be involved in the pathogenesis of a variety of cancers. They are highly expressed in hepatocellular carcinoma, head and neck and pancreatic cancer, in lung adenocarcinoma and squamous cell carcinoma, where their expression is typically associated with more aggressive behaviour and poorer clinical outcomes [Rosen and Lemjabbar-Alaoui, 2010]. In Chapter 3 we showed for the first time that SULF2 is

specifically overexpressed in a subgroup of NBL cells in which MYCN plays an important role. SULF2 expression *in vivo* in primary human NBL tumours has subsequently been investigated (see Chapter 5).

Data from this chapter suggest that SULF2 mediates the oncogenic effect of MYCN by increasing cell proliferation and survival through a yet to be determined mechanism that involves increased cell cycle entry and decreased spontaneous apoptosis.

In the previous chapter our immunofluorescence studies demonstrated lower levels of sulfation in HSPG in cells expressing SULF2. This raises the possibility that SULF2 may promote the release of growth factors and other ligands from undersulfated HSPG, allowing them to interact with their respective receptors at the cell surface. In support of this concept is the recent observation that in malignant glioma, loss of SULF2 expression decreases PDGF-PDGFRα interaction and PDGFR-mediated activation of the mitogen activated protein kinase (MAPK) pathway [Phillips et al., 2012]. This resulted in a growth inhibition *in-vivo*, in particular in a subset of gliomas that are more dependent on exogenous growth factors [Phillips et al., 2012]. Neuroblastoma cells express a variety of receptor tyrosine kinases (RTK) such as neurotrophin tyrosine kinase receptor (NTKR), insulin-like growth factor receptor (IGFR), C-kit, VEGFR, epithelial growth factor receptor (EGFR) and PDGFR [Nilsson et al., 2010; Fakhari et al., 2002]. It is conceivable that as shown in glioma and breast cancer cells [Brodeur, 2003], SULF2 promotes the release of these heparin (HS)-bound growth factors and allows them to better interact with the receptors. One possible candidate for the activity of SULF2 is NTKR2 (TRKB),

which is abundantly expressed in MYCN-A tumours [Poluha et al., 1995]. Brain-derived neurotrophic factor (BDNF) is the ligand for TRKB, which via a paracrine and autocrine loop, promotes tumour growth, drug resistance and angiogenesis in neuroblastoma [Brodeur, 2003; Light et al., 2012]. Like many other neurotrophic and growth factors, BDNF binds to oversulfated proteoglycans [Nandini et al., 2004]. There is presently no data supporting the concept that SULF2 could regulate BDNF-TRKB interaction. However the published observation that SULF1 and SULF2 positively regulate glial cell-derived factor (GDNF)-mediated signalling and oesophageal innervation [Lui et al., 2012], suggests that SULF2 could regulate neurotrophic factor-mediated signalling. This line of investigation is currently the focus of further work.

Second, another important observation reported in this chapter is that SULF2 is a possible downstream target of MYCN and that its protumorigenic function is independent of MYCN. This was first suggested in the previous chapter by the striking observation that SULF2 was specifically overexpressed in neuroblastoma cell lines with MYCN amplification and high levels of MYCN protein expression. A causal relationship between MYCN expression and SULF2 expression was then established by demonstrating that SULF2 was a downstream target of MYCN since its expression was found to be dependent on MYCN expression. The data establish that SULF2 not only contributes to MYCN oncogenesis but is a downstream target of MYCN expression. Over the last few years, a large number of transcriptional targets of MYCN have been reported through the use of expression array analysis, chromatin immunoprecipitation and serial analysis of gene expression (SAGE). Initial

studies using SAGE identified mainly genes involved in ribosome biogenesis and protein synthesis [Boon et al., 2001] but more recent studies included a larger variety of genes including miRNA [Buechner and Einvik, 2012]. SULF2 has been reported to be a direct downstream transcriptional target of p53 and to mediate some aspect of p53 function such as DNA damage induced senescence [Chau et al., 2009]. Interestingly, SULF2 was recently identified among 36 genes down-regulated in 2 MYCN-A neuroblastoma cell lines treated with the bromodomain and extra-terminal domain (BET) inhibitor JQ1, that downregulates MYCN and its transcriptional program [Puissant et al., 2013]. By demonstrating that SULF2 overexpression increases the viability of NB cells independently of MYCN expression, evidence is provided that the pro-tumorigenic function of SULF2, although regulated by MYCN, is MYCN-independent.

Chapter 5: *In-vivo* expression and alterations of SULF2 in neuroblastoma

5.1. Introduction

In Chapter 4 we showed that amongst several enzymes that generate and edit the HS chain, SULF2 has a tumour promoting role in neuroblastoma. Studies showed that SULF2 is overexpressed in several human cancers where it plays a tumourigenic role [Bret et al., 2011]. Furthermore, studies have reported that, *in vivo* down-regulation of SULF2 resulted in a decreased tumour growth [Phillips et al., 2012; Lemjabbar-Alaoui et al., 2010].

We reported in previous chapters that, when compared to other cell lines, SULF2 is overexpressed in NBL cells that have MYCN amplification and that it promotes cell proliferation and decreases apoptosis *in vitro*. We also noticed that 6O-sulfation is decreased on the cell surface when SULF2 is overexpressed, which may lead to an increased release of growth factors and ligands into the extracellular space promoting the interaction with their receptors. In this Chapter we characterise the *in vivo,* expression status of SULF in human neuroblastoma tumours using large scale gene expression analysis and immunohistochemistry. To further confirm the observations made so far in this work, we also analysed the gene expression of SULF2 in two large and independent cohorts of NBL primary tumours. As SULF2 may have either promoting [Nawroth et al., 2007; Yang et al., 2005; Lai et al., 1998; Lai et al., 2004; Lemjabbar-Alaoui et al., 2010] or inhibiting functions, depending on the signalling pathway [Dai et al., 2005; Peterson et al., 2010], we wanted to test the effects of alterating the levels of SULF2 in a neuroblastoma xenograft model by genetic modification of its expression.

Here we have examined 1) the expression of SULF2 in primary human NBL tumour samples, 2) the effects that modulation of sulfation (by altering SULF2 expression) has on tumour cells survival *in vivo*.

5.2. Hypothesis and Aims

In this chapter we hypothesised that SULF2 is highly expressed in human primary NBL and that its alterations regulate tumour growth.

To test this hypothesis the aims of this chapter were

- To evaluate the expression of SULF2 in a cohort of primary human NBL tumour samples.
- To further analyse the effects of SULF2 levels on human neuroblastoma growth in a xenograft model.

5.3. Results

5.3.1 SULF2 expression in primary human neuroblastoma tumours

In order to validate the observations made *in vitro* on established cell lines, the expression of SULF2 *in vivo* in human NBL tissue was examined by immunohistochemistry (IHC). We wanted also to know whether the expression of SULF2 was restricted to NBL cells *in situ* and whether it was also present in the ECM and the surrounding cancer stroma cells. For this, a total of 65 primary human NBL samples were analysed; 22 tumours with MYCN amplification and unfavourable histology (UH), 23 tumours with UH but without MYCN amplification, and 20 tumours with favourable histology (FH) and without MYCN amplification. The staining of SULF2 was predominantly present in the plasma membrane and in the pericellular space surrounding tumour cells, although

some cells showed a marked cytoplasmic staining (Figure 5.1).

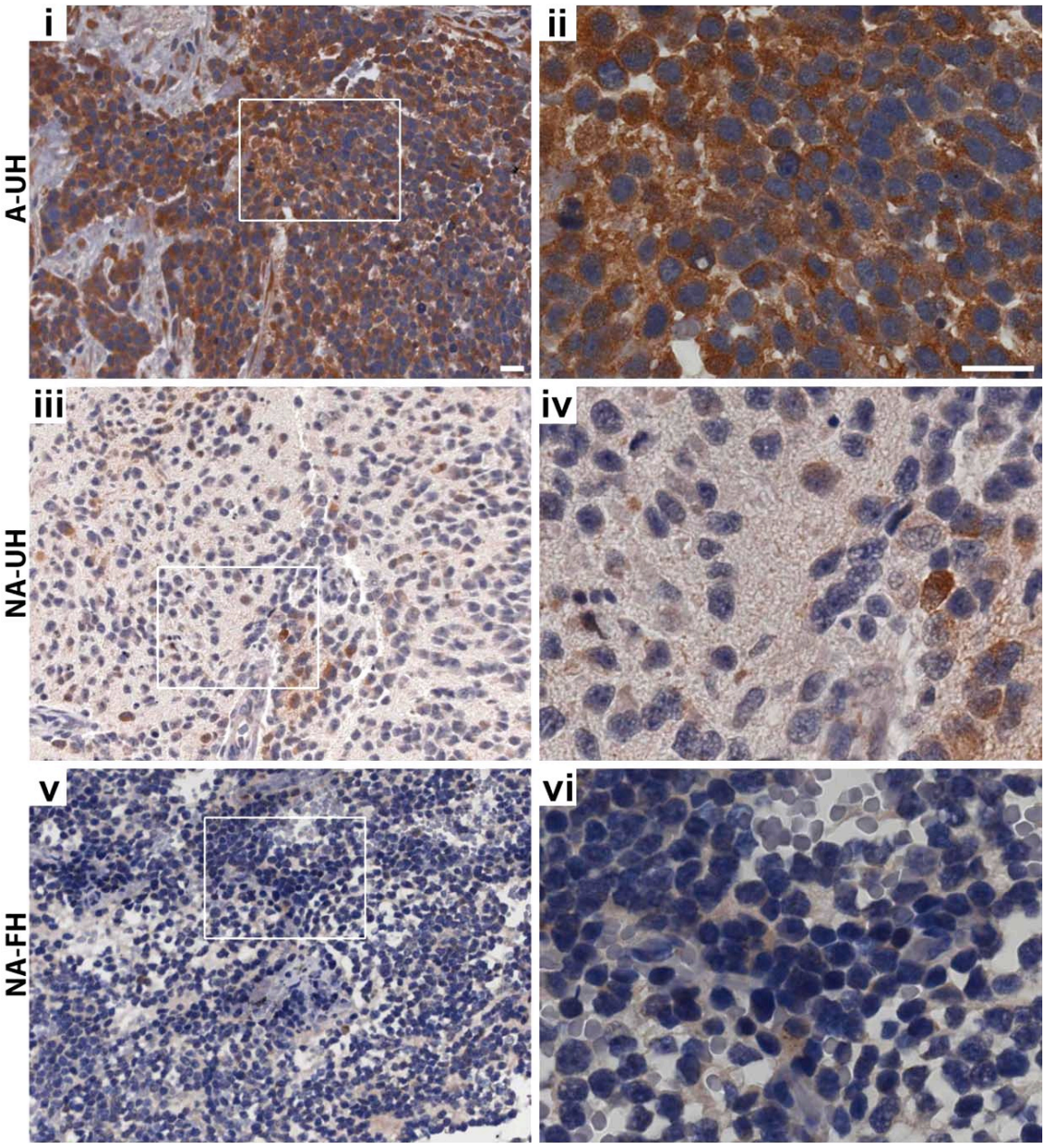

Figure 5.1 Analysis of SULF2 expression in FFPE sections of primary human neuroblastoma tumours. Representative sections of tumours stained with an anti SULF2 antibody. (i and ii) MYCN-A and unfavourable histology (UH), (iii and vi) MYCN-NA and unfavourable histology (UH) and (v and vi) are MYCN -NA with FH. Scale bar = 20 µm.

Stage 4S NBL (without MYCN A) showed weak immunoreactivity for SULF2 (Figure 5.2). Therefore, the expression of SULF2 was apparently restricted to NBL cells.

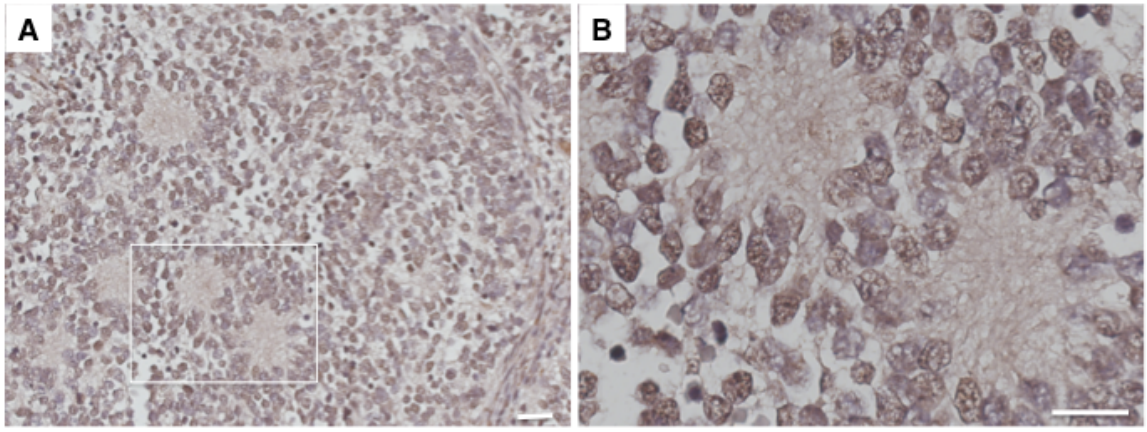

Figure 5.2 SULF2 expression in stage 4S NBL tumour. (A) Overall a weak SULF2 staining across the tissue section. (B) Higher magnification of Homer-Wright rosettes with a halo of differentiated neuroblasts showing a weak to moderate immunoreactivity for SULF2 and non-stained neuropil at the centre. Scale bars are 20 µm.

We noticed that there was a clear consistency amongst tissue sections when stained with the anti-SULF2 antibody. This was very prominent when comparing tissue sections that belonged to the MYCN amplified group versus the MYCN non-amplified ones (favourable histology); indicating that perhaps MYCN amplification was the crucial factor. However, sections belonging to the MYCN non-amplified and unfavourable histology showed some potentially different expression levels of SULF2. Owing to the expression patterns of SULF2 in NBL tissue a manual quantification of the immunoreactivity was difficult. We decided to measure the optical density (OD) of the immunoreactivity by colour deconvolution as the best option for our experiment.

This is a fast and quantitative method that can be used on standard RGB (red/green/blue) images acquired with a standard digital camera. Other methods such the “area method” using the ‘ImageJ’ thresholding tool were found to be time consuming and less reproducible. The IHC data were then quantified by colour deconvolution and optical density (OD) reading of digital images obtained from stained FFPE tissue sections as described in Materials and Methods. The method allowed a good separation of the DAB staining obtained with the anti-SULF2 antibody from the haematoxylin component (Figure 5.3).

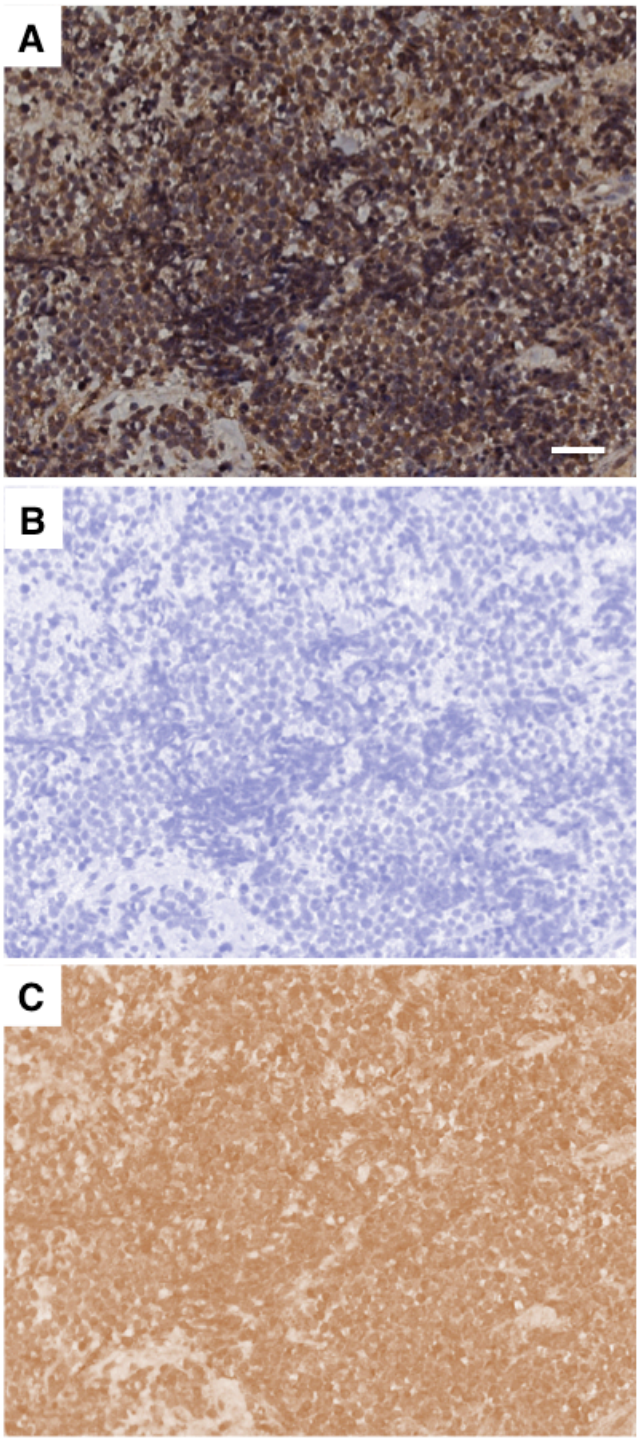

Figure 5.3 Representation of colour deconvolution of SULF2 immunohistochemistry in a MYCN amplified NBL tissue section. (A) NBL tissue section with a strong immunoreactivity for SULF2 with DAB (brown) and hematoxylin to stain nuclei (blue). Colour deconvolution results separating the contributions of hematoxylin (B) and DAB (C) to the original image. Scale bars are 20 µm.

The OD analysis (Figure 5.4) indicated a strong level of SULF2 expression in all MYCN-A tumours and an almost complete absence of expression in MYCN-NA tumours, whether they were of favourable or unfavourable histology (p= 0.0001); this clearly indicated that SULF2 expression was linked to MYCN expression and not to other markers of unfavourable outcome independent of MYCN. The results for the NBL tumours analysed are shown in Table 5.1.

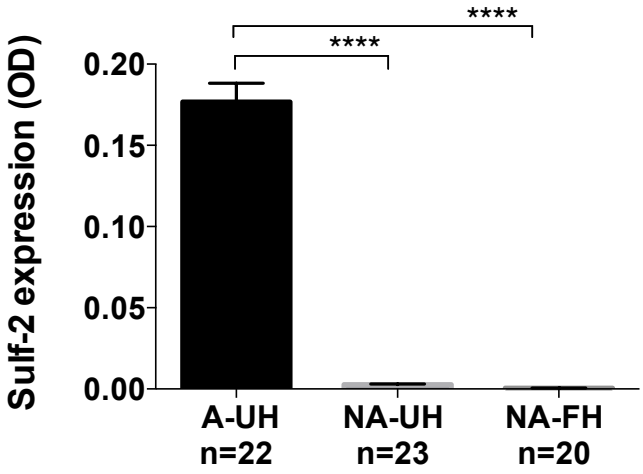

Figure 5.4 Colour deconvolution analysis of SULF2 staining in human NBL tissue samples. Quantification of the immunohistochemistry data was obtained by colour deconvolution of DAB staining as described in Materials and Methods. The data represent the mean (+SD) OD obtained from 10 fields (20x) for each tumour section from MYCN-A (n=22), MYCN-NA, UH (n=23) and MYCN-NA, FH (n=20) tumours as shown in Table 5.1. ****p<0.0001.

No.	Age at diagnosis	Primary site	Stage	Subtype	Histology	MKI	MYCN	DNA index	Average OD	SD of OD
1	10mo	adrenal gland	4	poorly differentiated	UH	High	A	1.1	0.0027	0.001992496
2	2y0mo	retroperitoneum	4	poorly differentiated	UH	High	A	1.877	0.3091	0.248114242
3	2y8mo	adrenal gland	4	poorly differentiated	UH	High	A	1	0.1939	0.042128442
4	1y7mo	retroperitoneum	4	poorly differentiated	UH	High	A	1.675	0.0295	0.018730881
5	3y3mo	adrenal gland	4	poorly differentiated	UH	Intermediate	A	1	0.0972	0.035885966
6	2y8mo	mediastinum	4	poorly differentiated	UH	High	A	1.422	0.1223	0.025680735
7	1y3mo	adrenal gland	4	poorly differentiated	UH	High	A	1.624	0.0582	0.042359791
8	6y1mo	adrenal gland	4	poorly differentiated	UH	High	A	1	0.0834	0.022527494
9	1y10mo	retroperitoneum	4	poorly differentiated	UH	High	A	1	0.0188	0.015517873
10	1y11mo	abdomen	4	poorly differentiated	UH	High	A	1.875	0.0197	0.016469964
11	1y3mo	retroperitoneum	4	poorly differentiated	UH	High	A	1	0.0365	0.013236271
12	1y7mo	abdomen	4	poorly differentiated	UH	High	A	1	0.0574	0.034012183
13	1y9mo	abdomen	4	undiff	UH	High	A	1	0.2783	0.05787682
14	2y0mo	abdomen	4	poorly differentiated	UH	High	A	1.727	0.1403	0.047433617
15	1y0mo	adrenal gland	4	poorly differentiated	UH	Intermediate	A	1	0.2284	0.061628232
16	1y11mo	adrenal gland	4	poorly differentiated	UH	Intermediate	A	US	0.0494	0.032324485
17	2y8mo	adrenal gland	4	poorly differentiated	UH	High	A	1	0.4873	0.080288318
18	11mo	abdomen	4	poorly differentiated	UH	High	A	1	0.5881	0.062665786
19	5mo	adrenal gland	2B	poorly differentiated	UH	High	A	1.704	0.2159	0.04150953
20	4y2mo	abdomen	4	undiff	UH	High	A	US	0.4260	0.099869974
21	4y9mo	abdomen	4	poorly differentiated	UH	High	A	1.594	0.0538	0.008393583
22	3y7mo	abdomen	4	poorly differentiated	UH	High	A	1.66	0.0223	0.004559016
1	6y2mo	adrenal gland	4	poorly differentiated	UH	Intermediate	NA	1	0.0018	0.002083645
2	4y1mo	posterior mediastinum	3	poorly differentiated	UH	Intermediate	NA	1	0.0057	0.003749105
3	8y3mo	retroperitoneum	2A	poorly differentiated	UH	Low	NA	1.42	0.0001	9.50145E-05
4	1y6mo	adrenal gland	1	poorly differentiated	UH	Intermediate	NA	1.628	0.0002	0.000195319
5	1y10mo	neck	4	poorly differentiated	UH	Intermediate	NA	1.332	0.0019	0.001140052
6	2y3mo	pelvis	4	poorly differentiated	UH	Intermediate	NA	2.373	0.0093	0.007758074
7	3y10mo	retroperitoneum	4	poorly differentiated	UH	Intermediate	NA	1	0.0030	0.002563447
8	2y7mo	adrenal gland	4	poorly differentiated	UH	Low	NA	1.718	0.0025	0.004247806
9	1y11mo	adrenal gland	4	poorly differentiated	UH	Intermediate	NA	1	0.0180	0.01387578
10	4y5mo	posterior mediastinum	4	poorly differentiated	UH	High	NA	1.067	0.0091	0.002960215
11	9y5mo	retroperitoneum	4	poorly differentiated	UH	Intermediate	NA	1.466	0.0088	0.004694647
12	6mo	adrenal gland	4	poorly differentiated	UH	High	NA	1.953	0.0036	0.003134973
13	3y9mo	adrenal gland	4	poorly differentiated	UH	Intermediate	NA	1	0.0087	0.006636563
14	5y7mo	adrenal gland	4	poorly differentiated	UH	Low	NA	1	0.0062	0.005790541
15	4y6mo	suprarenal mass	4	poorly differentiated	UH	Intermediate	NA	1	0.0011	0.000750488
16	3y11mo	retroperitoneum	4	poorly differentiated	UH	Intermediate	NA	1.852	0.0007	0.000660758
17	3y9mo	no data	4	poorly differentiated	UH	Intermediate	NA	1	0.0012	0.001254473
18	3y7mo	retroperitoneum	4	poorly differentiated	UH	Intermediate	NA	1.992	0.0025	0.001914191
19	4y10mo	abdomen	3	poorly differentiated	UH	High	NA	1.613	0.0000	7.16375E-06
20	3y5mo	abdomen	4	poorly differentiated	UH	Low	NA	1	0.0014	0.000922693
21	9y6mo	paraspinal mass	4	poorly differentiated	UH	Low	NA	1.411	0.0000	1.89826E-05
22	3y8mo	neck	4	poorly differentiated	UH	high	NA	1	0.0005	0.000329807
23	8y5mo	retroperitoneum	2B	poorly differentiated	UH	Intermediate	NA	1	0.0000	7.66176E-06
1	9mo	adrenal gland	1	poorly differentiated	FH	Intermediate	NA	1.614	0.0000	1.58005E-05
2	1mo	abdomen	1	poorly differentiated	FH	Low	NA	1.525	0.0000	5.68577E-05
3	3mo	retroperitoneum	3	poorly differentiated	FH	Intermediate	NA	US	0.0001	4.5818E-05
4	6mo	adrenal gland	4	poorly differentiated	FH	Intermediate	NA	1.437	0.0001	6.35906E-05
5	25days	retroperitoneum	2B	poorly differentiated	FH	Intermediate	NA	1.399	0.0001	5.27509E-05
6	2mo	adrenal gland	2B	poorly differentiated	FH	Low	NA	1.183	0.0002	0.0001847
7	3mo	paravertebral	2A	poorly differentiated	FH	Low	NA	ND	0.0002	0.000226281
8	1mo	adrenal gland	1	poorly differentiated	FH	Low	NA	1.471	0.0002	0.000241229
9	6mo	retroperitoneum	4s	poorly differentiated	FH	Low	NA	1.524	0.0003	0.000390292
10	5mo	posterior mediastinum	1	poorly differentiated	FH	Low	NA	1.486	0.0003	0.000227276
11	1y10mo	retroperitoneum	3	differentiating	FH	Low	NA	1.415	0.0003	0.000396476
12	2mo	adrenal gland	4s	poorly differentiated	FH	Intermediate	NA	1.47	0.0004	0.000360389
13	1y0mo	retroperitoneum	3	poorly differentiated	FH	Low	NA	1.48	0.0005	0.000433776
14	2mo	retroperitoneum	2B	poorly differentiated	FH	Low	NA	1.357	0.0007	0.000508782
15	1mo	adrenal gland	4S	poorly differentiated	FH	Low	NA	1.18	0.0008	0.000366443
16	8y8mo	abdomen	4	poorly differentiated	FH	Intermediate	NA	1	0.0008	0.000920497
17	1y4mo	retroperitoneum	4	poorly differentiated	FH	Intermediate	NA	1.252	0.0012	0.001652937
18	11mo	neck	3	poorly differentiated	FH	Intermediate	NA	1.17	0.0020	0.001199686
19	5mo	retroperitoneum	3	poorly differentiated	FH	Low	NA	1.298	0.0022	0.003131543
20	1w	adrenal gland	4s	poorly differentiated	FH	Low	NA	1.24	0.0002	0.0018045

Table 5.1 Neuroblastoma tissue samples data and OD measurements. A total of 65 primary human NBL tumours were analysed. Information includes age, primary tumour location, stage, histology subtype, MKI, MYCN status, DNA index and OD measurements by colour deconvolution. MKI=mitosis-karyorrhexis-index; (high, ≥200/5,000 cells, intermediate, 100-200/5,000 cells and low, <100/5,000 cells). MYCN: A (amplified), NA (non-amplified); and Stage: 1 to 3: non-metastatic; 4: metastatic; 4S: metastatic with good prognosis. DNA index (1 or >1); Diff+ grade of neuroblastic differentiation: differentiated, poorly differentiated and undifferentiated. Histology: FH (Favourable Histology) and UH (Unfavourable Histology).

5.3.2 Microarray analysis of human neuroblastoma tumours

To further confirm the link between SULF2 and MYCN expression in primary neuroblastoma tumours, information was obtained through an analysis of gene expression arrays in a cohort of 416 tumour samples from the patients enrolled in GPOH clinical trials [Asgharzadeh et al., 2012]. This analysis revealed a statistically significant higher level of expression of SULF2 mRNA in tumours derived from patients with high-risk disease and MYCN amplification compared to tumours of patients with high risk disease, but lacking MYCN amplification, and tumours of patients with low risk disease ($p < 0.0001$; Figure 5.5). Similar results were obtained from a second cohort of 162 samples obtained from children enrolled in the COG clinical trials ($p < 0.0005$). These data provided further support to the observation that SULF2 is a direct target of MYCN in neuroblastoma and contributes to its tumourigenic function.

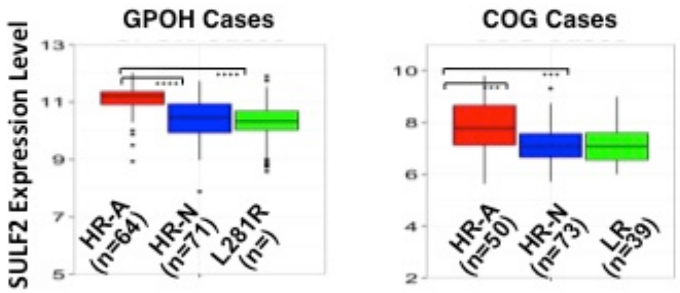

Figure 5.5 Expression of SULF2 RNA by gene array expression analysis generated from primary tumours. Two cohorts of patients treated in clinical trials conducted by GPOH (n=416) and COG (n=162) were analysed. The data were analysed by comparing 3 groups according to their clinical risk stratification (HR-A = high risk with MYCN-A, HR-N = high risk with MYCN NA and LR = low risk). **** $p < 0.0001$ in GPOH group and *** $p < 0.0005$ in COG group based on ANOVA.

5.3.3 SULF2 in a xenograft model of neuroblastoma

To validate our hypothesis that SULF2 modulates tumour growth, we used a genetic approach to either overexpress or knock down the expression of SULF2 in a xenograft model of NBL. To examine the consequences of SULF2 expression on tumour growth, we developed gene expression constructs with either the active (SULF2) or inactive SULF2 (S2ΔCC), as described in the Methods chapter (section 2.6.2). These constructs were transfected into CHLA-255 NBL cells, and injected into NOD/SCID mice (Figure 5.6). The harvested tumours showed an increase in weight for the SULF2 and also unexpectedly for the control group. Transduction with the mutated and inactive SULF2 (S2ΔCC) did not show any growth (Figure 5.6).

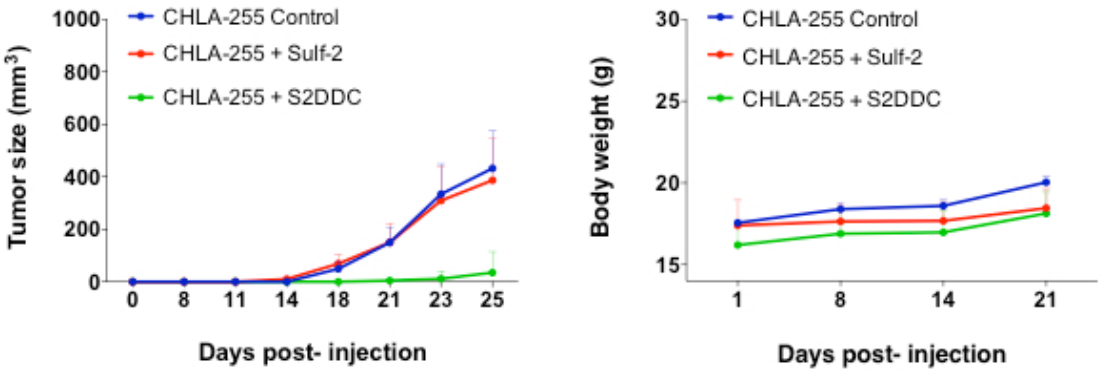

Figure 5.6 Tumour size and body weight in NOD/SCID mice after SULF2 overexpression. Size of the tumours (left) was evaluated until day 25 post injection. Both groups of CHLA-255 cells transfected with the control (scramble sequence) and or SULF2 overexpressing vector grew large tumours. As expected, cells with the mutated inactive SULF2 did not form tumours [Lemjabbar-Alaoui et al., 2010]. Graph on the right shows the body size in the three groups with equal values.

To further examine the effects of SULF2 on NBL cells *in vivo*, we used a xenograft model in NOD/SCID mice. We selected the human neuroblastoma cell SK-N-BE(2), a cell line that is known to have high levels of SULF2 and

MYCN expression, and transfected with a tet-inducible shRNA-targeting SULF2 vector (developed specifically in these studies and described in Methods, section 2.6.3). The cells were tested for doxycycline toxicity and grown in culture at a doxycycline concentration of 1 µg/ml to activate the shRNA to knockdown the expression of SULF2 (Figure 5.7). Transfected cells were positive for GFP and sorted by FACS to obtain a high concentration of transfected cells prior the injection into NOD/SCID mice (Figure 5.8).

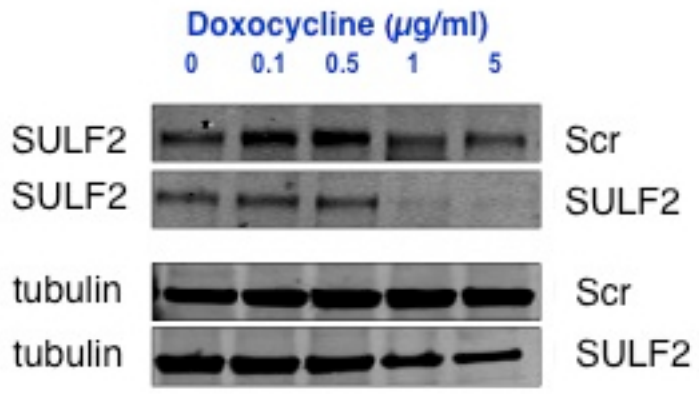

Figure 5.7 Western blot of SK-N-BE(2) cells transfected with the tet-inducible shRNA-targeting SULF2 vector **and treated with doxycycline.** The H1 promoter was activated by the presence of doxycycline and induced a knock down of SULF2. Scr, scramble (control) sequence maintained the elevated levels for SULF2.

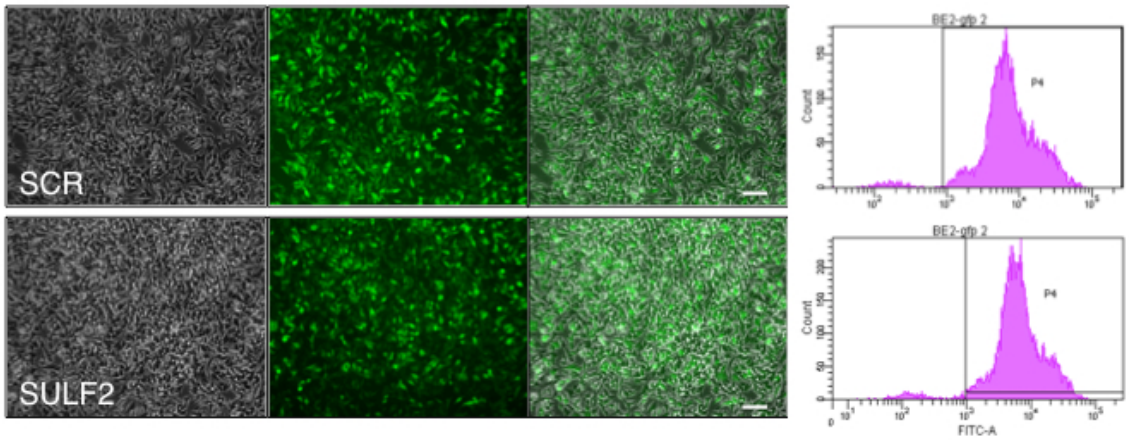

Figure 5.8 FACS sorting for GFP positive cells. Cells transfected with tet-inducible shRNA-targeting SULF2 vector are positive for GFP and have high transfection efficiency by microscopy (images on left, for x, y and z = 3 panel types) and by FACS sorting (image far right). Bar scale is 20 μm.

These transfected SK-N-BE(2) cells were then injected subcutaneously at 2 sites in NOD/SCID mice and monitored for growth (Figure 5.9 A and B). In each group (n=9 or 10 mice), 5 mice received doxycycline in the drinking water (to activate the knockdown of SULF2). In the 9 mice injected with SKNBE(2) pKRAB-SCR vector(scramble sequence), 8 mice developed bilateral tumours and the administration of doxycycline had no effect on the rate of tumour growth (one mouse in the doxycycline negative group did not develop tumours). By day 31 after tumour cell implantation, all mice had to be euthanized because one or both tumours had reached a volume greater than 1,500 mm^3 (Figure 5.9 A).

In the group of mice injected with SKNBE(2) pKRAB-SULF2 vector, treatment with doxycycline resulted in a tumour formation rate of 50 % only and in a significant delay in tumour growth with an average time for tumours to reach 500 mm^3 of 28 ±3.7 days compared to a tumour formation rate of 75 % and 100 % and an average time for tumours to reach 500 mm^3 of 20±5 and 18±2.3 days in the pKRAB-SCR control group (untreated and treated with doxycycline respectively). Unexpectedly, the pKRAB-SULF2 group untreated with doxycycline, although having an expected tumour formation rate of 100 % showed a delay in tumour growth with an average time to reach 500 mm^3 25 ± 3.2 days. This suggested that SULF2 expression might have been down regulated in this group due to the leakiness of the vector. This was confirmed by an analysis of SULF2 mRNA expression in tumour samples by RT-PCR

(Figure 5.9 C), which revealed a statistically significant decrease in SULF2 expression in the pKRAB-SULF2 subgroup (average ΔCT of 12.7 ± 0.8) not treated with doxycycline (p=0.008). An analysis of the expression of SULF2 protein by immunohistochemistry (Figure 5.9 D) confirmed the down regulation of SULF2 in tumours derived from mice implanted with pKRAB-SULF2 cells and untreated with doxycycline. The data in this group of mice are explained by the leakiness of the pKRAN-SULF2 vector and further demonstrate that down regulation of SULF2 expression in MYCN A cells inhibits tumourgenesis.

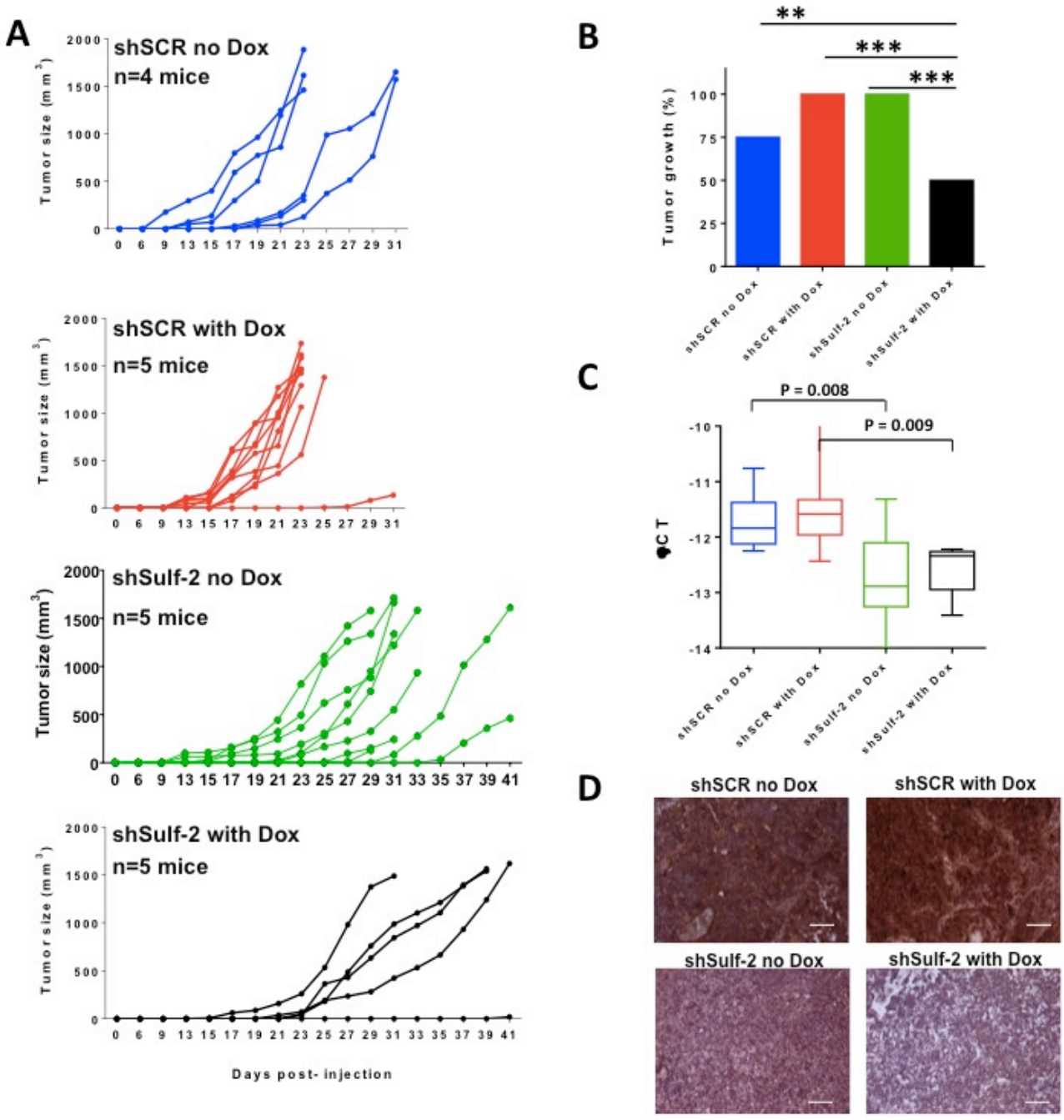

Figure 5.9 Loss of SULF2 expression in MYCN tumour cells inhibits tumour formation and growth. MYCN-A-SKNBE(2) cells were stably transfected with pKRABDULF2 and pKRABSCR and sorted for GFP expression. (A), Cells were injected in the right and left flank of NOD/SCID mice and monitored for development and growth. The graph represents the tumour diameter (in mm^3) of each tumour measured at the indicated times in the four groups. (B), The graph represents the percentage of tumours that developed in the 4 groups of mice. (C), pRT-PCR analysis

for SULF2 mRNA expression in tumours harvested at time of sacrifice. (D), Analysis of SULF2 expression by immunohistochemistry in sections of tumours derived from the 4 groups of mice. Scale bar = 20 µm.

In conclusion, in this Chapter we have demonstrated that SULF2 is significantly increased at protein and mRNA levels in a large cohort of human primary neuroblastoma when MYCN is amplified. We also demonstrated in an *in vivo* model that knock down of SULF2 in MYCN A NBL cells inhibits tumour growth. This data are encouraging and are consistent with SULF2 having a pro-tumourigenic role in neuroblastoma.

5.4. Discussion

In the previous chapters we observed that SULF2 was strikingly overexpressed in NBL cell lines that are MYCN amplified. In this Chapter we provide the first evidence that SULF2 is also over-expressed in a subgroup of primary human NBL tumours with the amplification of MYCN, a marker for poor survival, consistent with an important role for this endosulfatase in cancer. SULF2 was almost absent in the tumour tissue of MYCN non-amplified tumours and with favourable histology. The observation that SULF2 is increased in NBL patients with poor prognosis is similar to the previously reported findings in human oesophageal cancer and glioma [Lui et al., 2012; Phillips et al., 2012]. Often there has been discrepancy between *in vitro* and *in vivo* findings regarding SULFs. Both enzymes showed signalling inhibition for certain growth factors *in vitro* but, had antagonistic activities for cell proliferation and angiogenesis in *in vivo* [Lai et al., 2004; Lai et al., 2008; Uchimura et al., 2006; Morimoto-Tomita et

al., 2005]. This could be due to distinct effects on spatially separate substrates. For example, 6O-desulfation of cell surface HS could result in the reduction of growth factor binding at the cell, whereas 6O-desulfation of HS in the matrix could cause a release of growth factors from the ECM.

The *ex vivo* studies in human NBL tissue were extended by showing that SULF2 mRNA levels are significantly elevated in a large number of non-correlated primary human NBL tumours. We have demonstrated in two large cohorts (416 patients in the CPOH cohort and 162 from the COG cohort described, Figure 5.4) that SULF2 expression in primary NBL tumours was significantly elevated in high-risk NBL when MYCN was amplified compared to high-risk without MYCN amplification and low-risk. It is notable that there is no huge difference in the overall survival of children with HR disease. Those dependent on MYCN have been shown to have shorter time to progression and in general shorter time to death compared to patients whose tumour does not have MYCN amplification [London et al., 2011]. However, patients in the HR group without MYCN eventually succumb to their disease, and hence have similar overall outcomes. NBL patients with HR and MYCN A have a slightly but not significantly poorer outcome than HR patients with MYCN NA [London et at, 2011]. MYCN amplified NBL tumours are thought to use different mechanism to evade the immune system and have different metabolic profiles [Song et al., 2009]. It has been noted that MYCN NA HR patients tend to utilise the tumour microenvironment and express different pathways with higher proliferation capabilities [Metelitsa et al., 2004], and this would also be consistent with the observed effects of SULF2 on proliferation, and other effects

that might be rendered by SULF2 induced alterations in HS sulfation. Thus, SULF2 levels are quite conceivably a key aspect that explains at least in significant part the differences between the NBL sub-types.

Interestingly, both SULF2 and MYCN gene transcripts were found to be strongly over-expressed in B cells of patients with chronic lymphocytic leukaemia (CLL) resistant to treatment with fludarabine [Moussay et al., 2010]. This was seen in both *in vivo* and in *vitro* with both genes over-expressed in samples of resistant patients obtained before treatment. Based on our previous *in vitro* findings and on the central role that SULF2 has in promoting tumourigenesis, we hypothesised that its forced expression in a MYCN non-amplified NBL cell line will induce tumour growth *in vivo*. Unfortunately, our initial xenograft experiments with forced SULF2 expression described in this chapter did not reveal the expected results in full; although the NBL cells with SULF2 overexpression showed good tumour growth similar to the control (scrambled construct). In contrast, the NBL cells overexpressing catalytically inactive SULF2 (S2DCC) did not grow; this was also an unexpected finding, as an inactive SULF2 should not have arrested tumour formation to this extent. The function of the mutated SULF2 is not clear; it is however know to accumulate in the lipid raft with a more even distribution on the cell surface [Tang and Rosen, 2009]. Here the mutated SULF2 could compete with the endogenous SULF2 to bind to target sequences and block them. As known from the literature [Lemjabbar-Alaoui et al., 2010] and our data from Chapter 4, an overexpression of SULF2 should have promoted tumour growth compared to the control. Cells with forced overexpression of SULF2 are known to have a

transformed phenotype with increased proliferation and survival, whereas transfection with the mutated and inactive SULF2 did not show any changes [Lemjabbar-Alaoui et al., 2010]. Thus we could not confirm entirely *in vivo* our hypothesis that SULF2 has a tumour promoting role in NBL. It is not clear why the scrambled control and the inactive SULF2 gave unexpected results, and further experiments are required. The possibilities for the incongruent results obtained could lie in a technical problem with the transduction of the sequences, as they can be lost over a number of cell cycles and cells from the inactive SULF2 might have lost their viability during the injection into the mice. To avoid the possibility that the cells will lose expression of the shRNA construct, further repeats of this set of experiments after a clonal selection have being carried out. However, this experiment was not repeated due to a lack of time available in the fellowship. In contrast, the SULF2 knockdown *in vivo* experiment has provided some good results, consistent with our hypothesis, that the effect of genetic ablation of SULF2 on neuroblastoma growth will match the reports in the literature that reported a pro-tumourigenic effect of SULF2 [Nawroth et al., 2007, Yang et al., 2005, Lai et al., 2005, Lemjabbar-Alaoui et al., 2010].

In conclusion, our data have demonstrated that SULF2 is elevated in high-risk neuroblastoma patients with MYCN amplification, a marker of poor outcome and therapy resistance; and its promotes tumourgenesis in an *in vivo* model. SULF2 might represent a target for therapeutic intervention in NBL as reported for other cancers with elevated SULF2 levels and clearly warrants further investigation.

Chapter 6. Conclusions and Future Directions

6.1 Summary of key findings

This thesis sets out the findings of investigations into the role of HS, and in particular its sulfation patterns, in neuroblastoma. All the data presented in this thesis come from *in vitro* studies using established cell lines, human primary neuroblastoma tumours, and preliminary experiments with *in vivo* models using xenografts in immunodeficient mice.

The major findings presented in this thesis are:

- Amongst several HS biosynthetic and modification enzymes SULF2 is over-expressed in neuroblastoma cell lines when MYCN is amplified.
- SULF2 is also over-expressed in a large cohort of human primary high-risk neuroblastoma samples that have MYCN amplification
- SULF2 regulates neuroblastoma cell survival independently of MYCN status
- SULF2 is a direct target of MYCN in neuroblastoma and contributes to its tumourigenic functions.

  The above findings strongly support the main initial hypothesis of this study, that HSPGs and their sulfation status are involved in the regulation of NBL cell survival.

6.2 General discussion

The studies presented in this thesis have focussed on the role of SULF2 in neuroblastoma and the effects of its manipulation on tumour growth. It makes a contribution towards understanding the role of glycosylation in cancer and in particular reports the novel implications of a key enzyme responsible for the HS sulfation status in neuroblastoma.

Neuroblastoma is still a lethal disease for many patients despite multimodal treatment strategies that have reached their maximum potential, and new treatment approaches are required. MYCN amplification still plays a central role in the pathology of this cancer. MYCN is the major negative prognostic marker in NBL with amplification in 25 % of primary tumours and nearly half of high-risk cases [Maris and Matthay, 2010; Brodeur 1984]. It is known to play a crucial role in proliferation, differentiation and apoptosis. MYCN expression is essential during normal neural crest development and other neuronal organs and becomes down-regulated only towards the end of terminal tissue differentiation [Thomas et al., 2004]. Importantly, MYCN alone is sufficient for transformation [Weiss et al., 1997]. Despite many genomic studies, it has not been possible to identify new molecular targets in NBL [Molenaar et al., 2012] and the need to study the role of the microenvironment of cancer cells is becoming more widely accepted [Hanahan and Coussen, 2012].

The hypothesis of the work presented here was based on some preliminary data that indicated altered HS signatures amongst NBL cells and primary tumours with an increase in 6O-sulfation in HS chains (*see* Appendix 1). Here, a panel of 16 cancerous cell lines, of which 8 were NBL with various NMYC

amplification status, was screened for the major HS biosynthetic and modification enzymes. It was established that SULF2 was significantly increased in all MYCN amplified NBL cell lines tested. Increased levels of SULF2 expression would be expected to lead to decreased levels of 6-O sulfation as shown in our preliminary data (see Appendix 1) and in the literature [Phillips et al., 2012; Lemjabbar-Alaoui et al., 2010]; however further biochemical work is needed to study the sulfation status in NBL cell lines.

This data was confirmed in a large cohort of human primary NBL samples with MYCN amplification at both mRNA and protein levels. Manipulation of SULF2 expression by siRNA was found to induce cell apoptosis and reduce cell proliferation, without affecting the expression of MYCN. Forced over-expression of SULF2 in the absence of MYCN increased cell proliferation, consistent with previous studies [Lemjabbar-Alaoui et al., 2010] and from observation made in other human cancer types such as chronic lymphatic leukaemia [Moussay et al., 2010]. Our work suggests that SULF2 is a down stream target of MYCN and furthermore that it mediates the oncogenic effect of MYCN by a mechanism not yet identified. The data presented in this thesis clearly indicate that a direct result of SULF2 overexpression is enhanced proliferation and reduced apoptosis, both of which would be consistent with more aggressive tumour behaviour. There may well be other mechanisms related to tumour dissemination, which could result from over-expression of SULF2 and its consequences in terms of altered HS sulfation patterns and thus interactions with the extracellular matrix. Further work is needed on *in vivo* model studies of

forced over-expression of SULF2 in NBL to investigate these mechanisms in more detail.

Several transcription targets for MYCN have been identified by a ChiP assay study, one of which is the tumour suppressor p53, which also has SULF2 as a transcriptional target [Chau et al., 2009]. Induced expression of MYCN resulted in increased SULF2 expression, but not *vice versa*, strongly indicating that SULF2 is a down stream target of MYCN. It has always been considered that MYCN is a non-druggable target. Several therapeutic strategies investigated included small molecule inhibition to disrupt the Aurora-A/MYCN complex [Brockmann et al., 2013] and the PI3K/AKT/mTOR network [Gustafson and Weiss, 2010]. Despite being promising potential therapeutic approaches, these also target other kinases and biological processes and organs systems raising concerns about off-target effects and toxicity. However, recent studies found that inhibition of the BET bromodomain by JQ1 knocked down the expression of MYCN, impaired growth and induced apoptosis [Puissant et al., 2013]. In this study several genes responded to the treatment by being knocked down, and SULF2 was part of the response signature. Interestingly many of the genes (such as PHOX2B and SULF2) are associated with neuronal crest differentiation.

Recently SULF2 has been considered important to drive tumourigenesis through the action of several growth factors [Phillips et al., 2012; Bret et al., 2011; Lemjabbar-Alaoui et al., 2010]. Several treatment strategies in the modulation of heparan sulfate and SULF2 have been the focus of recent studies. PI-88, initially developed as an anti-heparanase agent (which is also

anti-angiogenic and inhibits some growth factors), has also been shown to have SULF2 inhibitory functions [Hossain et al., 2010]. PI-88 has been tested in clinical trials for liver cancer but was found to have a lack of efficacy due to dosage limitations of toxicity and off-target effects [Wang et al., 2013]. In addition, other protease inhibitors suppress SULF2 expression levels in some cancer cell lines, and reduce tumour size in mice xenografts [Khurana et al., 2013; Garteiser et al., 2010]. Some of these inhibitors have been tested in clinical trial for the treatment of lung and prostate cancer but unfortunately, showed some serious side effects due to their broad range of activities [Kudchadkar et al., 2008; Schelwies et al., 2010]. Other therapeutic possibilities would include the development of small molecule inhibitors or antibody-based therapies targeted more specifically against SULF2. However, the success of further treatments is dependent on a better knowledge of the mechanisms by which SULF2 plays roles in neuroblastoma behaviour, particularly when MYCN is amplified. Additionally, the information available so far SULF2 suggests to have an extremely complex molecule; this may improve the chances of it being a successful target for drug development.

6.3 Concluding remarks and future investigations

This thesis set out to investigate the relationship between sulfation of HS and neuroblastoma. All the data presented in this thesis derive from *in vitro* studies using establishes cell lines and primary human neuroblastoma tumours. Experiments *in vivo* used xenografts in immunedeficient NOD/SCID mice.

Our data point to SULF2 as regulator of HS sulfation, being downstream of MYCN and an important contributor to its oncogenic function. They also emphasize the critical role that HSPGs could play as regulators of survival and proliferation in neuroblastoma, a subject that has not been investigated so far.

A number of avenues for future investigations arise from the work presented in this thesis:

6.3.1 Effects of SULF2 overexpression in the mouse xenograft model

The experiments from which preliminary data is described in Chapter 5 will be completed, in order to assess the effect of SULF2 overexpression down *in vivo*.

6.3.2 To characterise biochemical changes in HS in neuroblastoma.

Some preliminary studies on HS structure were undertaken and are presented in Appendix 3. We aim to further characterise, initially by disaccharide composition analysis, the sulphation status of HS in neuroblastoma cell lines and human tissue, and in particular the consequences of over-expresssion or siRNA knock-down of SULF2. These experiments will allow a better understanding of the functional effects of SULF2, and the mechanisms by which changes in HS mediate biological effects in NBL.

6.3.3 To study the signalling pathways regulated by SULF2 in neuroblastoma

Using our established methods for genetically altering the expression of SULF2, we aim to examine the effects on regulation of critical growth factor signalling pathways in NBL. This is expected to include FGFs and VEGF, but may reveal

additional growth factor targets of potential biological and therapeutic significance. Additionally because SULFs are expressed in soluble as well as cell-surface associated forms, SULF2 might also have non-cell autonomous or paracrine activity which needs to be addressed in future work.

Publications

Part of the work of this thesis has been published:

Solari V, Borriello L, Turcatel G, Shimada H, Sposto R, Fernandez GE, Asgharzadeh S, Yates EA, Turnbull JE, DeClerck YA. MYCN-dependent expression of Sulfatase2 regulates neuroblastoma cell survival. *Cancer Research* (in press).

Solari V, Jesudason EC, Turnbull JE, Yates EA Determining the anti-coagulant-independent anti-cancer effects of heparin. *Br J Cancer* 103:593-4, 2010

References

Ai X, Do AT, Lozynska O, Kusche-Gullberg M, Lindahl U, Emerson CP Jr. QSulf1 remodels the 6-O sulfation states of cell surface heparan sulfate proteoglycans to promote Wnt signaling. J Cell Biol 162:341-51, 2003

Aikawa J, Esko JD. Molecular cloning and expression of a third member of the heparan sulfate/heparin GlcNAc N-deacetylase/ N-sulfotransferase family. J Biol Chem 274:2690-5, 1999

Ara T, DeClerck YA. Mechanisms of invasion and metastasis in human neuroblastoma. Cancer Metastasis Rev 25:645-57, 2006

Arvanitis C, Felsher DW. Conditional transgenic models define how MYC initiates and maintains tumorigenesis. Semin Cancer Biol 16:313-7, 2006

Asgharzadeh S, Salo JA, Ji L, Oberthuer A, Fischer M, Berthold F, et al. Clinical significance of tumor-associated inflammatory cells in metastatic neuroblastoma. J Clin Oncol 30:3525-32, 2012

Ashikari-Hada S, Habuchi H, Kariya Y, Itoh N, Reddi AH, Kimata K. Characterization of growth factor-binding structures in heparin/heparan sulfate using an octasaccharide library. J Biol Chem 279:12346-54, 2004

Backen AC, Cole CL, Lau SC, Clamp AR, McVey R, Gallagher JT, Jayson GC. Heparan sulphate synthetic and editing enzymes in ovarian cancer. Br J Cancer 96:1544-8, 2007

Basta NO, James PW, Gomez-Pozo B, Craft AW, McNally RJ. Survival from childhood cancer in northern England, 1968-2005. Br J Cancer 105:1402-8, 2011

Beard J. The Enzyme Treatment of Cancer and its Scientific Basis, 1911

Beckwith JB, Martin RF. Observations on the histopathology of neuroblastomas. J Pediatr Surg 3:106-10, 1968

Beckwith JB, Perrin EV. In situ neuroblastomas: contribution to the natural history of neural crest tumors. Am J Pathol 43:1089-104, 1963

Bell E, Chen L, Liu T, Marshall GM, Lunec J, Tweddle DA. MYCN oncoprotein targets and their therapeutic potential. Cancer letters. 293:144-157, 2010

Biedler J, Roffler-Tarlov S, Schachner M, Freeman LS. Multiple neurotransmitter systems by human neuroblastoma cell lines and clones. Cancer Res 38:3751-7, 1978

Boon K, Caron HN, van AR, Valentijn L, Hermus MC, van SP, et al. N-myc enhances the expression of a large set of genes functioning in ribosome biogenesis and protein synthesis. EMBO J 20:1383-93, 2001

Boveri T. Concerning the origins of malignant tumours by Theodor Boveri. Translated and annotated by Henry Harris. Cold Spring Harbor Laboratory Press. 2008

Bregman MD, Meyskens Jr FL. *In vitro* modulation of human and murine melanoma growth by prostanoid analogues. Prostaglandins 26: 449–456, 1983

Bret C, Moreaux J, Schved JF, Hose D, Klein B. SULFs in human neoplasia: implication as progression and prognosis factors. J Transl Med 9:72, 2011

Brockmann M, Poon E, Berry T, Carstensen A, Deubzer HE, Rycak L, Jamin Y, Thway K, Robinson SP, Roels F, Witt O, Fischer M, Chesler L, Eilers M. Small molecule inhibitors of aurora-a induce proteasomal degradation of N-myc in childhood neuroblastoma. Cancer Cell 24:75-89, 2013

Brodeur GM. Neuroblastoma: biological insights into a clinical enigma. Nat Rev Cancer 3:203-16, 2003

Brodeur GM, Pritchard J, Berthold F, et al. Revisions of the international criteria for neuroblastoma diagnosis, staging, and response to treatment. J Clin Oncol 11:1466-1477, 1993

Brodeur GM, Seeger RC, Barrett A, Berthold F, Castleberry RP, D' Angio G, De Bernarid B, Evans AE, Favrot M, et al. International criteria for diagnosis, staging, and response to treatment in patients with neuroblastoma. J Clin Oncol 6:1874-1881, 1988

Buechner J, Einvik C. N-myc and noncoding RNAs in neuroblastoma. Mol Cancer Res 10:1243-53, 2012

Brugal G. Pattern recognition, image processing, related data analyssi and expert system integrated in medical microscopy 286-287, 1988

Bullock SL, Fletcher JM, Beddington RS, Wilson VA. Renal agenesis in mice homozygous for a gene trap mutation in the gene encoding heparan sulfate 2-sulfotransferase. Genes Dev 12:1894-906, 1998

Bunin GR, Ward E, Kramer S, Rhee CA, et al. Neuroblastoma and parental occupation. Am J Epidemiol 131:776-780, 1990

Carmeliet P, Jain RK. Molecular mechanisms and clinical applications of angiogenesis. Nature 473:298-307, 2011

Carr-Wilkinson J, Griffiths R, Elston R, Gamble LD, Goranov B, Redfern CP, Lunec J, Tweddle DA. Outcome of the p53-mediated DNA damage response in neuroblastoma is determined by morphological subtype and MYCN expression. Cell Cycle 10:3778-87, 2011

Casu B, Lindahl U. Structure and biological interactions of heparin and heparan sulfate. Adv Carbohydr Chem Biochem 57:159-206, 2001

Chau BN, Diaz RL, Saunders MA, Cheng C, Chang AN, et al. Identification of SULF2 as a novel transcriptional target of p53 by use of integrated genomic analyses. Cancer Research 69:1368–1374, 2009

Cheung, Nai-Kong. Neuroblastoma. Springer-Verlag. ISBN 3-540-40841- p. 63, 2005

Cheung NK, Dyer MA. Neuroblastoma: developmental biology, cancer genomics and immunotherapy. Nat Rev Cancer 13:397-411, 2013

Clausen DM, Guo J, Parise RA, Beumer JH, Egorin MJ, Lazo JS, Prochownik EV, Eiseman JL. In vitro cytotoxicity and in vivo efficacy, pharmacokinetics, and metabolism of 10074-G5, a novel small-molecule inhibitor of c-Myc/Max dimerization. J Pharmacol Exp Ther 335:715-27, 2010

Cohn SL, Pearson AD, London WB et al. The international Neuroblastoma Risk Group (INRG) classification system: an INRG Task Force report. J Clin Oncol 27:289-297, 2009

Conrad HE. Heparin-binding Proteins Academic Press, San Diego, 1998

Crawford BE, Garner OB, Bishop JR, Zhang DY, Bush KT, Nigam SK, Esko JD. Loss of the heparan sulfate sulfotransferase, Ndst1, in mammary epithelial cells selectively blocks lobuloalveolar development in mice. PLoS One 5:e10691, 2010

Dai Y, Yang Y, MacLeod V, Yue X, Rapraeger AC, Shriver Z, Venkataraman G, Sasisekharan R, Sanderson RD.HSulf-1 and HSulf-2 are potent inhibitors of myeloma tumor growth in vivo. J Biol Chem 280:40066-73, 2005

Danesin C, Agius E, Escalas N, Ai X, Emerson C, Cochard P, Soula C. Ventral neural progenitors switch toward an oligodendroglial fate in response to increased Sonic hedgehog (Shh) activity: involvement of Sulfatase 1 in modulating Shh signaling in the ventral spinal cord. J Neurosci 26:5037-48, 2006

Dang CV. MYC on the path to cancer. Cell 149:22-35, 2012

David G, Bai XM, Van der Schueren B, Cassiman JJ, Van den Berghe H. Developmental changes in heparan sulfate expression: in situ detection with mAbs. J Cell Biol 119:961-75, 1992

Davies JA, Yates EA, Turnbull JE. Structural determinants of heparan sulphate modulation of GDNF signalling. Growth Factors 21:109-19, 2003

Davies PC, Lineweaver CH. Cancer tumors as Metazoa 1.0: tapping genes of ancient ancestors. Phys Biol 8:015001, 2011.

Delcommenne M, Klingemann HG. Detection and characterization of syndecan-1-associated heparan sulfate 6-O-sulfated motifs overexpressed in multiple myeloma cells using single chain antibody variable fragments. Hum Antibodies 21:29-40, 2012

Dennissen MA, Jenniskens GJ, Pieffers M, Versteeg EM, Petitou M, Veerkamp JH, van Kuppevelt TH. Large, tissue-regulated domain diversity of heparan sulfates demonstrated by phage display antibodies. J Biol Chem 277:10982-6, 2002

Dhoot G K, Gustafsson MK, Ai X, Sun W, Standiford DM, Emerson CP, Jr. Regulation of Wnt Signaling and Embryo Patterning by an Extracellular Sulfatase. Science 293, 1663-1666, 2001

Dierks T, Schmidt B, von Figura K. Conversion of cysteine to formylglycine: a protein modification in the endoplasmic reticulum. Proc Natl Acad Sci U S A 94:11963-8, 1997

Esko JD, Lindahl U. Molecular diversity of heparan sulfate. J Clin Invest 108:169-73, 2001

Esko JD, Selleck SB. Order out of chaos: assembly of ligand binding sites in heparan sulfate. Annu Rev Biochem 71:435-471, 2002

Fakhari M, Pullirsch D, Paya K, Abraham D, Hofbauer R, Aharinejad S. Upregulation of vascular endothelial growth factor receptors is associated with advanced neuroblastoma. J Pediatr Surg 37:582-7, 2002

Fan G, Xiao L, Cheng L, Wang X, Sun B, Hu G. Targeted disruption of NDST-1 gene leads to pulmonary hypoplasia and neonatal respiratory distress in mice. FEBS Lett 467:7-11, 2000

Ferguson BW, Datta S. Role of heparan sulfate 2-o-sulfotransferase in prostate cancer cell proliferation, invasion, and growth factor signaling. Prostate Cancer 2011:893208, 2011

Fernández-Vega I, García O, Crespo A, Castañón S, Menéndez P, Astudillo A, Quirós LM. Specific genes involved in synthesis and editing of heparan sulfate proteoglycans show altered expression patterns in breast cancer. BMC Cancer 13:24, 2013

Ferrara N. VEGF-A: a critical regulator of blood vessel growth. Eur Cytokine Netw 20:158-63, 2009

Feyzi E, Lustig F, Fager G, Spillmann D, Lindahl U, Salmivirta M. Characterization of heparin and heparan sulfate domains binding to the long splice variant of platelet-derived growth factor A chain. J Biol Chem 272:5518-24, 1997

Folkman J. Tumor angiogenesis: therapeutic implications. N Engl J Med 285:1182-6, 1971

Follis AV, Hammoudeh DI, Daab AT, Metallo SJ. Small-molecule perturbation of competing interactions between c-Myc and Max. Bioorg Med Chem Lett 19:807-10, 2009

Forsberg E, Pejler G, Ringvall M, Lunderius C, Tomasini-Johansson B, Kusche-Gullberg M, Eriksson I, Ledin J, Hellman L, Kjellén L. Abnormal mast cells in mice deficient in a heparin-synthesizing enzyme. Nature 400:773-6, 1999

French AE, Grant R, Weitzman S, Ray JG, et al. Folic acid food fortification is associated with a decline in neuroblastoma. Clin Pharmacol Ther 74:288-294, 2003

Furuta J, Umebayashi Y, Miyamoto K, Kikuchi K, Otsuka F, Sugimura T, Ushijima T. Promoter methylation profiling of 30 genes in human malignant melanoma. Cancer Sci 95:962-8, 2004

Fuster MM, Esko JD. The sweet and sour of cancer: glycans as novel therapeutic targets. Nat Rev Cancer 5:526-4, 2005

Fuster MM, Wang L, Castagnola J, Sikora L, Reddi K, Lee PH, Radek KA, Schuksz M, Bishop JR, Gallo RL, Sriramarao P, Esko JD. Genetic alteration of endothelial heparan sulfate selectively inhibits tumor angiogenesis. J Cell Biol 177:539-49, 2007

Gallagher JT, Walker M. Molecular distinctions between heparan sulphate and heparin. Analysis of sulphation patterns indicates that heparan sulphate and heparin are separate families of N-sulphates polysaccharides. Biochem J 230:665-74, 1985

Garteiser P, Doblas S, Watanabe Y, Saunders D, Hoyle J, Lerner M, He T, Floyd RA, Towner RA. Multiparametric assessment of the anti-glioma

properties of OKN007 by magnetic resonance imaging. J Magn Reson Imaging 31:796-806, 2010

George RE, Lipshultz SE, Lipsitz SR, Colan SD, Diller L. Association between congenital cardiovascular malformations and neuroblastoma. J Pediatr 144:444-448, 2004

Germain M, Affar EB, D'Amours D, Dixit VM, Salvesen GS, Poirier GG. Cleavage of automodified poly(ADP-ribose) polymerase during apoptosis. Evidence for involvement of caspase-7. J Biol Chem 274:28379-84, 1999

Goh YI, Bollano E, Einarson TR, Koren G. Prenatal multivitamin supplementation and rates of pediatric cancers: a meta analysis. Clin Pharmacol Ther 81:685-691, 2007

Gorsi B, Whelan S, Stringer SE. Dynamic expression patterns of 6-O endosulfatases during zebrafish development suggest a subfunctionalisation event for Sulf2. Dev Dyn 239:3312-23, 2010

Grimmer MR, Weiss WA. Childhood tumors of the nervous system as disorders of normal development. Curr Opin Pediatr 18:634-8, 2006

Grobe K, Esko JD. Regulated translation of heparan sulfate N-acetylglucosamine N-deacetylase/n-sulfotransferase isozymes by structured 5'-untranslated regions and internal ribosome entry sites. J Biol Chem 277:30699-706, 2002

Gross RE, Farber S, Martin LW. Neuroblastoma sympatheticum; a study and report of 217 cases. Pediatrics 23:1179-91, 1959

Guimond S, Maccarana M, Olwin BB, Lindahl U, Rapraeger AC. Activating and inhibitory heparin sequences for FGF-2 (basic FGF). Distinct requirements for FGF-1, FGF-2, and FGF-4. J Biol Chem 268:23906–23914, 1993

Guiral EC, Faas L, Pownall ME. Neuronal crest migration requires the activity of the extracellular sulfatases XtSulf1 and XtSulf2. Dev Biol 341:375-88, 2010

Gurel B, Iwata T, Koh CM, Jenkins RB, Lan F, Van Dang C, Hicks JL, Morgan J, Cornish TC, Sutcliffe S, Isaacs WB, Luo J, De Marzo AM. Nuclear MYC protein overexpression is an early alteration in human prostate carcinogenesis. Mod Pathol 21:1156-67, 2008

Gustafson WC, Weiss WA. Myc proteins as therapeutic targets. Oncogene 29:1249-59, 2010

Haase D, Ablin AR, Miller C, Zoger S, Matthay KK. Complete pathologic maturation and regression of stage IVS neuroblastoma without treatment. Cancer 62:818-825, 1988

Haase GM, Wong KY, deLorimier AA, Sather HN, HammonGD. Improvement in survival after excision of primary tumor in stage III neuroblastoma. J Pediatr Surg 24:194-200, 1989

Habuchi H, Tanaka M, Habuchi O, Yoshida K, Suzuki H, Ban K, Kimata K. The occurrence of three isoforms of heparan sulfate 6-O-sulfotransferase having different specificities for hexuronic acid adjacent to the targeted N-sulfoglucosamine. J Biol Chem 275:2859-68, 2000

Habuchi H, Miyake G, Nogami K, Kuroiwa A, Matsuda Y, Kusche-Gullberg M, Habuchi O, Tanaka M, Kimata K., Biosynthesis of heparan-sulphate with diverse structures and functions: two alternatively spliced forms of human heparan sulphate 6-O-sulphotransferase-2 having different expression patterns and properties. Biochem J 371:131-42, 2003

Häcker U, Nybakken K, Perrimon N. Heparan sulphate proteoglycans: the sweet side of development. Nat Rev Mol Cell Biol 6:530-41, 2005

Hampson IN, Kumar S, Gallagher JT. Differences in the distribution of O-sulphate groups of cell-surface and secreted heparan sulphate produced by human neuroblastoma cells in culture. Biochim Biophys Acta 763:183-90, 1983

Hampson IN, Kumar S, Gallagher JT. Heterogeneity of cell-associated and secretory heparan sulphate proteoglycans produced by cultured human neuroblastoma cells. Biochim Biophys Acta 801:306-13, 1984

Hamrick SEG, Olshan AF, Neglia JP, Pollock BH. Association of pregnancy history and birth characteristics with neuroblastoma. A report from the Children's Cancer Group and Pediatric Group. Paediatr Perinat Epidemiol 15:328-337, 2001

Hanahan D, Coussens LM. Accessories to the crime: functions of cells recruited to the tumor microenvironment. Cancer Cell 21:309-22, 2012

Hanahan D, Weinberg RA. Hallmarks of cancer: the next generation.
Cell 144:646-74, 2011

Hileman RE, Fromm JR, Weiler JM Linhardt RJ. Glycosaminoglycanprotein interactions: definition of consensus sites in glycosaminoglycan binding proteins. Bioessays. 20, 156-67, 1998

Holst CR, Bou-Reslan H, Gore BB, Wong K, Grant D, Chalasani S, Carano RA, Frantz GD, Tessier-Lavigne M, Bolon B, French DM, Ashkenazi A. Secreted sulfatases Sulf1 and Sulf2 have overlapping yet essential roles in mouse neonatal survival. PLoS One 2:e575, 2007

Hossain MM, Hosono-Fukao T, Tang R, Sugaya N, van Kuppevelt TH, Jenniskens GJ, Kimata K, Rosen SD, Uchimura K. Direct detection of HSulf-1 and HSulf-2 activities on extracellular heparan sulfate and their inhibition by PI-88. Glycobiology 20:175-86, 2010

Hughes M, Marsden HB, Palmer MK. Histologic patterns of neuroblastoma related to prognosis and clinical staging. Cancer 34:1706-11, 1974

Hur K, Han TS, Jung EJ, Yu J, Lee HJ, Kim WH, Goel A, Yang HK.
Up-regulated expression of sulfatases (SULF1 and SULF2) as prognostic and metastasis predictive markers in human gastric cancer. J Pathol 228:88-98, 2012

Ikeda Y, Lister J, Bouton JM, Buyukpamukcu M. Congenital neuroblastoma, neuroblastoma in situ and the normal fetal development of the adrenal gland. J Ped Surg 16:636-44, 1981

Irie A, Yates EA, Turnbull JE, Holt CE. Specific heparan sulfate structures involved in retinal axon targeting. Development 129:61-70, 2002

Ishihara M, Takano R, Kanda T, Hayashi K, Hara S, Kikuchi H, Yoshida K. Importance of 6-O-sulfate groups of glucosamine residues in heparin for activation of FGF-1 and FGF-2. J Biochem 118:1255-60, 1995

Iozzo RV. Basement membrane proteoglycans: from cellar to ceiling. Nat Rev Mol Cell Biol 6:646-56, 2005

Iwao K, Inatani M, Matsumoto Y, Ogata-Iwao M, Takihara Y, Irie F, Yamaguchi Y, Okinami S, Tanihara H. Heparan sulfate deficiency leads to Peters anomaly in mice by disturbing neural crest TGF-beta2 signaling. J Clin Invest 119:1997-2008, 2009

Jain RK, Duda DG, Clark JW, Loeffler JS. Lessons from phase III clinical trials on anti-VEGF therapy for cancer. Nat Clin Pract Oncol 3:24-40, 2006

Jayson GC, Lyon M, Paraskeva C, Turnbull JE, Deakin JA, Gallagher JT. Heparan sulfate undergoes specific structural changes during the progression from human colon adenoma to carcinoma in vitro. J Biol Chem 273:51-7, 1998

Jia J, Maccarana M, Zhang X, Bespalov M, Lindahl U, Li JP. Lack of L-iduronic acid in heparan sulfate affects interaction with growth factors and cell signaling. J Biol Chem 284:15942–15950, 2009

Johnson CC, Spitz MR. Neuroblastoma: case-control analysis of birth characteristics. J Natl Cancer Inst 74:789-92, 1985

Joshi VV, Cantor AB, Altshuler A, Larkin EW, Neill JSA, Shuster JJ, et al. Age-linked prognostic categorization based on a new histologic grading system of neuroblastomas: a clinical pathologic study of 211 cases from the Pediatric Oncology Group. Cancer 69:2197-2211, 1992

Joyce JA, Pollard JW. Microenvironmental regulation of metastasis. Nat Rev Cancer 9:239-52, 2009

Kaatsch P. Epidemiology of childhood cancer. Cancer Treat Rev 36:277-85, 2010

Keshelava N, Seeger RC, Groshen S, Reynolds CP. Drug resistance patterns of human neuroblastoma cell lines derived from patients at different phases of therapy. Cancer Res 58:5396-405, 1998

Keshelava N, Zuo JJ, Chen P, Waidyaratine SN, Luna MC, Gomer CJ, Triche TJ, Reynolds C P. Loss of p53 function confers high-level multi-drug resistance in neuroblastoma cell lines. *Cancer Res.* 61:6185-93, 2001.

Kan M, Wang F, Xu J, Crabb JW, Hou J, McKeehan WL. An essential heparin-binding domain in the fibroblast growth factor receptor kinase. Science 259:1918-21, 1993

Khurana A, Beleford D, He X, Chien J, Shridhar V. Role of heparan sulfatases in ovarian and breast cancer. Am J Cancer Res 3:34-45, 2013

Kobayashi M, Habuchi H, Yoneda M, Habuchi O, Kimata K. Molecular cloning and expression of Chinese hamster ovary cell heparan-sulfate 2-sulfotransferase. J Biol Chem 272:13980-5, 1997

Kota J, Chivukula RR, O'Donnell KA, Wentzel EA, Montgomery CL, Hwang HW, Chang TC, Vivekanandan P, Torbenson M, Clark KR, Mendell JR, Mendell JT. Therapeutic microRNA delivery suppresses tumorigenesis in a murine liver cancer model. Cell 137:1005-17, 2009

Kreuger J, Salmivirta M, Sturiale L, Giménez-Gallego G, Lindahl U. Sequence analysis of heparan sulfate epitopes with graded affinities for fibroblast growth factors 1 and 2. J Biol Chem 276:30744-52, 2001

Kreuger J, Jemth P, Sanders-Lindberg E, Eliahu L, Ron D, Basilico C, Salmivirta M, Lindahl U. Fibroblast growth factors share binding sites in heparan sulphate. Biochem J 389:145-50, 2005

Kudchadkar R, Gonzalez R, Lewis KD. PI-88: a novel inhibitor of angiogenesis. Expert Opin Investig Drugs 17:1769-76, 2008

Lai J, Chien J, Staub J, Avula R, Greene EL, Matthews TA, Smith DI, Kaufmann SH, Roberts LR, Shridhar V. Loss of HSulf-1 up-regulates heparin-binding growth factor signaling in cancer. J Biol Chem 278:23107-17, 2003

Lai JP, Chien JR, Moser DR, Staub JK, Aderca I, Montoya DP, Matthews TA, Nagorney DM, Cunningham JM, Smith DI, Greene EL, Shridhar V, Roberts LR. hSulf1 Sulfatase promotes apoptosis of hepatocellular cancer cells by decreasing heparin-binding growth factor signaling. Gastroenterology 126:231-48, 2004

Lai JP, Sandhu DS, Yu C, Moser CD, Hu C, Shire AM, Aderca I, Murphy LM, Adjei AA, Sanderson S, Roberts LR. Sulfatase 2 protects hepatocellular carcinoma cells against apoptosis induced by the PI3K inhibitor LY294002 and ERK and JNK kinase inhibitors. Liver Int 30:1522-8, 2010

Lakhani SA, Masud A, Kuida K, Porter GA Jr, Booth CJ, Mehal WZ, Inayat I, Flavell RA. Caspases 3 and 7: key mediators of mitochondrial events of apoptosis. Science 311:847-51, 2006

Lamanna WC, Baldwin RJ, Padva M, Kalus I, Ten Dam G, van Kuppevelt TH, Gallagher JT, von Figura K, Dierks T, Merry CL. Heparan sulfate 6-O-endosulfatases: discrete in vivo activities and functional co-operativity. Biochem J 400:63-73, 2006

Lamanna WC, Frese MA, Balleininger M, Dierks T. Sulf loss influences N-, 2-O-, and 6-O-sulfation of multiple heparan sulfate proteoglycans and modulates fibroblast growth factor signaling. J Biol Chem 283:27724-35, 2008

Landau M. Verhandlungen des Internationalen Pathologischen Kongresses, Turin 1911

Leder A, Pattengale PK, Kuo A, Stewart TA, Leder P. Consequences of widespread deregulation of the c-myc gene in transgenic mice: multiple neoplasms and normal development. Cell 45:485-95, 1986

Lee RE, Young RH, Castleman B. James Homer Wright: a biography of the enigmatic creator of the Wright stain on the occasion of its centennial. Am J Surg Pathol 26:88–96, 2002

Lemjabbar-Alaoui H, van Zante A, Singer MS, Xue Q, Wang YQ, Tsay D, He B, Jablons DM, Rosen SD. Sulf-2, a heparan sulfate endosulfatase, promotes human lung carcinogenesis. Oncogene 29:635-46, 2010

Lidholt K, Lindahl U. Biosynthesis of heparin. The D-glucuronosyl- and N-acetyl-D-glucosaminyltransferase reactions and their relation to polymer modification. Biochem J 287:21-9, 1992

Light JE, Koyama H, Minturn JE, Ho R, Simpson AM, Iyer R, Mangino JL, Kolla V, London WB, Brodeur GM. Clinical significance of NTRK family gene expression in neuroblastomas. Pediatr Blood Cancer 59:226-32, 2012

Lin A, Ardinger HH, Pierpont ME. Classification of cardiovascular malformations associated with neuroblastoma. J Pediatr 146:439-441, 2005

London WB, Castel V, Monclair T, Ambros PF, Pearson AD, Cohn SL, Berthold F, Nakagawara A, Ladenstein RL, Iehara T, Matthay KK. Clinical and biological features predictive of survival after relapse of neuroblastoma: a report from the International Neuroblastoma Risk Group project. J Clin Oncol 29:3286-92, 2001

Lui NS, van Zante A, Rosen SD, Jablons DM, Lemjabbar-Alaoui H.SULF2 expression by immunohistochemistry and overall survival in oesophageal cancer: a cohort study. BMJ Open 2:6, 2012

Lundin L, Larsson H, Kreuger J, Kanda S, Lindahl U, Salmivirta M, Claesson-Welsh L. Selectively desulfated heparin inhibits fibroblast growth factor-induced mitogenicity and angiogenesis. J Biol Chem 275:24653–24660, 2000

Lutz W, Stöhr M, Schürmann J, Wenzel A, Löhr A, Schwab M. Conditional expression of N-myc in human neuroblastoma cells increases expression of alpha-prothymosin and ornithine decarboxylase and accelerates progression into S-phase early after mitogenic stimulation of quiescent cells. Oncogene 13:803-12, 1996

Lyon M, Deakin JA, Rahmoune H, Fernig DG, Nakamura T, Gallagher JT. Hepatocyte growth factor/scatter factor binds with high affinity to dermatan sulfate. J Biol Chem 273:271-8, 1998

Lyon M, Rushton G, Gallagher JT. The interaction of the transforming growth factor-betas with heparin/heparan sulfate is isoform-specific. J Biol Chem 272:18000-6, 1997

Mahalingam Y, Gallagher JT, Couchman JR. Cellular adhesion responses to the heparin-binding (HepII) domain of fibronectin require heparan sulfate with specific properties. J Biol Chem 282:3221-30, 2007

Makinen T, Olofsson B, Karpanen T, Hellman U, Soker S, Klagsbrun M, Eriksson U, Alitalo K. Differential binding of vascular endothelial growth factor B splice and proteolytic isoforms to neuropilin-1. J Biol Chem 274:21217-22, 1999

Mäkinen J. Microscopic patterns as guide to prognosis of neuroblastoma in childhood. Cancer 29:1637-1646, 1972

Maresh GA, Chernoff EA, Culp LA. Heparan sulfate proteoglycans of human neuroblastoma cells: affinity fractionation on columns of platelet factor-4+. Arch Biochem Biophys 233:428-37, 1984

Maris JM, Matthay KK. Molecular biology of neuroblastoma. J Clin Oncol 17:2264-79, 1999

Maris JM, Weiss MJ, Mosse Y, et al. Evidence for a hereditary neuroblastoma predisposition locus at chromosome 16p12-13. Cancer Res 62:6651-6658, 2002

Metelitsa LS, Wu HW, Wang H, Yang Y, Warsi Z, Asgharzadeh S, Groshes S, Wilson, Seeger RC. Natural killer T cells infiltrate neuroblastomas expressing the chemokine CCL2. J Exp Med 199: 1213–1221, 2004

Michalek AM, Buck GM, Nasca PC, Freedman AN, Baptiste MS, Mahoney MC. Gravid health status, medication use, and risk of neuroblastoma. Am J Epidemiol 143:996-1001, 1996

Miller RW. Childhood cancer and congenital defects. A study of U.S. death certificates during the period 1960-1966. Pediatr Res 3:389-97, 1969

Miyamoto K, Asada K, Fukutomi T, Okochi E, Yagi Y, Hasegawa T, Asahara T, Sugimura T, Ushijima T. Methylation-associated silencing of heparan sulfate D-glucosaminyl 3-O-sulfotransferase-2 (3-OST-2) in human breast, colon, lung and pancreatic cancers. Oncogene 22:274-80, 2003

Mochizuki H, Yoshida K, Gotoh M, Sugioka S, Kikuchi N, Kwon YD, Tawada A, Maeyama K, Inaba N, Hiruma T, Kimata K, Narimatsu H. Characterization of a heparan sulfate 3-O-sulfotransferase-5, an enzyme synthesizing a tetrasulfated disaccharide. J Biol Chem 278:26780-7, 2003

Mohammadi M, Olsen SK, Goetz R. A protein canyon in the FGF-FGF receptor dimer selects from an à la carte menu of heparan sulfate motifs. Curr Opin Struct Biol 15:506-16, 2005

Molenaar JJ, Koster J, Zwijnenburg DA, van Sluis P, Valentijn LJ, van der Ploeg I, Hamdi M, van Nes J, Westerman BA, van Arkel J, Ebus ME, Haneveld F, Lakeman A, Schild L, Molenaar P, Stroeken P, van Noesel MM, Ora I, Santo EE, Caron HN, Westerhout EM, Versteeg R. Sequencing of neuroblastoma identifies chromothripsis and defects in neuritogenesis genes. Nature 483:589-93, 2012

Moll UM, LaQuaglia M, Benard J, Riou G. Wild-type p53 protein undergoes cytoplasmic sequestration in undifferentiated neuroblastomas but not in differentiated tumors. Proc Natl AcadSci USA 92: 4407–11, 1995

Monclair T, Brodeur GM, Ambros PF, et al. The International Neuroblastoma Risk Group (INRG) staging system: an INRG Task Force report. J Clin Oncol 27: 298-303, 2009.

Moodley Y, Thompson P, Warburton D. Stem cells: a recapitulation of development. Respirology 18:1167-76, 2013

Morimoto-Tomita M, Uchimura K, Werb Z, Hemmerich S, Rosen SD. Cloning and Characterization of Two Extracellular Heparin-degrading Endosulfatases in Mice and Humans. J. Biol. Chem. 277, 49175-49185, 2002

Morimoto-Tomita M, Uchimura K, Bistrup A, Lum DH, Egeblad M, Boudreau N, Werb Z, Rosen SD. Sulf-2, a proangiogenic heparan sulfate endosulfatase, is upregulated in breast cancer. Neoplasia 7:1001-10, 2005

Moussay E, Palissot V, Vallar L, Poirel HA, Wenner T, El Khoury V, Aouali N, Van Moer K, Leners B, Bernardin F, Muller A, Cornillet-Lefebvre P, Delmer A, Duhem C, Ries F, van Dyck E, Berchem G. Determination of genes and microRNAs involved in the resistance to fludarabine in vivo in chronic lymphocytic leukemia. Mol Cancer 9:115, 2010

Nagamine S, Keino-Masu K, Shiomi K, Masu M. Proteolytic cleavage of the rat heparan sulfate 6-o-endosulfatase SulfFP2 by furin-type proprotein convertases. Biochem Biophys Res Commun 391:107-12, 2010

Nandini CD, Mikami T, Ohta M, Itoh N, Akiyama-Nambu F, Sugahara K. Structural and functional characterization of oversulfated chondroitin sulfate/dermatan sulfate hybrid chains from the notochord of hagfish. Neuritogenic and binding activities for growth factors and neurotrophic factors. J Biol Chem 279:50799-809, 2004

Narita K, Staub J, Chien J, Meyer K, Bauer M, Friedl A, Ramakrishnan S, Shridhar V.HSulf-1 inhibits angiogenesis and tumorigenesis in vivo. Cancer Res 66:6025-32, 2006

Nawroth R, van Zante A, Cervantes S, McManus M, Hebrok M, Rosen SD. Extracellular sulfatases, elements of the Wnt signaling pathway, positively regulate growth and tumorigenicity of human pancreatic cancer cells. PLoS One 2:e392, 2007

Nilsson MB, Zage PE, Zeng L, Xu L, Cascone T, Wu HK, Wu HK, Saigal B, Zweidler-McKay PA, Heymach JV. Multiple receptor tyrosine kinases regulate HIF-1alpha and HIF-2alpha in normoxia and hypoxia in neuroblastoma: implications for antiangiogenic mechanisms of multikinase inhibitors. Oncogene 29:2938-49, 2010

Olshan AF, Bunin GR. Epidemiology of neuroblastoma. In: Brodeur GM, Sawada T, et al. Neuroblastoma. Elsevier, Amsterdam, pp 33-39, 2000

Ono K, Hattori H, Takeshita S, Kurita A, Ishihara M. Structural features in heparin that interact with VEGF165 and modulate its biological activity. Glycobiology 9:705-11, 1999

Ori A, Wilkinson MC, Fernig DG. The heparanome and regulation of cell function: structures, functions and challenges. Front Biosci 13:4309-38, 2008

Origone P, Defferrari R, Mazzocco K, Lo Cunsolo C, De Bernardi B, Tonini GP. Homozygous inactivation of NF1 gene in a patient with familial NF1 and disseminated neuroblastoma. Am J Med Genet A 118A:309-13, 2003

Otsuki S, Hanson SR, Miyaki S, Grogan SP, Kinoshita M, Asahara H, Wong CH, Lotz MK. Extracellular sulfatases support cartilage homeostasis by regulating BMP and FGF signaling pathways. Proc Natl Acad Sci U S A 107:10202-7, 2010.

Paget S. The distribution of secondary growths in cancer of the breast. Lancet 1:571–573, 1889

Palaskas N, Larson SM, Schultz N, Komisopoulou E, Wong J, Rohle D, Campos C, Yannuzzi N, Osborne JR, Linkov I, Kastenhuber ER, Taschereau R, Plaisier SB, Tran C, Heguy A, Wu H, Sander C, Phelps ME, Brennan C, Port E, Huse JT, Graeber TG, Mellinghoff IK. 18F-fluorodeoxy-glucose positron emission tomography marks MYC-overexpressing human basal-like breast cancers. Cancer Res 71:5164-74, 2011

Pallerla SR, Lawrence R, Lewejohann L, Pan Y, Fischer T, Schlomann U, Zhang X, Esko JD, Grobe K. Altered heparan sulfate structure in mice with deleted NDST3 gene function. J Biol Chem. 2008 Jun 13;283(24):16885-94

Pantoliano MW, Horlick RA, Springer BA, Van Dyk DE, Tobery T, Wetmore DR, Lear JD, Nahapetian AT, Bradley JD, Sisk WP. Multivalent ligand-receptor binding interactions in the fibroblast growth factor system produce a cooperative growth factor and heparin mechanism for receptor dimerization. Biochemistry 33: 10229-48, 1994

Park S, Hahm ER, Lee DK, Yang CH. Inhibition of AP-1 transcription activator induces myc-dependent apoptosis in HL60 cells. J Cell Biochem 91:973-86, 2004

Parkin DM, Kramarova E, Draper GJ, Masuyer E, Michaelis J, Neglia J et al. International Incidence of Childhood Cancer, Vol. 2. IARC Sci Pub 1-391, 1998

Pellegrini L, Burke DF, von Delft F, Mulloy B, Blundell TL.Crystal structure of fibroblast growth factor receptor ectodomain bound to ligand and heparin. Nature 407:1029-34, 2000

Peterson SM, Iskenderian A, Cook L, Romashko A, Tobin K, Jones M, Norton A, Gómez-Yafal A, Heartlein MW, Concino MF, Liaw L, Martini PG. Human Sulfatase 2 inhibits in vivo tumor growth of MDA-MB-231 human breast cancer xenografts. BMC Cancer 10:427, 2010

Peuchmaur M, d'Amore ES, Joshi VV, Hata J, Roald B, Dehner LP, Gerbing RB, Stram DO, Lukens JN, Matthay KK, Shimada H. Revision of the International Neuroblastoma Pathology Classification: confirmation of favorable and unfavorable prognostic subsets in ganglioneuroblastoma, nodular. Cancer 98:2274-81, 2003

Phillips JJ, Huillard E, Robinson AE, Ward A, Lum DH, Polley MY, Rosen SD, Rowitch DH, Werb Z.Heparan sulfate sulfatase SULF2 regulates PDGFRα signaling and growth in human and mouse malignant glioma. J Clin Invest 122:911-22, 2012

Plotnikov AN, Schlessinger J, Hubbard SR, Mohammadi M. Structural basis for FGF receptor dimerization and activation. Cell 98:641–650, 1999

Poluha W, Poluha DK, Ross AH. TrkA neurogenic receptor regulates differentiation of neuroblastoma cells. Oncogene 10:185-9, 1995

Puissant A, Frumm SM, Alexe G, Bassil CF, Qi J, Chanthery YH, et al. Targeting MYCN in neuroblastoma by BET bromodomain inhibition. Cancer Discov 3:308-23, 2013

Pye DA, Vivès RR, Hyde P, Gallagher JT. Regulation of FGF-1 mitogenic activity by heparan sulfate oligosaccharides is dependent on specific structural features: differential requirements for the modulation of FGF-1 and FGF-2. Glycobiology 10:1183-92, 2000

Quail DF, Joyce JA. Microenvironmental regulation of tumor progression and metastasis. Nat Med 19:1423-3, 2013

Raabe EH, Laudenslager M, Winter C, et al. Prevalence and functional consequence of PHOX2B mutations in neuroblastoma.Oncogene 27:469-476, 2008

Raman K, Kuberan B. Chemical tumor biology of heparan sulfate proteoglycans. Curr Chem Biol 4:20-31, 2012

Rapraeger AC, Krufka A, Olwin BB. Requirement of heparan sulfate for bFGF-mediated fibroblast growth and myoblast differentiation. Science 252:1705-

8 ,1991

Reynolds CP, Biedler JL, Spengler BA, Reynolds DA, Ross RA, Frenkel EP, Smith RG. Characterization of human neuroblastoma cell lines established before and after therapy. *J Natl Cancer I* 76:375-87, 1986

Rosen SD, Lemjabbar-Alaoui H. Sulf-2: an extracellular modulator of cell signaling and a cancer target candidate. Expert Opin Ther Targets 14:935-49, 2010

Rossler J, Schwab M, Havers W, Schweigerer L. Hypoxia promotes apoptosis of human neuroblastoma cell lines with enhanced N-myc expression. Biochem Biophys Res Commun 281:272-6, 2001

Rudd TR, Guimond SE, Skidmore MA, Duchesne L, Guerrini M, Torri G, Cosentino C, Brown A, Clarke DT, Turnbull JE, Fernig DG, Yates EA. Influence of substitution pattern and cation binding on conformation and activity in heparin derivatives. Glycobiology 17:983-93, 2007

Rudd TR, Yates EA. A highly efficient tree structure for the biosynthesis of heparan sulfate accounts for the commonly observed disaccharides and suggests a mechanism for domain synthesis. Mol Biosyst 8:1499-506, 2012

Sanderson RD, Yang Y, Kelly T, MacLeod V, Dai Y, Theus A. Enzymatic remodeling of heparan sulfate proteoglycans within the tumor microenvironment: growth regulation and the prospect of new cancer therapies. J Cell Biochem 96:897-905, 2005

Sasisekharan R, Shriver Z, Venkataraman G, Narayanasami U Roles of heparan-sulphate glycosaminoglycans in cancer. Nat Rev Cancer 2:521-8, 2002

Schelwies M, Brinson D, Otsuki S, Hong YH, Lotz MK, Wong CH, Hanson SR. Glucosamine-6-sulfamate analogues of heparan sulfate as inhibitors of endosulfatases. Chembiochem 11:2393-7, 2010

Schindelin J, Arganda-Carreras I, Frise E, Kaynig V, Longair M, Pietzsch T, et al. Fiji: an open-source platform for biological-image analysis. Nat Methods 9:676-82, 2012

Schlessinger J, Plotnikov AN, Ibrahimi OA, Eliseenkova AV, Yeh BK, Yayon A, Linhardt RJ, Mohammadi M. Crystal structure of a ternary FGF-FGFR-heparin complex reveals a dual role for heparin in FGFR binding and dimerization. Mol Cell 6:743-50, 2000

Schuz J, Kaletsch U, Meinert R, Kaatsch P, et al. Risk factors for neuroblastoma at different stages of disease. Results from a population-based case-control study in Germany. J Clin Epidemiol 54:702-709, 2001

Schwab M. MYCN in neuronal tumours. Cancer Lett 204:179-87, 2004

Shafat I, Barak AB, Postovsky S, Elhasid R, Ilan N, Vlodavsky I, Arush MW. Heparanase levels are elevated in the plasma of pediatric cancer patients and correlate with response to anticancer treatment. Neoplasia 9:909-16, 2007

Shimada H, Ambros IM, Dehner LP, et al. Terminology and morphologic criteria of neuroblastoma tumours: recommendations by the International Neuroblastoma Pathology Committee. Cancer 86:349-363, 1999[a]

Shimada H, Ambros IM, Dehner LP, et al. The International Neuroblastoma Pathology Classification (the Shimada system). Cancer 86:364-372, 1999[b]

Shimada H, Chatten J, Newton WA Jr, Sachs N, Hamoudi AB, Chiba T, Marsden HB, Misugi K. Histopathologic prognostic factors in neuroblastic tumors: definition of subtypes of ganglioneuroblastoma and an age-linked classification of neuroblastoma. J Natl Cancer Inst 73:405-16, 1984

Shuman C, Beckwith JB, Smith AC, et al. Beckwith-Wiedemann Syndrome. In: Pagon RA, Adam MP, Bird TD, et al. Editors. Seattle (WA): University of Washington, Seattle; 1993-2013.

Shworak NW, Liu J, Fritze LM, Schwartz JJ, Zhang L, Logeart D, Rosenberg RD. Molecular cloning and expression of mouse and human cDNAs encoding heparan sulfate D-glucosaminyl 3-O-sulfotransferase. J Biol Chem 272:28008-19, 1997

Shworak NW, Liu J, Petros LM, Zhang L, Kobayashi M, Copeland NG, Jenkins NA, Rosenberg RD. Multiple isoforms of heparan sulfate D-glucosaminyl 3-O-sulfotransferase. Isolation, characterization, and expression of human cdnas and identification of distinct genomic loci. J Biol Chem 274:5170-84, 1999

Skidmore MA, Guimond SE, Dumax-Vorzet AF, Atrih A, Yates EA, Turnbull JE. High sensitivity separation and detection of heparan sulfate disaccharides. J Chromatogr A 1135:52-6, 2006

Skidmore MA, Guimond SE, Dumax-Vorzet AF, Yates EA, Turnbull JE. Disaccharide compositional analysis of heparan sulfate and heparin polysaccharides using UV or high-sensitivity fluorescence (BODIPY) detection. Nat Protoc 5:1983-92, 2010

Slack A, Shohet JM. MDM2 as a critical effector of the MYCN oncogene in tumorigenesis. Cell Cycle 4:857-60, 2005

Slamon DJ, Boone TC, Seeger RC, Keith DE, Chazin V, Lee HC, Souza LM. Identification and characterization of the protein encoded by the human N-myc oncogene. Science 232:768-72, 1986

Song L, Ara T, Wu HW, Woo CW, Reynolds CP, Seeger RC, DeClerck YA, Thiele CJ, Sposto R, Metelitsa LS. Oncogene MYCN regulates localization of NKT cells to the site of disease in neuroblastoma. J Clin Invest 117:2702-12, 2007

Soucek L, Whitefield J, Martins CP, Finch AJ, Murphy DJ, Sodir NM, Karnezis AN, Swigart LB, Nasi S, Evan GI. Modelling Myc inhibition as a cancer therapy. Nature 455:679-83, 2008

Stauber DJ, DiGabriele AD, Hendrickson WA. Structural interactions of fibroblast growth factor receptor with its ligands. Proc Natl Acad Sci U S A 97:49–54, 2000

Stiller CA, Parkin DM. International variations in the incidence of neuroblastoma. Int J Cancer 52:538-543, 1992

Stovroff M, Dykes F, Teague WG. The complete spectrum of neurocristopathy in an infant with congenital hypoventilation, Hirschsprung's disease, and neuroblastoma. J Ped Surg 30:1218-12221, 1995

Su G, Meyer K, Nandini CD, Qiao D, Salamat S, Friedl A. Glypican-1 is frequently overexpressed in human gliomas and enhances FGF-2 signaling in glioma cells. Am J Pathol 168:2014–2026, 2006

Sugaya N, Habuchi H, Nagai N, Ashikari-Hada S, Kimata K. 6-O-sulfation of heparan sulfate differentially regulates various fibroblast growth factor-dependent signalings in culture. J Biol Chem 283:10366–10376, 2008

Takei Y, Ozawa Y, Sato M, Watanabe A, Tabata T. Three Drosophila EXT genes shape morphogen gradients through synthesis of heparan sulfate proteoglycans. Development 131:73-82, 2004

Tang R, Rosen SD. Functional consequences of the subdomain organization of the sulfs. J Biol Chem 284:21505-14, 2009

Tátrai P, Egedi K, Somorácz A, van Kuppevelt TH, Ten Dam G, Lyon M, Deakin JA, Kiss A, Schaff Z, Kovalszky I. Quantitative and qualitative alterations of heparan sulfate in fibrogenic liver diseases and hepatocellular cancer. J Histochem Cytochem 58:429-41, 2010

Thomas WD, Raif A, Hansford L, Marshall, G. N-myc transcription molecule and oncoprotein. Int J Biochem Cell Biol, 36, 771-775, 2004

Turnbull JE, Field RA. Emerging glycomics technologies. Nat Chem Biol 3:74-7, 2007

Turner N, Grose R. Fibroblast growth factor signalling: from development to cancer. Nat Rev Cancer 10:116–129, 2010

Tzeng ST, Tsai MH, Chen CL, Lee JX, Jao TM, Yu SL, Yen SJ, Yang YC. NDST4 is a novel candidate tumor suppressor gene at chromosome 4q26 and its genetic loss predicts adverse prognosis in colorectal cancer. PLoS One 8:e67040, 2013

Uchimura K, Morimoto-Tomita M, Rosen SD. Measuring the activities of the Sulfs: two novel heparin/heparan sulfate endosulfatases. Methods Enzymol 416:243-53, 2006

Valastyan S, Weinberg R. Tumour metastasis: molecular insights and evolving paradigms. Cell 147:275-292, 2011

Valentijn LJ, Koster J, Haneveld F, Aissa RA, van Sluis P, Broekmans ME, Molenaar JJ, van Nes J, Versteeg R. Functional MYCN signature predicts outcome of neuroblastoma irrespective of MYCN amplification. Proc Natl Acad Sci U S A 109:19190-5, 2012

van den Born J, Salmivirta K, Henttinen T, Ostman N, Ishimaru T, Miyaura S, Yoshida K, Salmivirta M. Novel heparan sulfate structures revealed by monoclonal antibodies. J Biol Chem 280:20516-23, 2005

Vivès RR, Seffouh A, Lortat-Jacob H. Post-synthetic regulation of HS structure: The yin and yang of the Sulfs in cancer. Front Oncol 3:331, 2014

Viviano BL, Paine-Saunders S, Gasiunas N, Gallagher J, Saunders S. Domain-specific modification of heparan sulfate by Qsulf1 modulates the binding of the bone morphogenetic protein antagonist Noggin. J Biol Chem 279:5604-11, 2004

Virchow R. Die krankhaften Geschwülste. Hirschwald H, Berlin,1865

Wade A, Robinson AE, Engler JR, Petritsch C, James CD, Phillips JJ. Proteoglycans and their roles in brain cancer. FEBS J 280:2399-417, 2013

Wahl HR. Neuroblastomata: with a Study of a Case illustrating the Three Types that arise from the sympathetic System. J Med Res 30:205-260.13, 1914

Wang L, Fuster M, Sriramarao P, Esko JD. Endothelial heparan sulfate deficiency impairs L-selectin- and chemokine-mediated neutrophil trafficking during inflammatory responses. Nat Immunol 6:902-10, 2005

Wang J, He XD, Yao N, Liang WJ, Zhang YC. A meta-analysis of adjuvant therapy after potentially curative treatment for hepatocellular carcinoma. Can J Gastroenterol 27:351-63, 2013

Weiss WA, Aldape K, Mohapatra G, Feuerstein BG, Bishop JM.
Targeted expression of MYCN causes neuroblastoma in transgenic mice. EMBO J 16:2985-95, 1997

Wenzel A, Cziepluch C, Hamann U, Schürmann J, Schwab M. The N-Myc oncoprotein is associated in vivo with the phosphoprotein Max(p20/22) in human neuroblastoma cells. EMBO J 10:3703-12, 1991

Whitelock JM, Iozzo RV. Heparan sulfate: a complex polymer charged with biological activity. Chem Rev 105:2745-64, 2005

Whiteside TL. The tumor microenvironment and its role in promoting tumor growth. Oncogene 27:5904-12, 2008

Whitfield JR, Soucek L. Tumor microenvironment: becoming sick of Myc. Cell Mol Life Sci 69:931-4, 2012

Williams CL, Bunch KJ, Stiller CA, Murphy MF, Botting BJ, Wallace WH, Davies M, Sutcliffe AG. Cancer risk among children born after assisted conception. N Engl J Med 369:1819-27, 2013

Yang JD, Sun Z, Hu C, Lai J, Dove R, Nakamura I, Lee JS, Thorgeirsson SS, Kang KJ, Chu IS, Roberts LR. Sulfatase 1 and sulfatase 2 in hepatocellular carcinoma: associated signaling pathways, tumor phenotypes, and survival. Genes Chromosomes Cancer 50:122-35, 2011

Yang Q, Olshan AF, Bondy ML, Shah NR, Pollock BH, Seeger RC, Look AT, Cohn SL. Parental smoking and alcohol consumption and risk of neuroblastoma. Cancer Epidemiol Biomarkers Prev 9:967-72, 2000

Yayon A, Klagsbrun M, Esko JD, Leder P, Ornitz DM. Cell surface, heparin-like molecules are required for binding of basic fibroblast growth factor to its high affinity receptor. Cell 64:841-8, 1991

Zheng LD, Tong QS, Tang ST, Du ZY, Liu Y, Jiang GS, Cai JB. Expression and clinical significance of heparanase in neuroblastoma. World J Pediatr 5:206-10, 2009

Appendix

Appendix 1 - Preliminary data that lead to the hypothesis of this thesis

This Appendix shows some of the preliminary PhD work done as part of the Academic Clinical Fellowship in paediatric surgery by the author (VS).

It was known that some heparan sulfate (HS) abnormalities were found in NBL in the 1980s [Hampson et al., 1983] and that elevated serum heparanase also correlates with poor prognosis in NBL [Shafat et al., 2007]. Initially when discovered, these HS abnormalities could not be pursued due to lack of technology that hampered its analysis. Also it became more apparent that NBL is a cancer of development where their few genetic mutations cannot explain entirely the complexity of their development and behaviour. The increasing evidence of the important role heparan sulfate as a regulator of cell interactions with the surrounding microenvironment became an important missing link. We started by hypothesising that HS is altered in NBL and that it regulates their phenotype.

In our preliminary work that lead to the MRC Clinical Research Fellowship that sponsored this PhD study we used for the first time phage-display antibodies to HS to study HS expression in NBL cells. The phage display antibody HS3B7V (Appendix Figure 1.1) shows differential HS staining between the NBL cell line SH-5YSY (neuronal type) and SHEP (stromal type). SH-5YSY and SHEP are MYCN NA cell lines. We also analysed archival tumour sections and showed that HS is overexpressed in primary human NBL tumours relative to surrounding non-tumour tissue (Appendix Figure 1.2). Additionally we

demonstrated that NBL cell lines with different phenotypes vary characteristically in their HS expression with reciprocally altered sulfation in SH-SY5Y compared to SHEP (Appendix Figure 1.3).

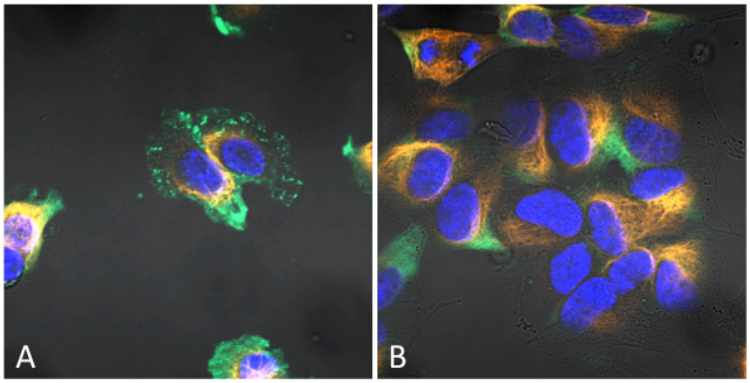

Appendix Figure 1.1 Immunocytochemistry with a phage display antibody. HS3B7V (green immunofluorescence), differential HS staining between the NB cell line SH-5YSY (A, neuronal type) and SHEP (B, stromal type). Vimentin is stained in red. We demonstrated NBL cell lines with different phenotypes that vary characteristically in their HS expression with reciprocally altered sulfation in SH-SY5Y compared to SHEP (*B*).

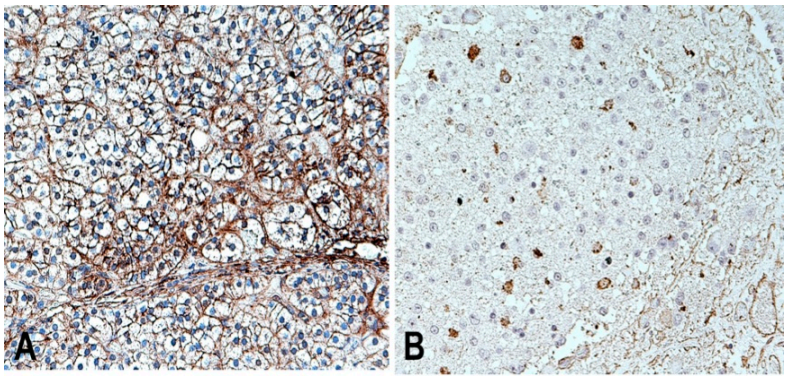

Appendix Figure 1.2 HS immunohistochemistry using 3G10 antibody. A representative stage 3 NBL tumour with a strong expression in the stroma and cell surface (A) and only a few HS positive cells in the normal adrenal gland.

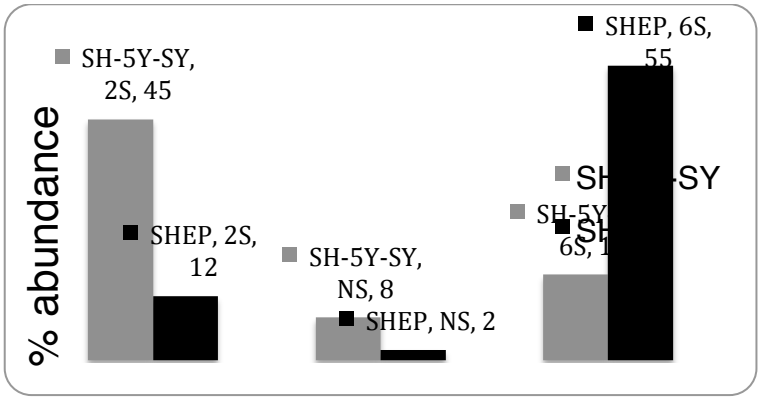

Appendix Figure 1.3 High performance liquid chromatography (HPLC) disaccharide analysis. Graph bar showing the three principal sulfation (S) positions with differences in 2S and 6S between the NBL cell lines SHEP and SH-5Y-SY.

Appendix 2 - Chromatin immunoprecipitation (ChIP) assay

The finding s from Chapter 3 and Chapter 4 suggested that SULF2 is a down stream target of MYCN. Here in this appendix we show a chromatin immunoprecipitation assay to test this hypothesis.

The work of this appendix was done by Mueller Fabbri, MD, PhD and Kishore Challagundla, PhD at the Children's Hospital Los Angeles (CHLA), USA.

Appendix 2 - Material and Methods

MYCN amplified SK-N-BE(2) cells were crosslinked with 1% formaldehyde for 10 minutes at RT followed by quench the cross linking reaction with 1.25M glycine at RT for 5 minutes. Cells were washed 3 times with ice cold PBS and lysed with RIPA buffer [50 mM Tris (pH 8.0), 150 mM NaCl, 5 mM EDTA, 1 % NP-40, 0.1 % SDS, 0.5 % Sodium deoxycholate] and protease inhibitor cocktail on ice for 10 minutes. Cell lysates were sonicated for 15 seconds for 5 times using a sonicator (Q Sonica, Q125). The average chromatin fragment size after sonication was approximately 600-1000 bp. After centrifugation, the soluble chromatin fraction was recovered and pre-cleared for 30mins h at 4°C with a mixture of Protein A and G-conjugated beads (Santa Cruz Biotechnologies) then blocked with BSA and salmon sperm DNA. Chromatin was immunoprecipitated overnight at 4°C with either an IgG or anti-MYCN antibodies. After antibody incubation protein A/G beads were added to the immuno-precipitates for additional 2 hours at 4°C. Immunoprecipitates were washed twice with RIPA buffer, four times with IP wash buffer (100 mM Tris [pH 8.5], 500 mM LiCl, 1 % NP-40, 1 % deoxycholic acid) and additional two more

times with RIPA buffer. Bound chromatin and input DNA were placed in elution buffer (50 mM NaHCO3, 1 % SDS) and reverse crosslinked. Immunoprecipitated DNA and input DNA were treated with RNase A and proteinase K and purified with a QIAquick PCR purification kit (Qiagen). Quantitative RT-PCR was performed with CFX96 Touch Real Time PCR using SYBR master mix (Biorad). All reactions were carried out in triplicate. Calculations were done using the ΔΔCt method. MYCN IP was normalized to IgG IP and presented as fold change of MYCN IPed DNA when compare to IgG. Primer sequences used in ChIP qRT-PCR analysis are F: 5'-AGGCGATGGAAACTCGTTCT-3' and R: 5'-CATGGCCTTGTTGACCCTTA-3'. Another portion of the cells were used for western blot analysis of MYCN.

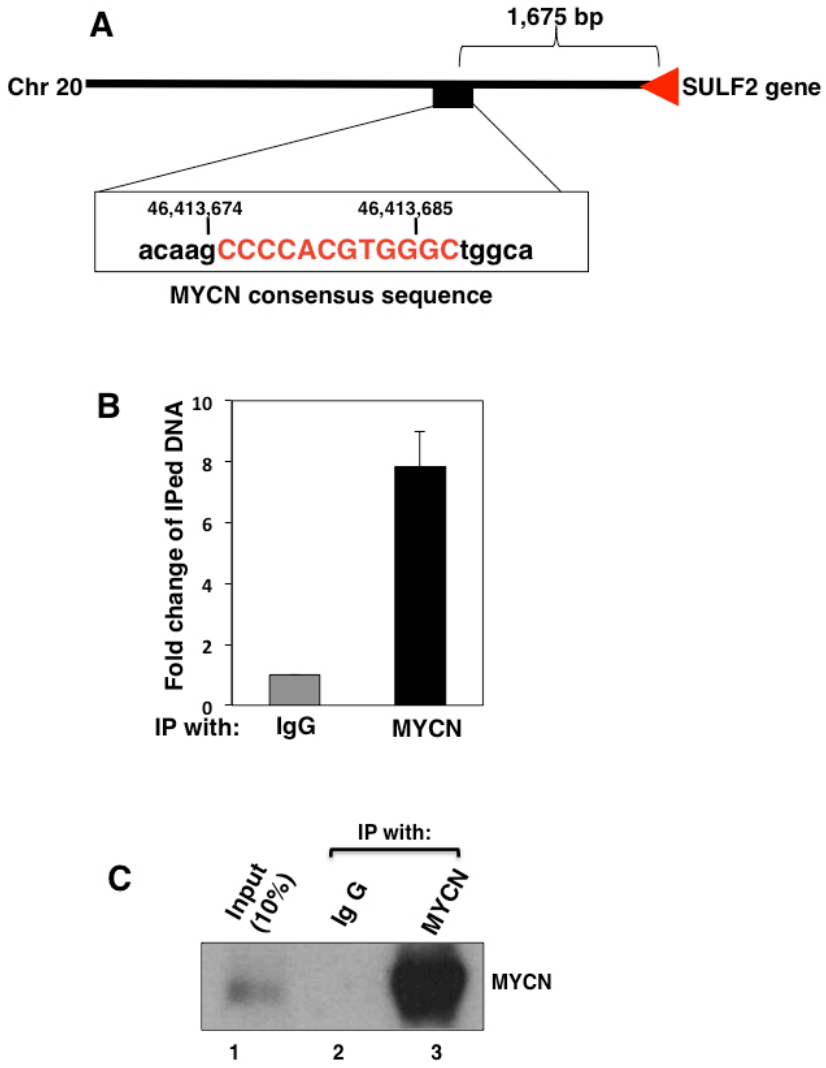

Appendix Figure 2.1 SULF2 is a target gene of MYCN.

(A) Diagram demonstrating the SULF2 gene location on Chromosome 20. Filled box indicate the exonic region amplified by ChIP-qPCR assay. Arrow indicates the transcription start point. (B) CHIP q-PCR assay showing the enrichment of MYCN on SULF2 gene promoter. ChIP-qPCR assays were conducted in SK-N-BE(2) cells using anti-MYCN antibody to detect the recruitment of endogenous MYCN at the SULF2 gene promoter. (C) Western blot showing the expression of endogenous MYCN in ChIP assay and no product for the IgG..

This assay showed that MYCN binds to the SULF2 promoter region. This supports our previous hypothesis in Chapter 4 that SULF is down stream of MYCN.

Appendix 3 - Disaccharide analysis

In initial efforts to explore changes in HS sulfation at the biochemical level in response to altered SULF2 expression, we purified HS from different NBL cell lines and genetically altered counterparts, and examined their disaccharide composition by HPLC employing fluorescence detection.

The work presented in this appendix is currently being performed by Becky Miller, PhD and Sophie Thompson, PhD at the University of Liverpool, UK.

Appendix 3: Material and Methods

HSPG extraction and purification of HSPGs using ion exchange chromatography : Cells were scraped from the flasks, sonicated and incubated at room temperature for 2 hours with agitation with TUT buffer (10 mM Tris base, 8 M urea, 1 % (v/v) Triton X-100, 1 mM Na_2SO_4, pH 8) at 1 mL/10 cm^2. Extracted sample/conditioned medium was applied to 100 ml DEAE-Sephacel beads per 5 mL sample (pre washed and equilibrated in PBS) and incubated overnight at room temperature with gentle agitation. Void volume material was discarded and the DEAE beads were washed three times in 10 column volumes of PBS, followed by 10 column volumes of 0.25 M NaCl in PBS. Bound material containing HSPGs was eluted with 10 column volumes of 2 M NaCl in PBS. The eluant was desalted over two, in-line 5 ml HiTrap desalting columns using an AKTA FPLC system and freeze dried

Digestion of HS into disaccharides: Freeze dried material was resuspended in heparin lyase buffer (100 mM sodium acetate, 0.1 mM calcium acetate, pH 7)

and 1.25 mU of heparinase I (heparitinase III) was added. Samples were incubated at 37°C. After 2 hours, 1.25 mU of heparinase III (heparitinase I) was added to samples and incubated for a further 2 hours at 37°C, followed by 1.25 mU of heparinase II incubated for another 2 hours at 37°C. All three enzymes were then added to each sample at 1.25 mU and incubated overnight at 37°C. Digested samples were then made up to 0.5 M NaCl, incubated at 95°C for 5 minutes and allowed to cool.

C18 recovery of HS disaccharides: C18 spin columns (#89873, Pierce) were washed as per the manufacturer's instructions. Each sample was added to a C18 column and centrifuged at 1,500 g for 1 minute. HS disaccharides present in the void volume were collected. Columns were washed three times with HPLC water and the washes added to the disaccharide samples.

Sample clean up using graphite: Graphite spin columns were washed as per the manufacturer's instructions. Samples were loaded onto the columns, mixed gently and incubated at room temperature for 10 minutes. Columns were then centrifuged at 3,000 g for 1 minute and the flow through discarded. The graphite was then washed three times with HPLC water and the bound disaccharides eluted in three washes of 40 % (v/v) acetonitrile, 0.5 % (v/v) TFA. Sampled were then dried to remove the acetonitrile and TFA.

Fluorescent labelling of HS disaccharides: Freeze-dried HS disaccharides were labelled with BODIPY FL hydrazide (5 mg/ml; 4,4-difluoro-5, 7-dimethyl-4-bora-3a, 4a-diaza-*s*-indacene-3-propionic acid hydrazide; Molecular Probes) as previously described [Skidmore et al., 2006; Skidmore et al., 2010]. Digested heparin control and HS disaccharide standards (Iduron, Manchester, UK) were

labelled in the same way. Labelled samples were applied to silica gel thin layer chromatography (TLC) aluminium plates and free BODIPY tag separated from labelled disaccharides with butanol. Labelled HS disaccharides were removed from the TLC plates and solubilised in HPLC grade water.

Ethanol precipitation: Sample volume was reduced to ~ 200 ml and incubated on ice. Ice cold saturated ethanol was added to samples at a final concentration of 80 % (v/v) and incubated on ice for 15 minutes. Samples were then centrifuged at 13000 rpm and the supernatant containing the HS disaccharides removed and dried by speed vac.

SAX-HPLC: SAX separations were performed on a Propac PA1 column (25 cm x 9 mm, 5 mm) using a Shimadzu SPD 10A HPLC system. Elution profiles were monitored by UV absorbance at 232 nm and fluorescent detection using a Shimadzu RF10AXL spectrofluorometer. Buffer A was 150 mM NaOH and Buffer B was 150 mM NaOH, 2 M NaCl. Elution profiles were monitored by UV absorbance at 232 nm and fluorescent detection at l_{ex} = 488 nm l_{em} = 520 nm. Samples were injected and the flow held at 2 ml min^{-1} in buffer A until all remaining free tag had been eluted. Fluorescently labelled disaccharides were then eluted using a linear gradient of 0-50% buffer B over 50 min at 1 ml min^{-1}. The column was then washed with a 10 min elution in 300 mM NaOH, 2 M NaCl, before returning to 150 mM NaOH.